Studies on Band Shape of UV Photoelectron Spectrum of Alkylamine

by Masao Takahashi

Studies on Band Shape of UV Photoelectron Spectrum of Alkylamine

by

Masao Takahashi

Department of Chemistry

Faculty of Science

Osaka University

June,1986

Contents

[Contents]

[Contents]

[Contents]

Chapter 1. Introduction

Spectroscopy based on measurement of energies of photoelectrons emitted from molecules by uv radiation was started by two research groups[1-5] and the method was named "molecular photoelectron spectroscopy" by Al-Joboury and Turner.[2] The photoelectron spectroscopy has been investigated extensively since then and has been reviewed thoroughly.[6-16] While a parallel technique, using X-ray as irradiation source instead of uv light, was developed by Siegbahn and named "ESCA".[17-19] These spectroscopy mutually compensate and are often called X-ray photoelectron spectroscopy (XPS) and UV photoelectron spectroscopy (UPS) distinguished by difference of the irradiation source. In this study the abbreviation "UPS" is used instead of "UV photoelectron spectrum". The methods are potentially of as great value to the chemist as are the well-established nmr, ir, and mass spectometry techniques.

Following informations are available from UPS of gaseous phase; first of all, ionization potential, I_p; bonding of the orbital in which the photoelectron has been binded; Substitution effect; Jahn-Teller effect; spin-orbit interaction; molecular structure. Steric hindrance and configuration have been discussed by means of I_p, e.g., dihedral angles of two phenyl groups were discussed using

difference in I_p's between two π-orbitals for biphenyl compounds.[20] Other studies on correlation between dihedral angles of planes included molecular orbitals and difference of their orbital I_p's, e.g., phenyl compounds,[21,22], butadiene derivatives[23], and hydrazine.[24-28] Substitution effects on I_p's have been discussed, e.g., variation of I_p's for aldehides, alcohols and ketones by alkyl substitution[29] and dialkylmercury conpounds.[30] Correlation between I_p's and Hammet σ or Taft σ^* has been discussed, e.g., in Ref. 31. Linear relation between I_p's of lone-pairs for halogen compounds and Pauling's electronegativity were found.[32]

Thus though numerous investigations on the chemical properties on the basis of their ionization energies have been executed, study on band shape has been a few and limited to qualitative one. Only difference between vertical I_p and adiabatic I_p was compared to the change in frequency on ionization,[33] and FWHM of the first band for methylamine, methanol, and methane thiol were compared to extent of contribution of lone-pair orbital to HOMO.[34] Quantitative treatment of difference between vertical I_p and adiabatic I_p was limited to hypothetical one.[35]

The band shape of UPS is affected by the degree of distortion of the molecular structure caused by the photoionization, viz., the larger the distortion, the wider

the band width.[16)]

And then the idea has been considered in general, i.e., the photoelectron band, assigned to *non- bonding molecular orbital* is sharper than the band, asssigned to *bonding* or *anti-bonding orbital* according to a molecular orbital model. However an exception was found on study for molybdenum complex.[36)] The instance is as follows. There is some analogy between thiolatomolybdenum, $Mo(t\text{-}BuS)_4$, and amidomolybdenum, $Mo(NMe_2)_4$ and $Mo(NEt_2)_4$ with respect to the molecular symmetry and the valence type of Mo. The DV-Xα MO calculations predict that the HOMO of the amidomolybdenum complex consists almost entirely of $Mo4d_{x^2-y^2}$ (88 %), while that of the thiolatomolybdenum complex delocalizes slightly. The contents of the theoretical calculation appear to be inconsistent with the experimental fact that the band width (FWHM) of the first band, corresponding to the ionization of the HOMO, in the UPS of $Mo(NMe_2)_4$ is estimated to be about twice as large as that of $Mo(t\text{-}BuS)_4$.

The difficulty to understand the contradiction has arisen in the same way on the studies of some metal halide complexes.[16)] For example, the photoionization of TlBr[37)] gives a broad peak due to the ejection of the electron localized on Br, i.e., the *non-bonding* or *lone-pair electron*, together with a sharp peak due to the ejection of the electron delocalized over the two atoms, i.e., the

bonding electron according to a molecular orbital model. The phenomenon was simply understood by taking account of the roles of localized and delocalized electrons in an ionic-bond. In the ionic-bond the electron on Br^- acts as a bonding electron, so its ionization causes a broad peak. In the case of amidomolybdenum and thiolatomolybdenum complexes the phenomenon also could be understood in quite the same manner. The DV-Xα calculations on $Mo(NH_2)_4$ and $Mo(SMe)_4$ also predict that the bond-overlap populations of Mo-N and Mo-S are 0.248 and 2.648, and that the net charge on Mo central atoms are +2.15 and +0.80, respectively. Therefore, it could be stated that the Mo-N bond is ionic in character but that the Mo-S bond is covalent if compared each other. Thus the electron in HOMO of amidomolybdenum plays a role as an anti-bonding electron with respect to the ionic Mo-N bond more strongly than the corresponding electron in thiolatomolybdenum does as a bonding electron with respect to the covalent Mo-S bond. Therefore, the spectra exhibit the broader first band for the amidomolybdenum complex than for the thiolatomolybdenum complex.

This evidence has been one of the motivation of this study. The other has been what the HOMO electron plays the most important role in regard to the chemical reactivity of the molecule. In order to investigate any informations of the chemical reactivity included in the band shape of the

UPS, a series of alkylamines have been choosen. Because alkylamine is simpler molecule whose first band is wide due to large distortion with photionization and is important on the environment science.

This thesis is constructed as follows. Chapter 2 is described about observed UPS for a series of alkylamines and their qualitative analysis. I_p's, band width δ's and vibrational frequencies for cation molecules are presented. Alkyl substitution effects on I_p and δ are discussed.

Chapter 3 deals with theoretical interpretation for the band shape. Ab initio MO calculations have been executed and using potential energy curves acquired, band width is discussed. And adiabatic I_p is also argued.

Chapter 4 states about a verification of the analysis of band shape of the UPS in this study and a determination method of adiabatic I_p by means of deuterium substitution. Observed UPS for deutrerium derivatives of alkylamines are presented.

In Chapter 5, electrochemical data are measured and are compared to photoelectron spectroscopic data. This discussion is done since the removal of a electron from the HOMO in vacuo is equivalent to one-electron oxidation at the electrode in solution. Correlation between I_p and oxidation potential and correlation between δ and one of the kinetic parameters in electrode reaction, transfer coefficient

(symmetry factor) are argued. The electrochemical oxidation reaction is discussed by using potential energy curves on both the neutral and the cationic states.

Chapter 6 deals a new quantity for the band shape, which express the band shape more generally. The discussion is done for the activation energy of the electrochemical oxidation at the equilibrium potential.

References

[1] M. I. Al-Joboury and D. W. Turner, *J. Chem. Phys.*, 37, 3007 (1962).

[2] M. I. Al-Joboury and D. W. Turner, *J. Chem. Soc.*, 1963, 5141.

[3] M. I. Al-Joboury and D. W. Turner, *ibid.*, 1964, 4434.

[4] F. I. Vilesov, B. L. Kurbatov, and A. N. Terenin, *Dokl. Akad. Nauk SSSR*, 138, 1329 (1961).

[5] B. L. Kurbatov, F. I. Vilesov, and A. N. Terenin, *Dokl. Akad. Nauk SSSR*, 140, 797 (1961).

[6] D. W. Turner, *Advan Phys. Org. Chem.*, 4, 31 (1966).

[7] D. W. Turner, *Advan. Mass. Spectrom.*, 4, 755 (1968).

[8] D. W. Turner, *Chem. Brit.*, 4, 435 (1968).

[9] R. S. Berry, *Ann. Rev. Phys. Chem.*, 20, 357 (1969).

[10] D. Betteridge and A. D. Baker, *Anal. Chem.*, 42, 43A (1970).

[11] A. D. Baker, *Acc. Chem. Res.*, 3, 17 (1970).

[12] S. D. Worley, *Chem. Rev.*, 71, 295 (1970).

[13] W. C. Price and D. W. Turner, *Phil. Trans. R. Soc. Lond.*, A268, 1 (1970).

[14] D. W. Turner, C. Baker, A. D. Baker, and C. R. Brundle, "Molecular Photoelectron Spectroscopy", Wiley-Interscience, New York (1970).

[15] H. Bock and B. Solouki, *Angew. Chem. Int. Ed. Engl.*,

20, 427 (1981).

[16] J. H. D. Eland, "Photoelectron Spectroscopy", Butterworths and Co., London (1974).

[17] K. Siegbahn, *Nova Acta Regae Soc. Sci. Upsal., Ser. IV*, 1967, 20.

[18] D. M. Hercules, *Anal. Chem.*, 42, 20A (1970).

[19] K. Siegbahn, *Phil. Trans. R. Soc. Lond.*, A268, 33 (1970).

[20] J. P. Maier and D. W. Turner, *Diss. Faraday Soc.*, 54, 149 (1972).

[21] J. P. Maier and D. W. Turner, *J. Chem Soc., Faraday Trans.* 2, 69, 196 (1973).

[22] J. P. Maier and D. W. Turner, *J. Chem. Soc., Faraday Trans.* 2, 69, 521 (1973).

[23] C. R. Brundle and M. B. Robin, *J. Am. Chem. Soc.*, 92, 5550 (1970).

[24] S. F. Nelson and J. M. Bunschek, *J. Am. Chem. Soc.*, 95, 2011 (1973).

[25] S. F. Nelson and J. M. Bunschek, *J. Am. Chem. Soc.*, 96, 2392 (1974).

[26] S. F. Nelson and J. M. Bunschek, *J. Am. Chem. Soc.*, 96, 6982 (1974).

[27] S. F. Nelson and J. M. Bunschek, *J. Am. Chem. Soc.*, 96, 6987 (1974).

[28] S. F. Nelson, *Acc. Chem. Res.*, 14, 131 (1981).

[29] B. J. Cocksey, J. H. D. Eland, and C. J. Danby, *J. Chem. Soc. (B)*, **1971**, 790.

[30] T. P. Fehlner, J. Ulman, W. A. Nugent, and J. K. Kochi, *Inorg. Chem.*, **15**, 2544 (1976).

[31] A. D. Baker, D. Betteridge, N. R. Kemp, and R. E. Kirby, *Anal. Chem.*, **43**, 375 (1971).

[32] A. D. Baker, D. Betteridge, N. R. Kemp, and R. E. Kerby, *Int. J. Mass Spectrom. Ion. Phys.*, **4**, 90 (1970).

[33] D. W. Turner, *Phil. Trans. R. Soc. Lond.*, **A268**, 7 (1970).

[34] H. Ogata, H. Onizuka, Y. Nihei, and H. Kamada, *Chem. Lett.*, **1972**, 895.

[35] A. W. Potts and W. C. Price, *Proc. R. Soc. Lond.*, **A326**, 165 (1971).

[36] M. Takahashi, I. Watanabe, S. Ikeda, M. Kamato, and S. Otsuka, *Bull. Chem. Soc. Jpn.*, **55**, 3757 (1982).

[37] J. Berkowitz, *J. Chem. Phys.*, **56**, 2766 (1972).

Chapter 2. UV Photoelectron Spectra for a Series of Alkylamines

2.1 Introduction

The shape of the first band in the UPS corresponding to the ionization of the HOMO electron should provide information on the chemical reactivity of the molecule. The UPS for a number of amines have been measured by many workers.[1-27] They are, however, inappropriate for discussion of the band shape because they were measured under different conditions, e.g., temperature, spectral resolution, etc. Accurate measurement of the UPS for a series of alkylamines was performed paying special attention to the first bands. In this chapter, all the spectra obtained under the same conditions are presented and interpreted qualitatively.

2.2 Experimental

The He(I) photoelectron spectrometer used has a hemispherical analyzer (127mm radius, constant pass energy of ∿1 eV) and was controlled by a mini-computer. The ionization energy scale was calibrated with argon (I_p=15.759 eV) or zenon (I_p=12.130 eV) used as an internal

reference. The computer acquisition provides accurately calibrated photoelectron spectra using a real-time energy calibration technique. Then the effect of any energy drift of the spectrometer during the measurement was compensated for. Spectral resolution defined by the full width at half-maximum (FWHM) of the $^2P_{3/2}$ argon or xenon peak was at 20-30 meV. Data points were taken every 10 meV for full scan spectra. The spectrometer was kept at about 300 K but the temperature of the ionization chamber was higher by 20 K because of the heat of the helium discharge lamp. In the case of triamylamine, having a low pressure, the spectrometer was heated to 307 K to obtain sufficient vapor pressure. Heating of the whole spectrometer gave a stronger signal without degradation of resolution. In addition to the measurements of full spectra, narrow scan measurement for the first bands were made. The narrow scan spectra were measured with data points every 5 meV except ammonia which was measured every 3 meV.

All samples were commercial products. The samples obtained in the form of aqueous solutions (ammonia, methylamine, dimethylamine, and trimethylamine) were evaporated from the solution by adding sodium hydroxide.

Vertical ionization potential I_{pv} was read at the maximum of the most intense vibrational component of the first band when vibrational progressions were well resolved.

Threshold ionization potential I_{Pth} was read at the first vibrational peak of the band. For the molecule which displays no vibrational fine structure, I_{Pv} was read at the maximum of the band, and I_{Pth} was determined as follows. We took the point where the spectral intensity was 1 % of the band maximum over the threshold region as the onset of the band. Then the I_{Pth} was obtained by adding 0.15 eV to the onset. 0.15 eV (0.148 ± 0.017 eV) is the average distance between the onset and the first vibrational peak of the band for those molecules which display vibrational progressions. Bandwidth δ was determined from the full width at half-maximum (FWHM) of the first band. When the band displayed vibrational fine structure, the δ was read from the FWHM of the envelope connecting vibrational peaks. Though the accuracies of I_P and δ depend on the band shape, we believe that they are better than 0.02 eV.

2.3 Results and Discussion

2.3.1 Spectra Observed

The first band of UPS of ammonia is shown in Fig. 2.1 and those of various alkylamines are shown in Figs. 2.2-2.7: The first bands of primary amines are collected in Figs. 2.2 and 2.3; those of secondary amines in Fig. 2.4 and 2.5; those of tertiary amines in Figs. 2.6 and 2.7. The full

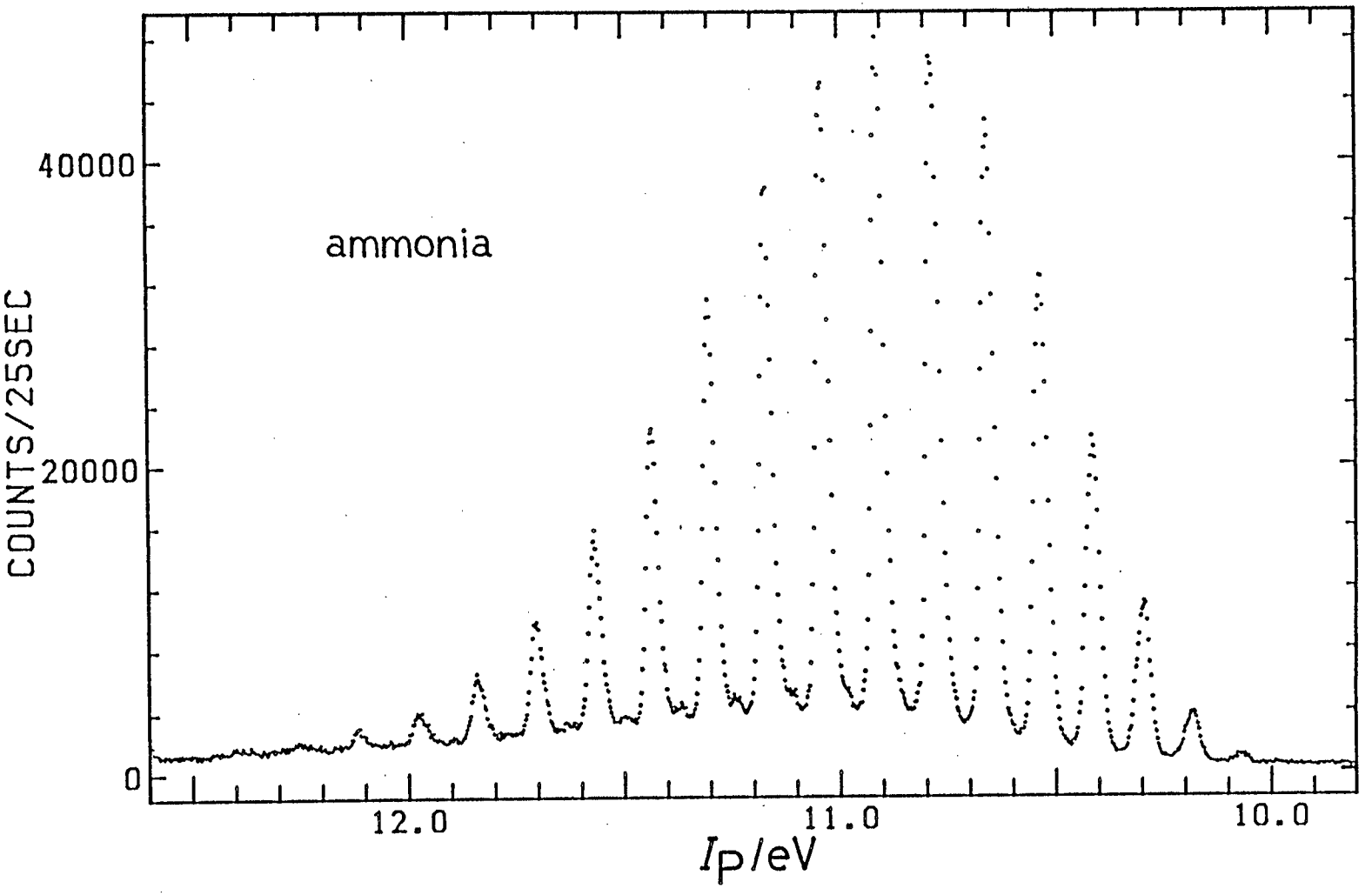

Fig. 2.1. First band of the UPS for ammonia.

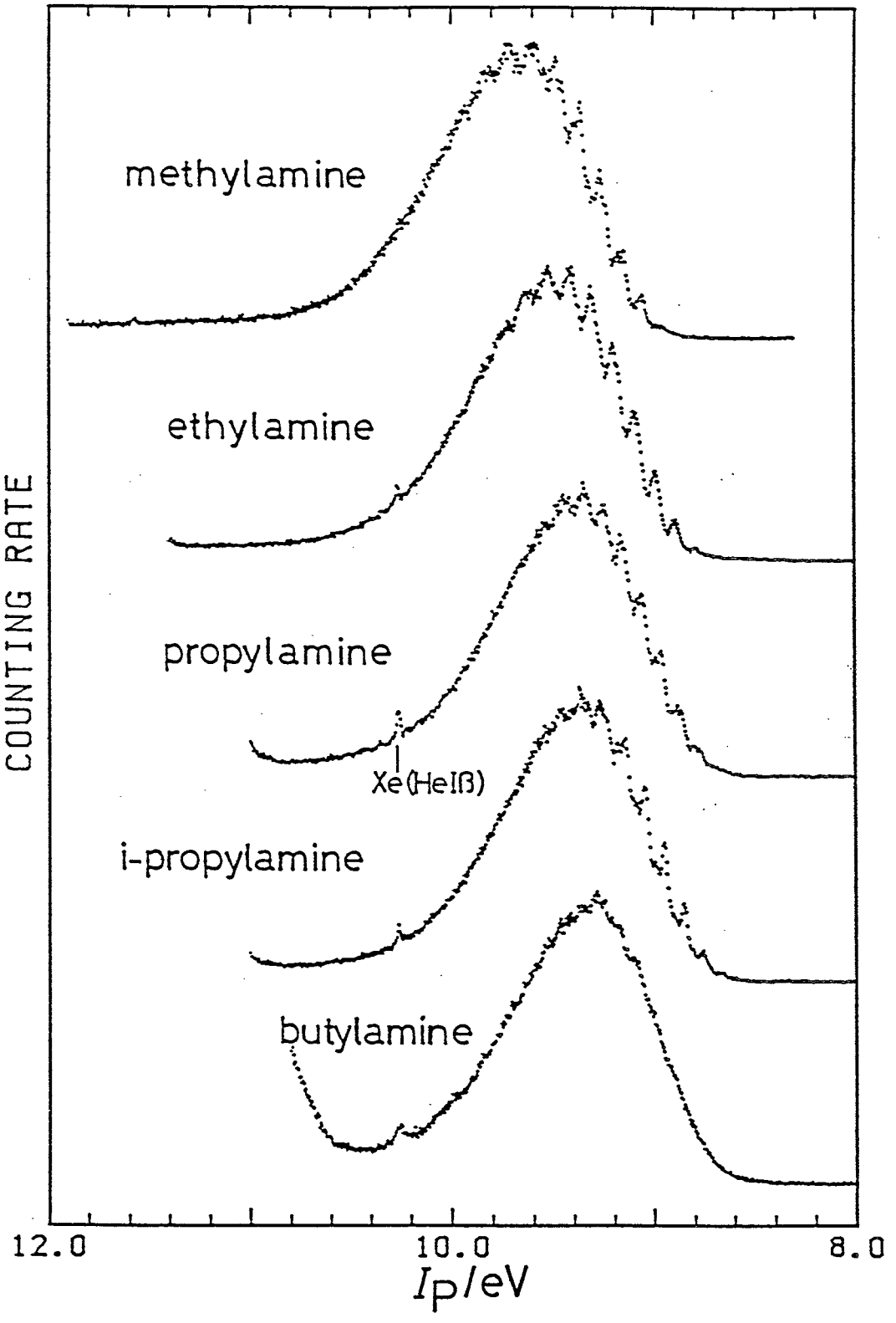

Fig. 2.2. First bands of the UPS for several primary alkylamines.

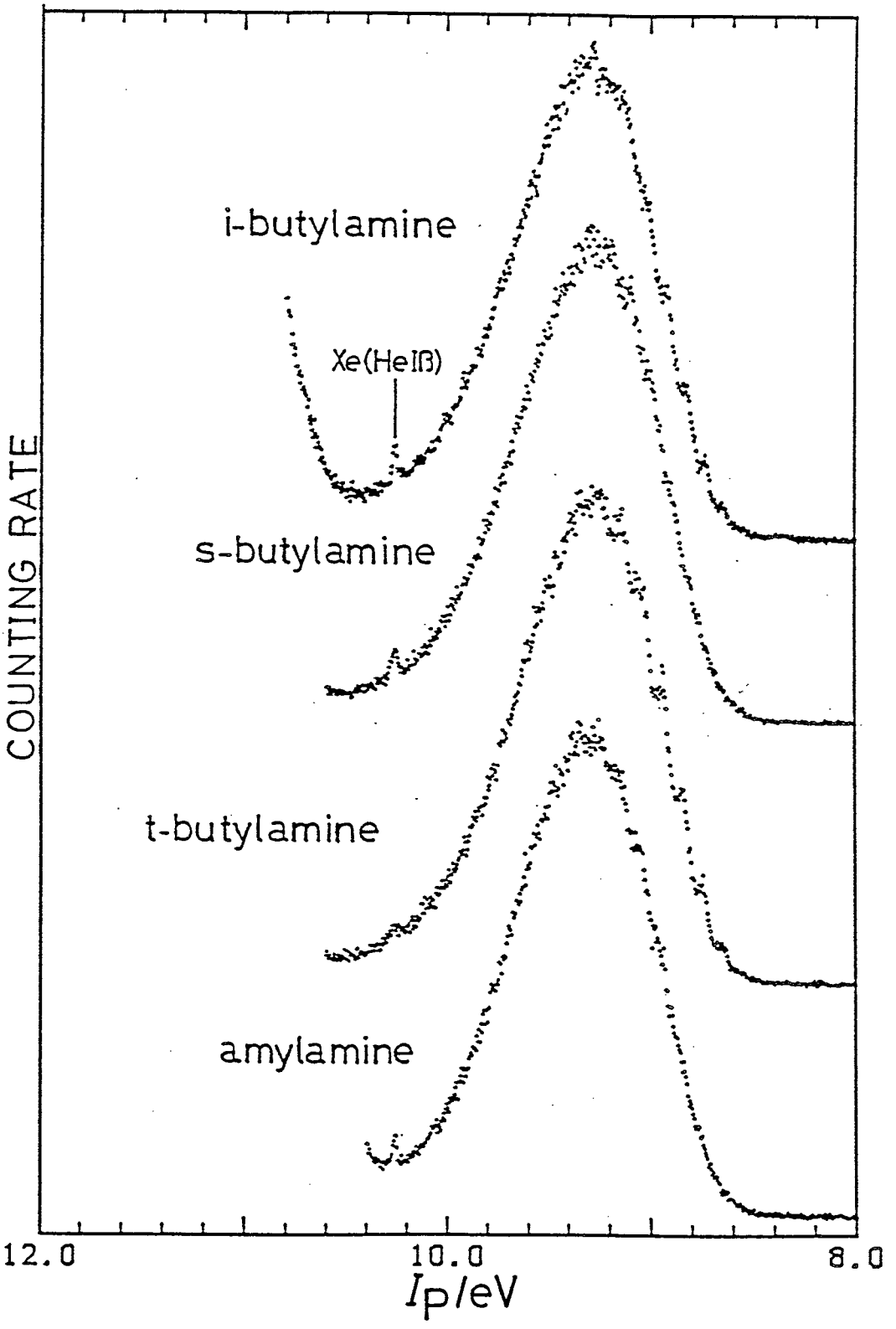

Fig. 2.3. First bands of the UPS for several primary alkylamines.

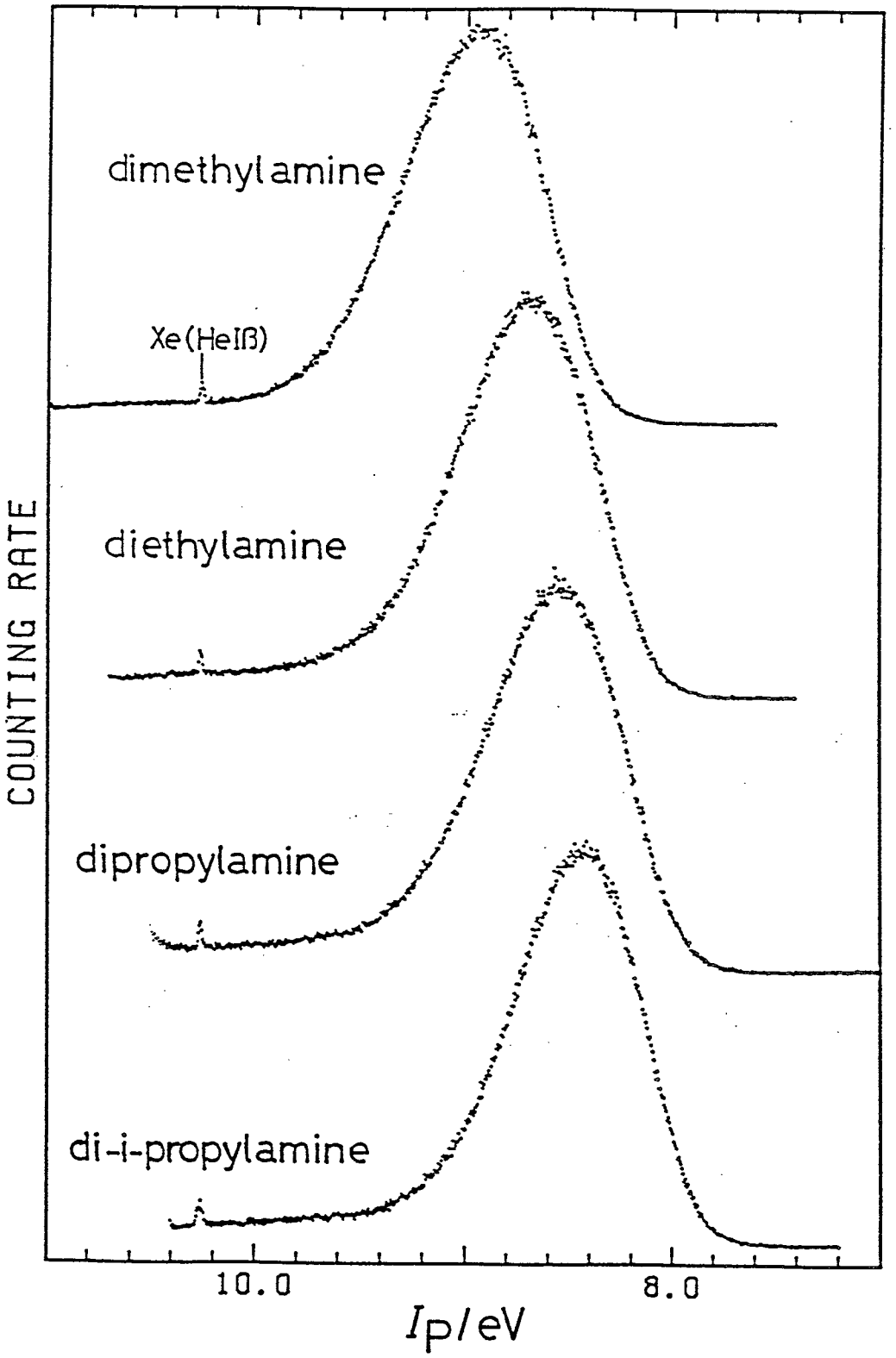

Fig. 2.4. First bands of the UPS for several secondary alkylamines.

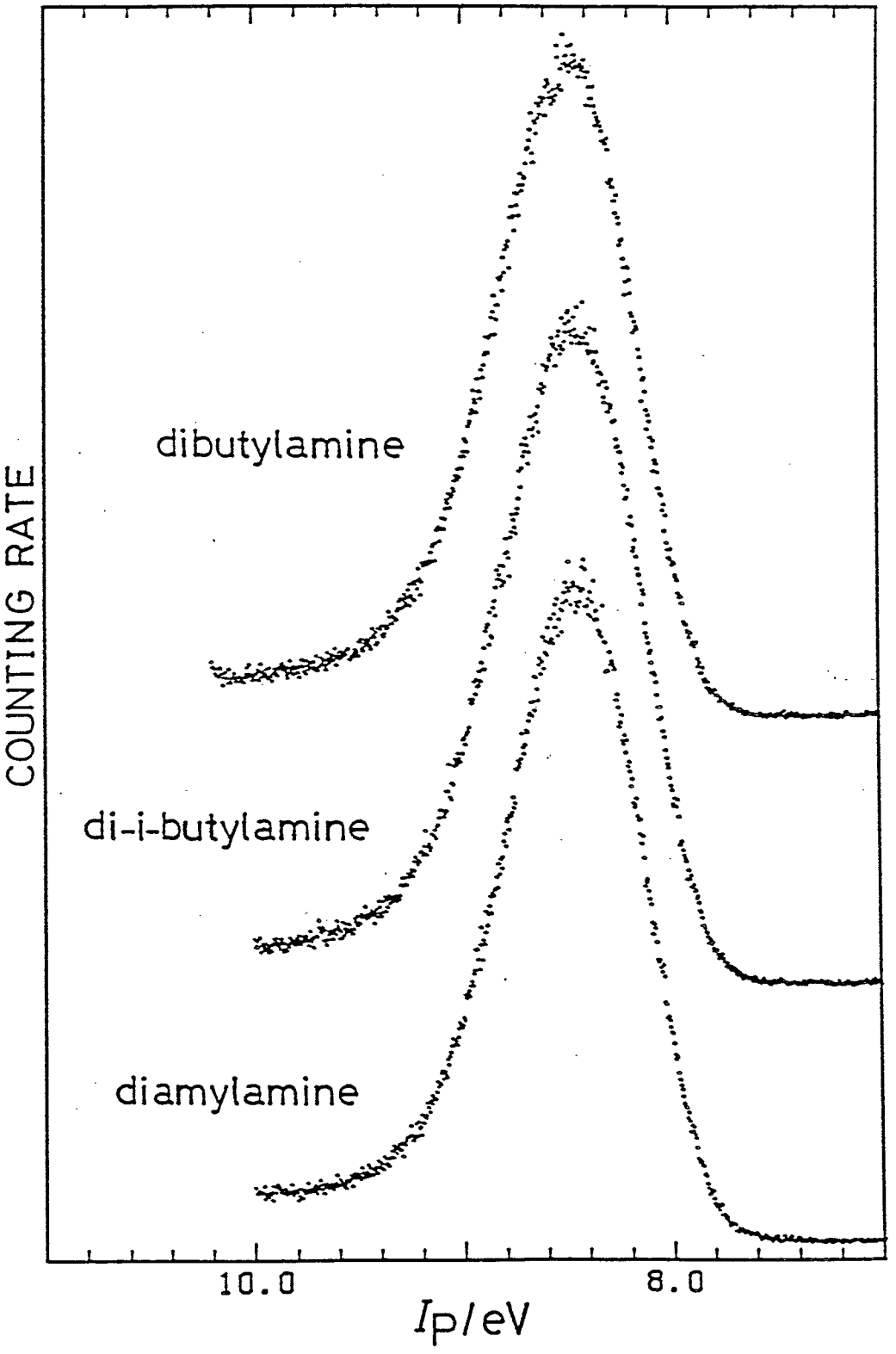

Fig. 2.5. First bands of the UPS for several secondary alkylamines.

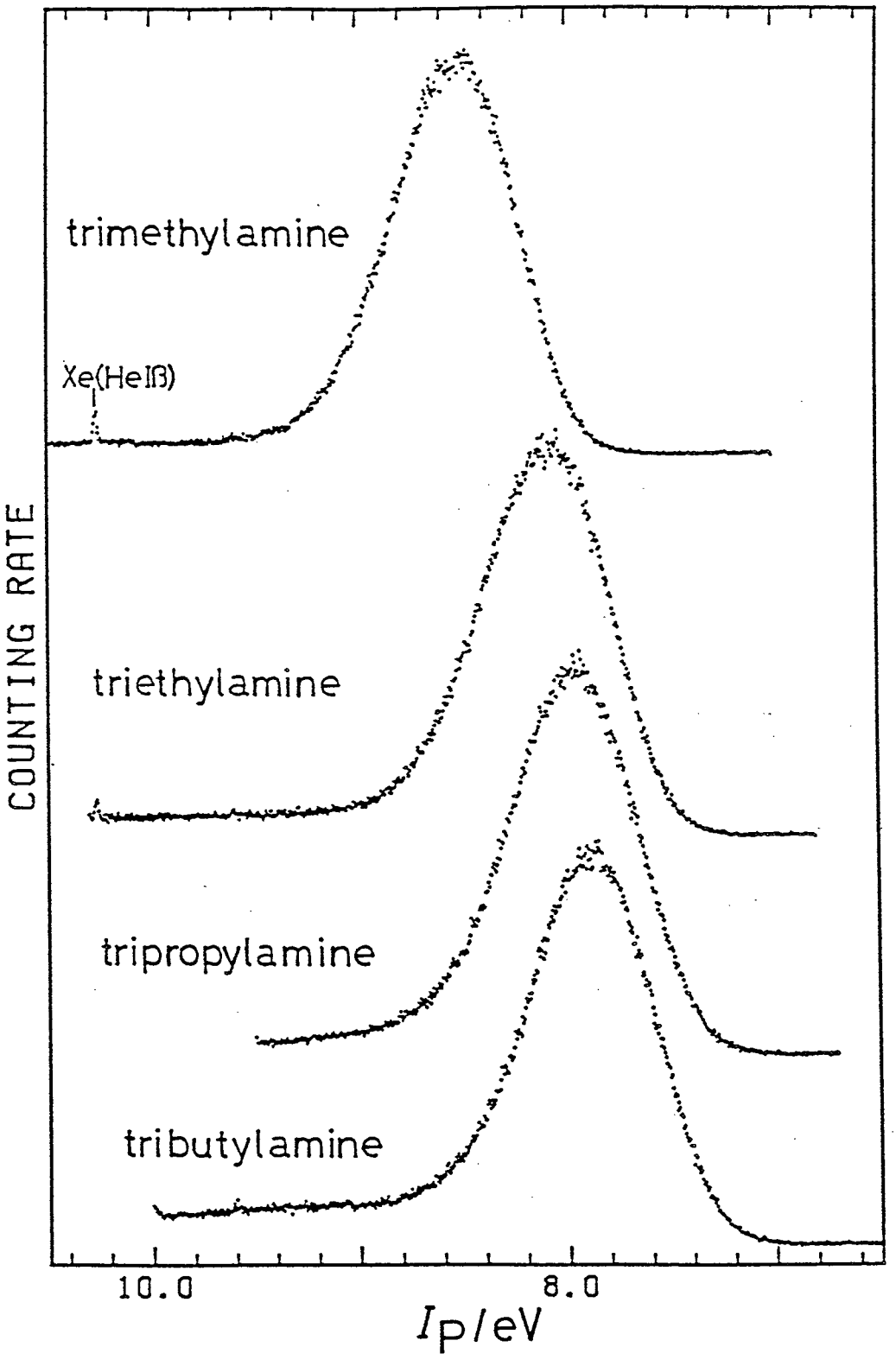

Fig. 2.6. First bands of the UPS for several tertiary alkylamines.

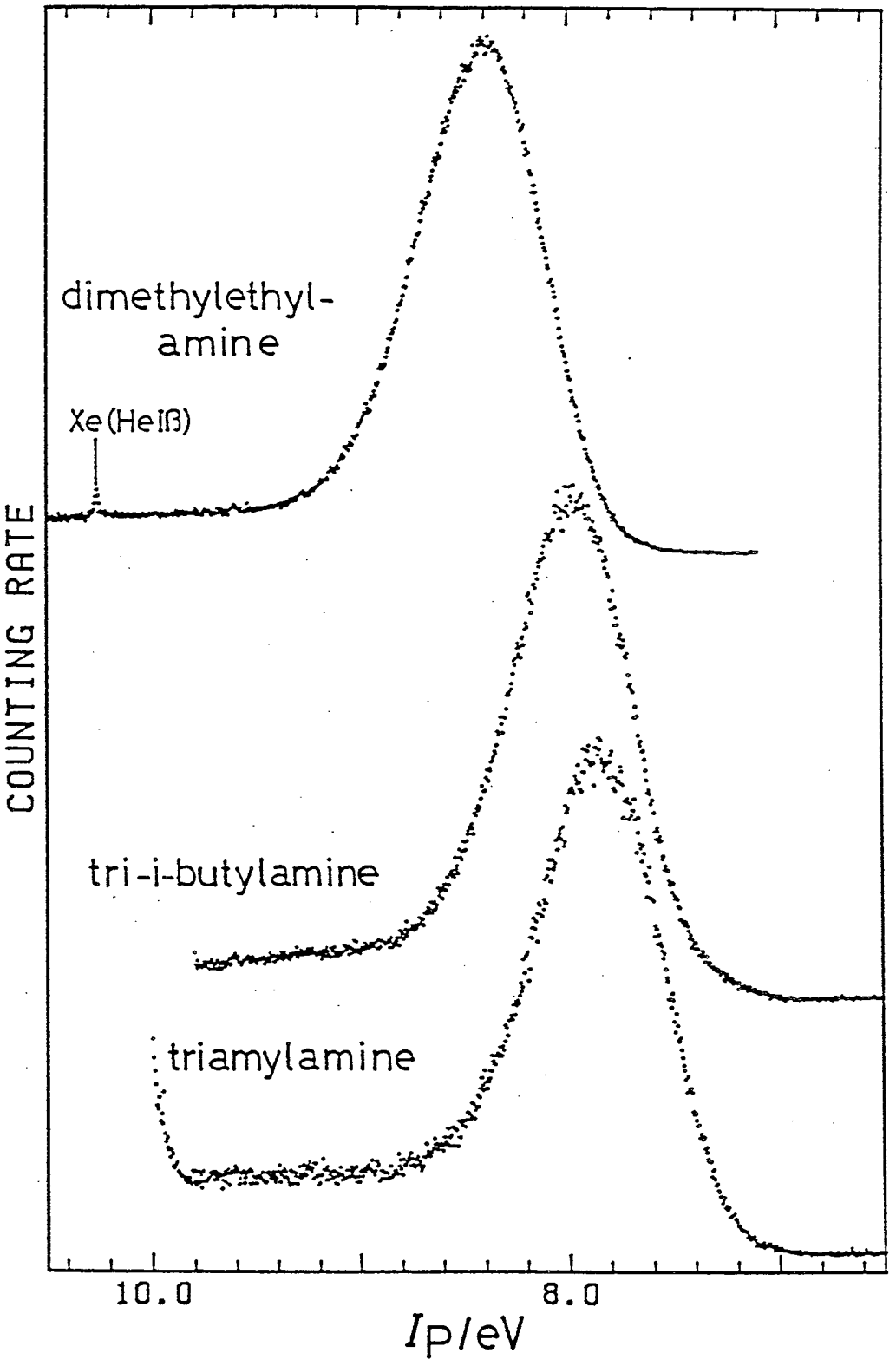

Fig. 2.7. First bands of the UPS for several tertiary alkylamines.

scan spectra are presented in appendix.

2.3.2 General Interpretation of the First Band

The first bands are broad and are ascribable to the photoionization of a 2p non-bonding electron on nitrogen. Vibrational progressions are observed in the first bands for all the primary amines. The first bands for some of the secondary and tertiary amines also have vibrational structures. The vibrational frequencies listed in Table 2.1 are to be comparable to the ones for the neutral state and will be discussed in the following chapter. The vibrational structures are composed almost entirely of angle deformation mode and the other vibrational modes are only slightly observable, e.g., in the case of ammonia,[4,7] i.e., the symmetric stretching vibration of NH, whose frequency is about three times that of the deformation vibration, is observed. The vibrational progressions show the negative anharmonicity for all compounds with well-resolved vibrational structure. This is because in the vibrations the restoring force does not become weaker as the amplitude increases, but is rather increased by steric interactions when the oscillating groups approach each other.

The first ionization peak 10.075 eV in the UPS of ammonia, observed also by several other workers,[2,4,7] has been regarded as the hot band.[2,4] However it has not yet

Table 2.1. Vertical I_{Pv} and Threshold I_{Pth} Ionization Potentials, Band Width δ, and Vibrational Frequencies, ν, for the First Bands

	Compound	I_{Pv}/eV	I_{Pth}/eV	δ/eV	ν/cm^{-1}
1	ammonia	10.90	10.08	0.95	900
2	methylamine	9.64	8.95	0.90	880
3	ethylamine	9.46	8.78	0.87	850
4	propylamine	9.34	8.68	0.85	770
5	*i*-propylamine	9.36	8.66	0.85	790
6	butylamine	9.29	8.59	0.84	(∿810)
7	*i*-butylamine	9.28	8.63	0.83	770
8	*s*-butylamine	9.27	8.60	0.81	740
9	*t*-butylamine	9.25	8.56	0.82	800
10	amylamine	9.30	8.61	0.81	(∿780)
11	dimethylamine	8.94	8.18	0.79	(∿520)
12	diethylamine	8.67	7.99	0.78	(∿310)
13	dipropylamine	8.55	7.80	0.77	(∿600)
14	diisopropylamine	8.42	7.75	0.75	
15	dibutylamine	8.49	7.74	0.79	
16	diisobutylamine	8.47	7.73	0.79	
17	diamylamine	8.45	7.68	0.78	

Table 2.1. (*continued*.)

18 trimethylamine	8.51	7.79	0.70	(∿400)
19 triethylamine	8.09	7.37	0.72	(∿280)
20 tripropylamine	7.94	7.18	0.72	(∿320)
21 tributylamine	7.88	7.15	0.72	
22 triisobutylamine	7.98	7.14	0.70	
23 triamylamine	7.85	7.11	0.72	
24 dimethylethylamine	8.39	7.61	0.73	

The following data are ionization potentials determined by other workers. I_{Pa}'s are in parentheses. Ammonia; (10.16),[1] 10.85 (10.16),[2] 10.85,[3] 10.88 (10.15),[4] (10.25),[5] (10.13),[6] (10.073),[7] 10.8 (10.073),[9]. Methylamine; (9.18),[1] 9.45 (8.80),[10] 9.67 (8.89),[2] 9.58,[11,12] 9.64,[13,14] 9.66 (9.08),[15] 9.7,[16] 9.65,[17]. Ethylamine; (9.19),[1] 9.44,[18] 9.47 (8.76),[2] 9.50,[12,13,19]. Propylamine; 9.41 (8.55),[2] 9.44,[13] 9.37,[20]. *i*-Propylamine; (8.86),[1] 9.32 (8.63),[2] 9.31,[13]. Butylamine; (8.79),[1] 9.40,[13]. *i*-Butylamine; 9.31 (8.50).[4] *s*-Butylamine; 9.31 (8.46).[2] *t*-Butylamine; (8.83),[1] 9.26 (8.46).[2] Dimethylamine; (8.36),[1] 8.93 (8.25),[10] 8.96 (8.07),[21] 8.93 (8.16),[2] 8.85,[22] 8.94 (8.30),[15] 8.97,[14] 8.95,[3] 8.9.[16] Diethylamine; (8.51),[1] 8.63 (7.85),[2] 8.68.[22] Dipropylamine; 8.54 (7.77),[2]

Table 2.1 (*continued*.)

8.59.[20] Diisopropylamine; 8.40 (7.59).[2] Trimethylamine; (8.12),[1] 8.54 (7.83),[10] 8.45,[3,23] 8.53 (7.77),[2] 8.47,[11,24] 8.55,[25] 8.54,[26] 8.50 (7.88),[15] 8.44,[14] 8.5.[16] Triethylamine; (7.84),[1] 8.19,[18] 8.08 (7.11),[2] 8.08.[27] Tripropylamine; 7.92 (7.03),[2] 8.04,[20] 7.94.[27] Tributylamine; 7.90 (6.98),[2] 7.80.[27]

been assured and the instance is discussed in the next chapter.

2.3.3 Alkyl Substitution Effect on Ionization Potential and Band Width

The I_{Pv} and the I_{Pth} for alkylamines decrease in the order of primary, secondary and tertiary as shown in Fig. 2.8. They also decrease with the length of alkyl group from the methyl to the propyl and level off. The successive decrease in ionization potential up to propyl substitution indicates that for small alkyl groups, the cationic state is stabilized to a greater extent than the neutral state by the introduction of a methylene group. It is a case for a series of aliphatic alcohols, in which the I_p values continue to decrease up to butyl substitution.[28] It seems that oxygen atom being more electronegative than nitrogen exhibits electron attracting effect extending to longer range in alcohol than that in amine.

The band width δ of the first band decreases in the order of primary, secondary, and tertiary amine as shown in Fig. 2.9. And in this order tailing to the higher I_p decreases, too. The systematic decrease of δ with the length of alkyl group is also indicated. However there is unexpected behavior of I_p shown in the same figure that the value of $\Delta I_{Pv,th}$, the difference between I_{Pv} and I_{Pth}, does

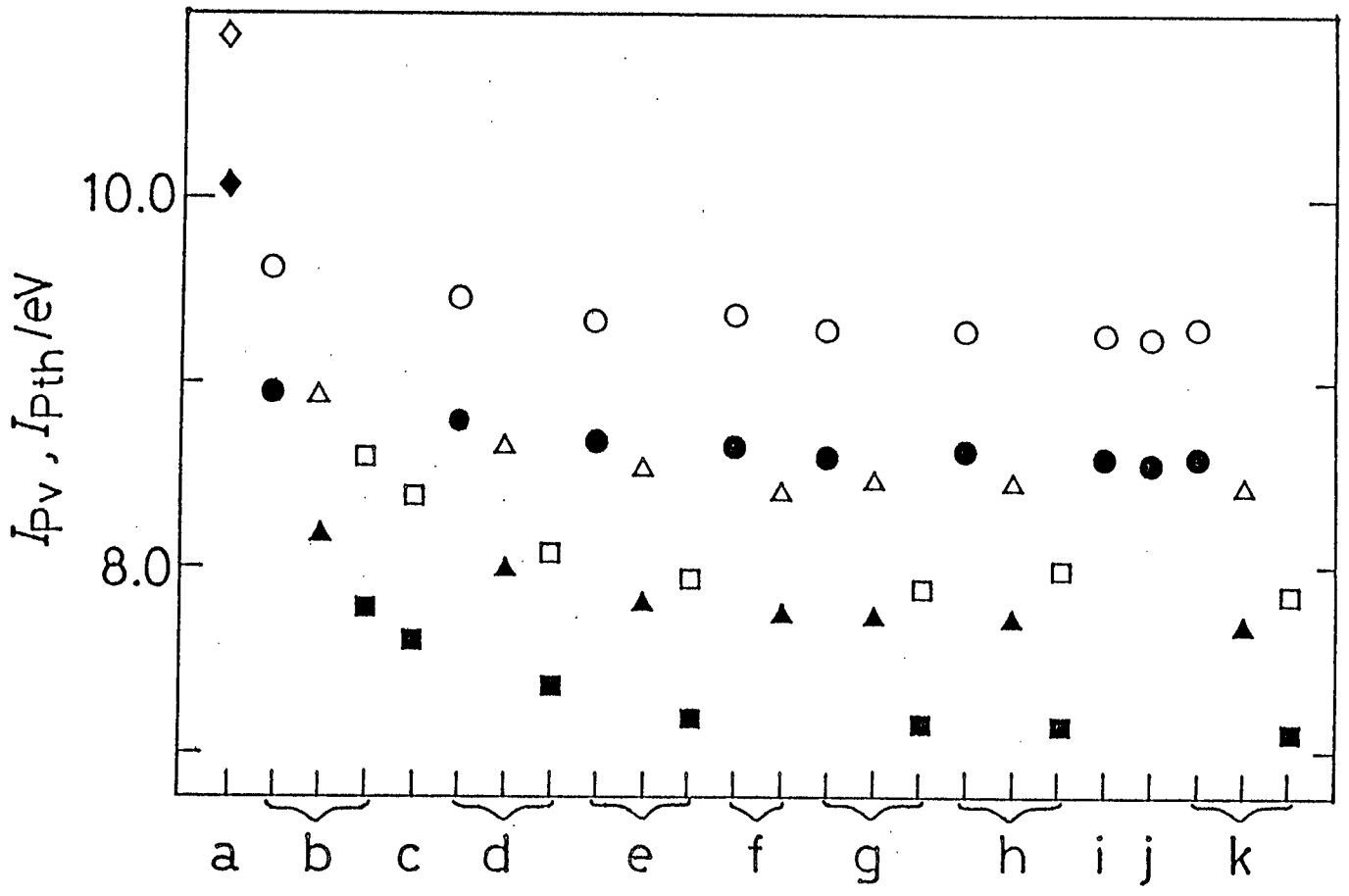

Fig. 2.8. Alkyl Substitution effect on I_{Pv} (open marks) and I_{Pth} (closed marks). Primary amines(○), secondary amines(△), tertiary amines(□), and ammonia(◇), (a) ammonia, (b) methyl-, (c) dimethylethyl-, (d) ethyl-, (e) propyl-, (f) isopropyl-, (g) butyl, (h) isobutyl-, (i) *s*-butyl-, (j) *t*-butyl-, and (k) amyl-.

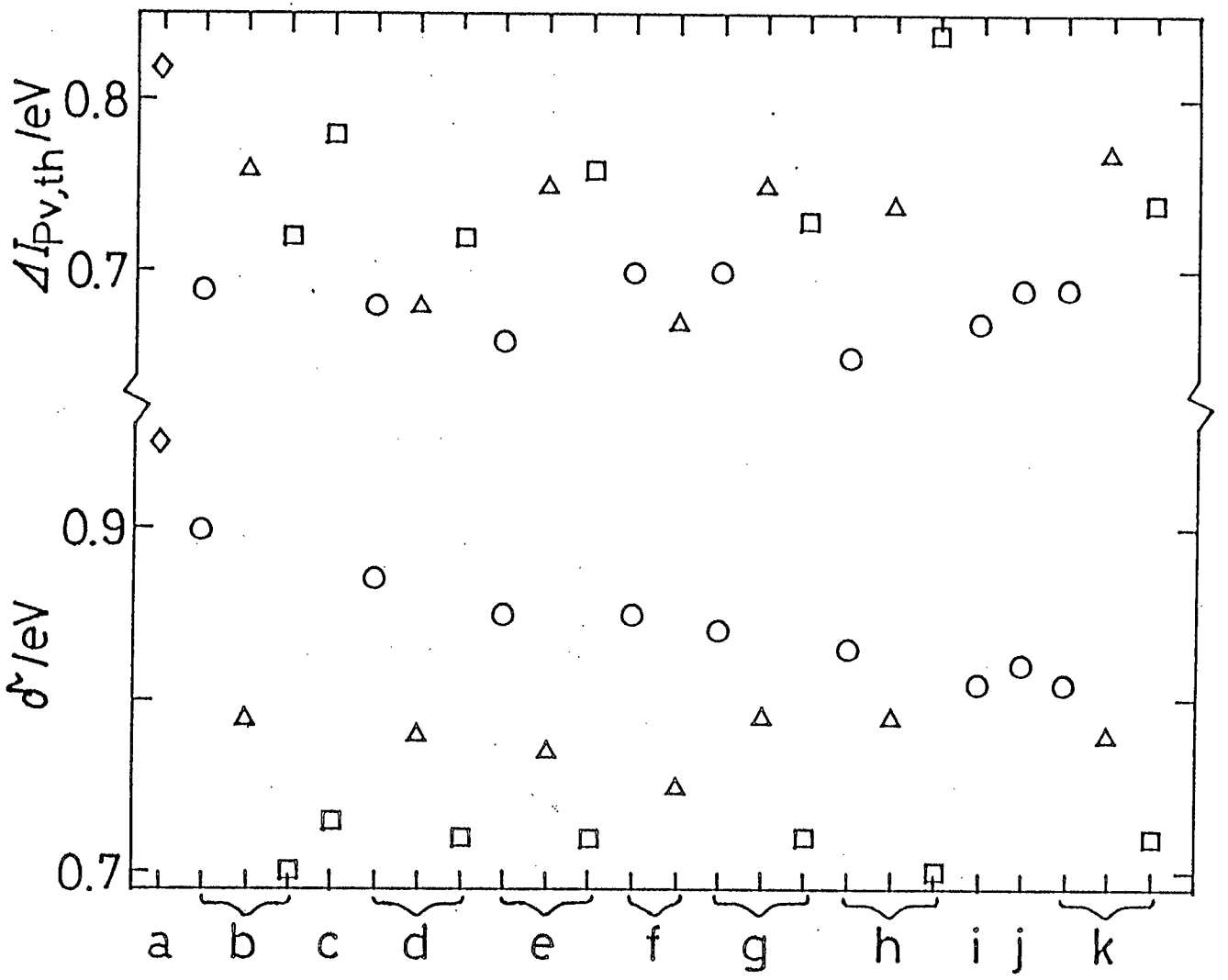

Fig. 2.9. Alkyl Substitution effect on $\Delta I_{Pv,th}$ and δ. Marks are the same as in Fig. 2.8.

not exhibit such trend against the alkyl substitution. The behavior of $\Delta I_{Pv,th}$ will be discussed in the following chapter.

2.3.4 Geometry and Band Width or Difference between Vertical Ionization Potential and Threshold Ionization Potential

Paying attention to δ and $\Delta I_{Pv,th}$ for the secondary amines, both for diisopropylamine are the lowest values. There is a bulky group at the α-carbon of alkyl group for diisopropylamine and then the difference in the geometries of nitrogen skeleton between the neutral and the cationic state for diisopropylamine may be not so large, judging from general considerations. Further δ values for the tertiary amines are almost similar, so the geometries of nitrogen skeleton in the tertiary amines may be less different, too. One must notice there is quite resolved vibrational structure in the first band of *t*-butylamine and it becomes worse resolved in the order of *i*-butylamine, butylamine, and *s*-butylamine within butyl-substituted primary amines. Besides, one peak in the first band of *i*-propylamine is sharper than that of propylamine. These seem to occur because of steric hindrance on α-carbon due to substituting second or third hydrogen by the methyl group. The vibrational fine structure becomes less resolved if a coupling of a vibrational mode with other vibrational mode

increases. One may expect that for *t*-butylamine barrier to rotation around the N-C axis is lowerer than for other butylamine isomers or for other simpler amines. However the barrier for *t*-butylamine is 0.10 eV[29] while that for methylamine is 0.09 eV[29,30] and then it is never considered that the former is expressly high. Therefore it may be considered that well resolved vibrational structure is observed for hardness of the above-mentioned coupling for those amines.

References

[1] M. I. Al-joboury and D. W. Turner, *J. Chem. Soc.*, 1964, 4434.

[2] D. H. Aue, H. M. Webb, and M. T. Bowers, *J. Am. Chem. Soc.*, 98, 311 (1976).

[3] H. Daamen and A. Oskam, *Inorg. Chim. Acta*, 26, 81 (1978).

[4] A. W. Potts and W. C. Price, *Proc. R. Soc. Lond.*, A326, 181 (1972).

[5] K. Watanabe, *J. Chem. Soc.*, 22, 1564 (1954).

[6] E. C. Y. Inn, *Phys. Rev.*, 91, 1194 (1953).

[7] J. W. Rabalais, L. Karlsson, L. O. Werme, T. Bergmark, and K. Siegbahn, *J. Chem. Phys.*, 58, 3370 (1973).

[8] G. Bieri, L. Åsbrink, and W. V. Niessen, *J. Electron Spectrosc. Relat. Phenom.*, 27, 129 (1982).

[9] M. J. Weiss and G. M. Lawrence, *J. Chem. Phys.*, 53, 214 (1970).

[10] J. P. Maier and D. W. Turner, *J. Chem. Soc. Faraday Trans* 2, 1973, 521.

[11] T. Kobayashi, *Phys. Lett. A.*, 69, 105 (1978).

[12] C. Utsunomiya, T. Kobayashi, and S. Nagakura, *Bull. Chem. Soc. Jpn.*, 53, 1216 (1980).

[13] S. Katsumata, T. Iwai, and K. Kimura, *Bull. Chem. Soc. Jpn.*, 46, 3391 (1973).

[14] K. Kimura and K. Osafune, *Mol. Phys.*, 29, 1073 (1975).

[15] V. I. Vovna and F. I. Vilesov, *Opt. Spectrosk.*, **36**, 463 (1974).

[16] A. B. Conford, D. C. Frost, F. G. Herring, and C. A. McDowell, *Can. J. Chem.*, **49**, 1135 (1971).

[17] H. Ogata, H. Onizuka, Y. Nihei, and H. Kamada, *Chem. Lett.*, **1972**, 895.

[18] S. Leavell, J. Steichen, and J. L. Franklin, *J. Chem. Phys.*, **59**, 4343 (1973).

[19] H. Ogata, H. Onizuka, Y. Nihei, and H. Kamada, *Bull. Chem. Soc. Jpn.*, **46**, 3036 (1973).

[20] J. B. Peel and G. D. Willett, *Aust. J. Chem.*, **30**, 2571 (1977).

[21] W. R. Cullen, G. D. Frost, and W. R. Leeder, *J. Fluorine Chem.*, **1**, 227 (1971/1972).

[22] S. G. Gibbins, M. F. Lappert, J. B. Pedley, and G. J. Sharp, *J. Chem. Soc., Dalton Trans.*, **1975**, 72.

[23] D. R. Lloyd and N. Lynaugh, *J. Chem. Soc., Faraday Trans. 2*, **1972**, 947.

[24] R. F. Lake, *Spectrochim. Acta*, **A27**, 1220 (1971).

[25] M. E. Akopyan and Y. V. Loginov, *Opt. Spectrosk.*, **37**, 442 (1974).

[26] S. Elbel, H. Bergmann, and W. Enβlin, *J. Chem. Soc., Faraday Trans. 2*, **1974**, 555.

[27] C. Utsunomiya, T. Kobayashi, and S. Nagakura, *Chem. Phys. Lett.*, **39**, 245 (1976).

[28] A. D. Baker, D. Betteridge, N. R. Kemp, and R. E. Kirby, *Anal. Chem.*, **43**, 375 (1971).

[29] M. Tsuboi, A. Y. Hirakawa, and K. Tamagake, *Nippon Kagaku Zasshi*, **89**, 821 (1968).

[30] K. Tamagake, M. Tsuboi, and A. Y. Hirakawa, *J. Chem. Phys.*, **48**, 5536 (1968).

Chapter 3. Band Shape of the UPS for Several Alkylamines

3.1 Introduction

Though numerous investigations on UPS for free molecules have been executed, most of them have been concerned only with thier ionization energies. The information contained in the band shape of the UPS has received special attention in this study. The attention has been paid to the first band of the UPS corresponding to the ionization of the HOMO electron which must play the most important role in regard to the chemical reactivity of the molecule. The band shape of the UPS is affected by the degree of distortion of the molecular structure caused by the photoionization, viz., the larger the distortion, the wider the band width.[1)]

Nitrogen skeleton of amine on the neutral state is known to take pyramidal geometry[2-4)] and that of the cationic state is planar.[5-7)] Thus the equilibrium structure of the amine cation produced by ejecting the HOMO electron differs substantially from that of the neutral one. It results in the broad first band in the UPS and a long vibrational progression even though the HOMO is a non-bonding orbital consisting mainly of nitrogen 2p electron. In order to discuss the band feature of the UPS, the Franck-

Condon factor for the transition from the neutral to cationic potential energy surfaces is necessary. The Franck-Condon factors were calculated and reported for simple molecules[8-12] by many workers. The calculations for ammonia were also performed and the first band of its UPS was theoretically obtained.[13-15] However the potential energy surfaces of neutral alkylamines and the corresponding cations are far more complex and have not yet been calculated due to the large number of intramolecular degrees of freedom.

One must also pay attention to whether the adiabatic ionization potential, I_{Pa}, can be determined from the UPS for the molecule which undergoes large change in the geometry after the photoionization process. For ammonia it remains uncertain whether the lowest ionization peak in the vibrational progressions for the first band corresponds to I_{Pa} or not.[6,16] It is known that I_{Pa} is intrinsically unobservable for in the case of water dimer molecule [17-19] and rare-gas van der Waals molecules.[11,12]

In this chapter, ab initio MO calculations for ammonia, the methylamines, and the ethylamines, with several different geometries both for the neutral and cationic state has been carried out and potential energy curves on the deformation coordinate of the bending vibration has beeen obtained. One can derive the theoretical photoelectron band

by using a simple Franck-Condon approach presented here. The band shape of UPS theoretically obtained will be compared with the UPS data experimentally obtained to test the validity of the present approach to understand the alkyl substitution effects on the band shape and ionization potentials.

3.2 Computational procedure

In the present chapter, ab initio MO calculations for ammonia, the methylamines, dimethylethylamine and the ethylamines has been performed. Calculations were carried out using the Gaussian 80 program and the IMSPACK program[20] with the minimal STO-3G basis set. For the cationic state, the open-shell calculations were performed with an unrestricted Hartree-Fock(UHF) procedure included in the programs.

The geometries for both neutral and cationic states were optimized by means of gradient method included in the Gaussian 80 program. The full-geometry optimization were carried out except for diethyl, dimethylethyl and triethyl amines, for which the structural parameters within ethyl group were fixed to the values optimized for ethylamine. The symmetries used for the calculations are; C_{3v} for ammonia and trimethylamine, C_3 for triethylamine, and C_s for

all the others and also ammonia and trimethylamine. The optimized geometries are described in Fig. 3.1, and the structural parameters obtained are listed in Table 3.1. The bond lengths and angles are in good agreement with those obtained experimentally and calculated by others.[21)]

As indicated in Table 3.1, the change in geometry of the cation from the neutral molecule is remarkable only in ψ or ϕ, which denotes the deformation angle as shown in Fig. 3.2. The first band of the UPS for the alkylamine has a very strong vibrational progression which corresponds to the deformation vibration. Thus a potential energy curve on the coordinate of ψ or ϕ, for the calculation of theoretical band shape of the UPS is choosen. Potential energy curves were also calculated by using the angles HNH for methylamine and CNC for dimethylamine as the reaction coordinate. During the calculations other structural parameters were fixed at the optimized values for the neutral state.

3.3 Derivation of *GF* Matrix Element

3.3.1 General Consideration for Molecular Vibration

A frequency of molecular vibration is decided by both the kinetic energy T and the potential energy V. The kinetic energy is expressed by the cartesian coordinates,

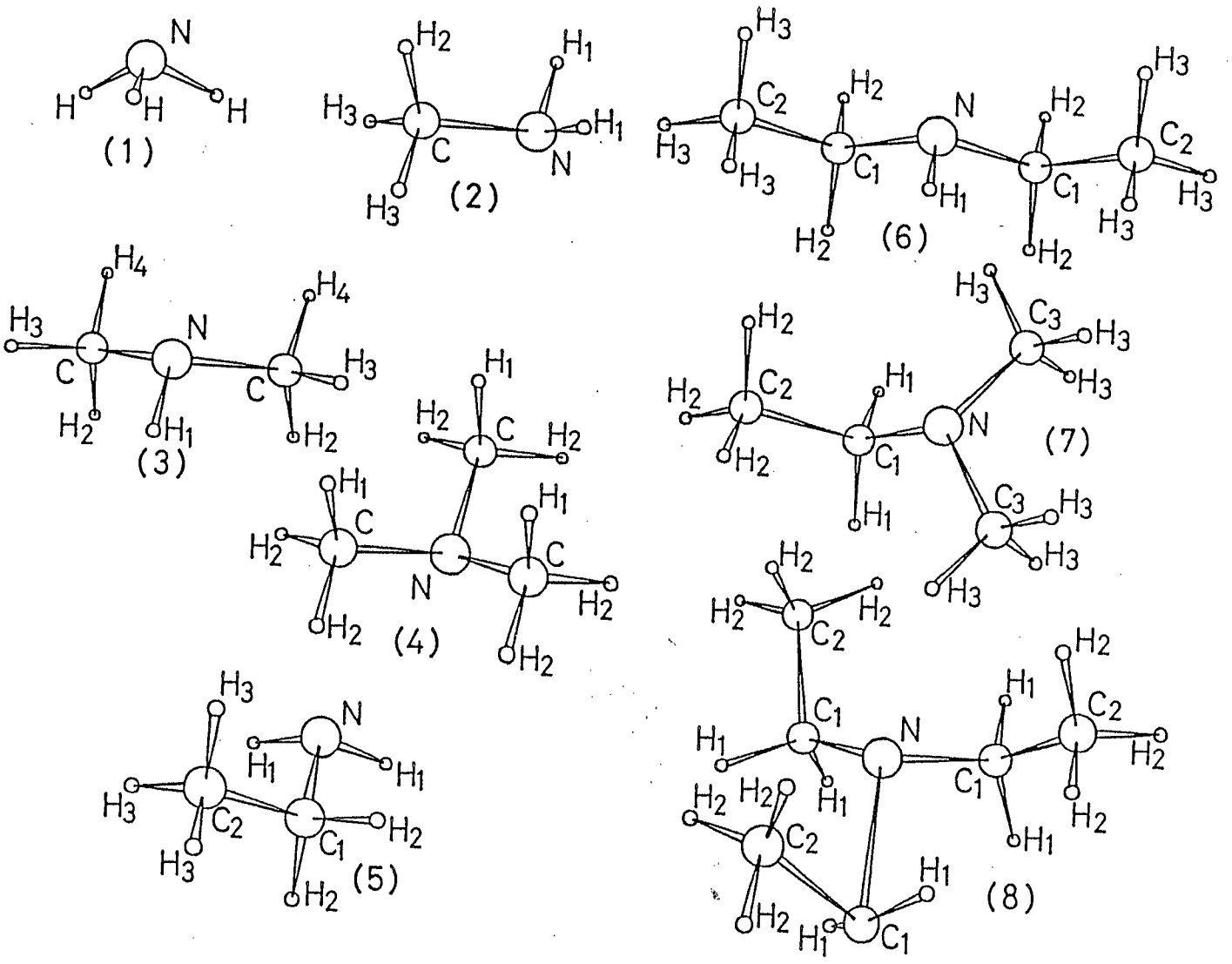

Fig. 3.1. Molecular geometries used for calculations for ammonia (1), methylamine (2), dimethylamine (3), trimethylamine (4), ethylamine (5), diethylamine (6), dimethylethylamine (7), and triethylamine (8).

Table 3.1. Optimized Structural Parameters and Total Energy

(Bond-length in nm, Bond-angle in degree, and Energy in a.u.)

	Neutral state	Cationic state
ammonia		
N-H	0.1033	0.1056
	(0.1006)	
ϕ	24.4	0.0
	(0.0)	
Total energy	-55.4554	-55.2070
	(-55.4377)	
methylamine		
N-C	0.1486	0.1509
	(0.1449)	
$N-H_1$	0.1033	0.1054
	(0.1009)	
$C-H_2$	0.1093	0.1098
	(0.1096)	
$C-H_3$	0.1089	0.1093
	(0.1091)	
H_2-C-N	113.7	106.6
	(113.6)	

Table 3.1. (*continued.*)

H_3-C-N	109.1	107.9
	(110.2)	
H_1-N-H_1 (η)	104.4	116.4
	(118.2)	
ψ	60.9	0.0
	(0.0)	
Total energy	-94.0329	-93.8167
	(-94.0162)	
dimethylamine		
N-C	0.1485	0.1506
	(0.1452)	
N-H_1	0.1034	0.1053
	(0.1011)	
C-H_2	0.1091	0.1093
	(0.1095)	
C-H_3	0.1089	0.1095
	(0.1089)	
C-H_4	0.1091	0.1093
	(0.1095)	

Table 3.1. (*continued.*)

H_2-C-N	113.4	108.7
	(112.1)	
H_3-C-N	109.0	107.4
	(109.4)	
H_4-C-N	109.2	107.4
	(111.8)	
C-N-C (η)	111.2	125.8
	(121.2)	
ψ	59.0	0.0
	(0.0)	
Total energy	-132.6122	-132.4215
	(-132.5968)	
trimethylamine		
N-C	0.1485	0.1508
	(0.1457)	
C-H_1	0.1094	0.1094
	(0.1096)	
C-H_2	0.1089	0.1091
	(0.1090)	
H_1-C-N	113.0	107.4
	(113.1)	

Table 3.1. (*continued.*)

H_2-C-N	109.3	108.6
	(110.1)	
ϕ	18.6	2.7
	(0.0)	
Total energy	-171.1919	-171.0214
	(-171.1755)	
ethylamine		
N-C_1	0.1490	0.1522
C_1-C_2	0.1541	0.1544
N-H_1	0.1033	0.1053
C_1-H_2	0.1093	0.1096
C_2-H_3	0.1086	0.1086
C_2-C_1-N	110.5	109.1
H_2-C_1-N	110.1	105.6
H_3-C_2-C_1	110.4	109.8
H-N-H (η)	104.4	116.2
ψ	61.5	0.0
Total energy	-132.6148	-132.4059
diethylamine		
N-H_1	0.1033	0.1052
N-C_1	0.1488	0.1519
C_1-C_2	0.1542	0.1541

Table 3.1. (*continued.*)

C_2-C_1-N	109.9	110.0
C_1-N-C_1 (η)	111.6	123.6
ψ	59.0	0.0
Total energy	-209.7757	-209.5970
dimethylethylamine		
N-C_1	0.1498	0.1510
C_1-C_2	0.1547	0.1552
N-C_3	0.1485	0.1500
C_2-C_1-N	110.6	108.0
C_3-N-C_3 (η)	110.2	119.0
ψ	49.9	1.4
Total energy	-209.7665	-209.6064
triethylamine		
N-C_1	0.1494	0.1523
C_1-C_2	0.1545	0.1547
C_2-C_1-N	111.1	111.6
φ	18.4	2.1
Total energy	-286.9283	-286.7754

ψ and φ are the angles defined in Fig. 3.2. Values in parenthesis are calculated for the planar form, i.e. ψ or φ=0°. The following parameters are fixed for the neutral and the cationic state respectively, for diethylamine(H_2-C_1; 0.1093 and 0.1096, H_3-C_2; 0.1086 and 0.1087, H_2-C_1-N; 110.5

Table 3.1. (*continued.*)

---

and 105.6, H_3-C_2-C_1; 110.5 and 110.0) and for triethylamine(C_1-H_1; 0.1093 and 0.1096, C_2-H_2; 0.1086 and 0.1087, H_1-C_1-N; 110.5 and 105.6, H_2-C_2-C_1; 110.5 and 110.0), and are fixed for both the neutral and the cationic states for dimethylethylamine(C_1-H_1; 0.1090, C_2-H_2; 0.1090, C_3-H_3; 0.1090, H_1-C_1-N; 110.0, H_2-C_2-C_1; 109.5, H_3-C_3-N; 110.0).

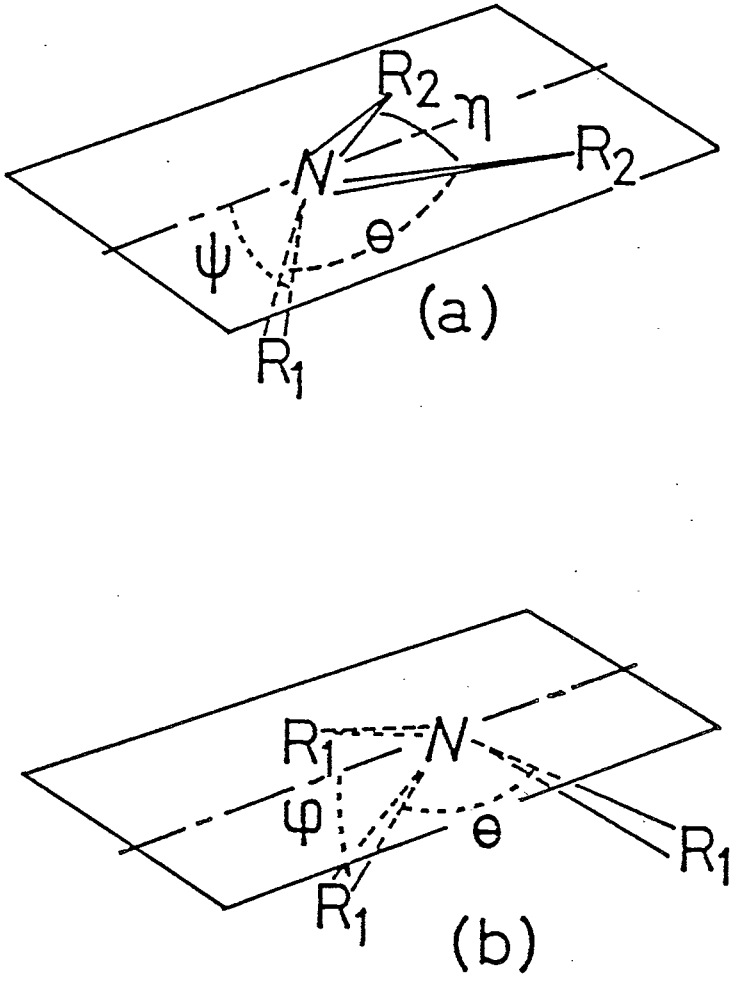

Fig. 3.2. Deformation angles and internal coordinates. R_1 and R_2 denote H, CH_3, or C_2H_5. (a) for C_s symmetry and (b) for C_3 and C_{3v}.

while the potential energy is expressed by the internal coordinates. Since there are only $3N$ degrees of freedom for a molecule of N atoms, there are six extra coordinates in the above coordinates. These six coordinates (for nonlinear molecules; while for linear molecules five coordinates) are removed by the separation of vibration, rotation and translation. Thus both the energies are given[22,23] by

$$2T=\sum_{i=1}^{3N}\dot{q}_i^2, \tag{3.1}$$

and

$$2V=2V_0+2\sum_{i=1}^{3N}f_i q_i+\sum_{i,j=1}^{3N}f_{i,j}q_i q_j+\text{ higher terms}, \tag{3.2}$$

in which the q_i's are mass-weighted cartesian displacement coordinates, the f_i's are constatnts given by

$$f_i=(\partial V/\partial q_i)_0, \tag{3.3}$$

and the $f_{i,j}$'s are constants given by

$$f_{i,j}=(\partial^2 V/\partial q_i \partial q_j)_0, \tag{3.4}$$

with $f_{i,j}=f_{j,i}$. As for the potential energy, V_0 may be eliminated by choosing the zero of energy so that the energy of the equilibrium configuration is zero. In addition, when all the q's are zero, the atoms are all in their equilibrium positions so that the energy must be a minimum for $q_i=0$, $i=1,2,\ldots 3N$, i.e.,

$$(\partial V/\partial q_i)_0=f_i=0 \quad i=1,2,\ldots 3N, \tag{3.5}$$

and that the higher terms can be neglected if amplitudes of

vibration are sufficiently small. Thus the potential energy is written by

$$2V=\sum_{i,j=1}^{3N} f_{i,j} q_i q_j . \qquad (3.6)$$

Now, considering a new set of coordinates, Q_k, $k=1,2,\ldots,3N$, called normal coordinates, the kinetic and potential energies have been translated as follows;

$$2T=\sum_{k=1}^{3N} \dot{Q}_k^2 , \qquad (3.7)$$

$$2V=\sum_{k=1}^{3N} \lambda_k' Q_k^2 . \qquad (3.8)$$

Where the normal coordinates Q's are defined in terms of the mass-weighted cartesian displacement coordinates q_i by the linear equations

$$Q_k=\sum_{i=1}^{3N} l''_{ki} q_i \qquad k=1,2,\ldots,3N, \qquad (3.9)$$

in which the coefficients l''_{ki} have been chosen so that in terms of the normal coordinates the kinetic and potential energies have the forms of Eqs. 3.7 and 3.8.

Then solving Newton's equations for each normal mode independently, wave numbers of vibrations are written by

$$\nu_k=(\lambda_k')^2/2\pi c. \qquad (3.10)$$

Thus a problem of normal vibration is solved.

3.3.2 Solution by the Use of Matrix---*GF* Matrix

Writing the equations mentioned in the previous section by matrixes, the expressions become simpler as follows. The potential energy V is expressed by both the matrix of the internal coordinates, R, and the matrix of the force constants, F

$$2V=\tilde{R}FR. \tag{3.11}$$

While the kinetic energy T is represented by both the cartesian coordinates, X, and the diagonal matrix of mass of each atom, M,

$$2T=\dot{\tilde{X}}M\dot{X}. \tag{3.12}$$

Where,

$$\dot{X}=\begin{pmatrix} \dot{x}_1 \\ \dot{y}_1 \\ \dot{z}_1 \\ \vdots \\ \dot{x}_N \\ \dot{y}_N \\ \dot{z}_N \end{pmatrix}, \qquad M=\begin{pmatrix} m_1 & & & & & & \\ & m_1 & & & & 0 & \\ & & m_1 & & & & \\ & & & \ddots & & & \\ & & & & m_N & & \\ & 0 & & & & m_N & \\ & & & & & & m_N \end{pmatrix}, \tag{3.13}$$

$$R=\begin{pmatrix} \Delta r_1 \\ \Delta r_2 \\ \vdots \\ \Delta r_n \end{pmatrix}, \qquad F=\begin{pmatrix} f_{11} & f_{12}\cdots f_{1n} \\ f_{21} & f_{22}\cdots f_{2n} \\ \vdots & \vdots \\ f_{n1} & f_{n2}\cdots f_{nn} \end{pmatrix}, \tag{3.14}$$

and in which $\tilde{X}$ and $\tilde{R}$ are transposed matrixs of X and R, respectively.

Hereupon, in order to connect the R and the X matrix B

defined in the way hereinafter prescribed may be introduced.

$$R=BX. \tag{3.15}$$

If the molecule does not rotate or undergoes translation, T is written in terms of the momenta, P,

$$2T=\tilde{P}GP, \tag{3.16}$$

where

$$G=BM^{-1}\tilde{B}. \tag{3.17}$$

While in terms of the normal coordinates, both T and V are expressed by

$$2T=\tilde{\dot{Q}}\dot{Q}, \tag{3.18}$$

$$2V=\tilde{Q}\Lambda Q, \tag{3.19}$$

In order to derive Eqs. 3.18 and 3.19 from Eqs. 3.11 and 3.16 the secular equation,

$$|GF-E\lambda|, \tag{3.20}$$

should be solved and eigen values, λ_1, λ_2,..., λ_n should be calculated. Thus finally each vibrational frequency is acquired.

3.3.3 Application to XYZ_2 Molecule with C_s Symmetry

In this study only deformation vibration has been considered, so the following internal coordinates are now adopted (Fig. 3.3a), i.e.,

$$R=\begin{pmatrix}\theta\\ \theta'\\ \eta\end{pmatrix}. \tag{3.21}$$

And

$$2V=\tilde{R}FR, \tag{3.22}$$

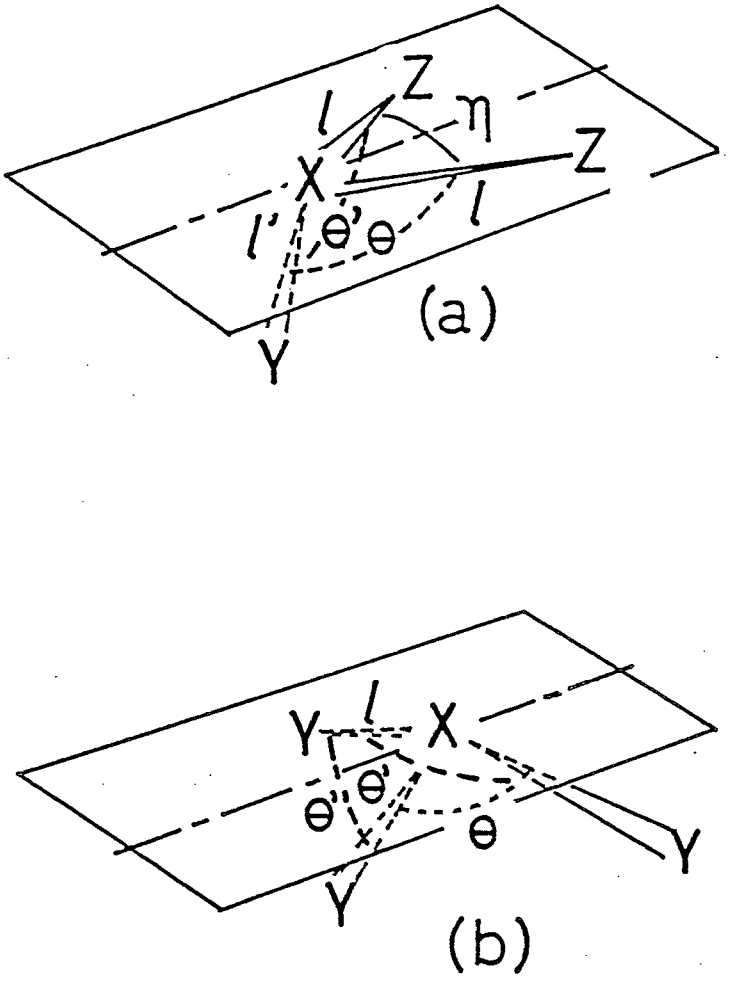

Fig. 3.3. Schematic drawings of internal coordinateds used in *GF* matrix method. (a) for XYZ_2 molecule with C_s symmetry, and (b) for XY_3 molecule with C_{3V} symmetry.

where
$$F=\begin{pmatrix}\theta\theta & \theta\theta' & \theta\eta\\ \theta\theta' & \theta\theta & \theta\eta\\ \theta\eta & \theta\eta & \eta\eta\end{pmatrix}=\begin{pmatrix}f_{11} & f_{12} & f_{13}\\ f_{12} & f_{11} & f_{13}\\ f_{13} & f_{13} & f_{33}\end{pmatrix}, \tag{3.23}$$

and
$$G=\begin{pmatrix}g_{11} & g_{12} & g_{13}\\ g_{12} & g_{11} & g_{13}\\ g_{13} & g_{13} & g_{33}\end{pmatrix}. \tag{3.24}$$

Replacing R to internal symmetry coordinate, R^{I}, i.e.,
$$R^{I}=\begin{pmatrix}(\Delta\theta+\Delta\theta')/\sqrt{2}\\ \Delta\eta\\ (\Delta\theta-\Delta\theta')/\sqrt{2}\end{pmatrix}, \tag{3.25}$$

where
$$R^{I}=U^{I}R, \tag{3.26}$$

and
$$U^{I}=\begin{pmatrix}1/\sqrt{2} & 1/\sqrt{2} & 0\\ 0 & 0 & 1\\ 1/\sqrt{2} & -1/\sqrt{2} & 0\end{pmatrix}, \tag{3.27}$$

then
$$F^{I}=U^{I}F\tilde{U}^{I}=\begin{pmatrix}f_{11}+f_{12} & \sqrt{2}f_{13} & 0\\ \sqrt{2}f_{13} & f_{33} & 0\\ 0 & 0 & f_{11}-f_{12}\end{pmatrix}, \tag{3.28}$$

and
$$G^{I}=U^{I}G\tilde{U}^{I}=\begin{pmatrix}g_{11}+g_{12} & \sqrt{2}g_{13} & 0\\ \sqrt{2}g_{13} & g_{33} & 0\\ 0 & 0 & g_{11}-g_{12}\end{pmatrix}. \tag{3.29}$$

Thus solving the determinant,
$$|G^{I}F^{I}-\lambda^{I}E|=0, \tag{3.30}$$

λ for $(\Delta\theta+\Delta\theta')$ is given by $(g_{11}+g_{12})(f_{11}+f_{12})$ and λ for η is by $g_{33}f_{33}$. Now the terms $(f_{11}+f_{12})$ and f_{33} are acquired from the potential energy curve calculated in this study.

And the terms $(g_{11}+g_{12})$ and g_{33} are calculated by using the method descrived in Ref. 23, i.e.,

$$g_{11}+g_{12}=(\cos\eta-\cos^2\theta)((1/l'-\cos\theta/l)^2/m_x+1/l'^2m_y)/\sin^2 2\theta$$
$$+\sin^2\theta/l^2m_x+1/l^2m_z+1/l'^2m_y$$
$$+(1/l^2+1/l'^2-2\cos\theta/ll')/m_x, \qquad (3.31)$$

and
$$g_{33}=2/l^2(m_y+(1-\cos\eta)/m_x), \qquad (3.32)$$

where m_i is mass of i-th atom.

3.3.4 Application to XY_3 molecule with C_{3v} symmetry

Using the following coordinates as the internal coordinates (Fig. 3.3b), i.e.,

$$\boldsymbol{R}=\begin{pmatrix}\Delta\theta\\ \Delta\theta'\\ \Delta\theta''\end{pmatrix}, \qquad (3.33)$$

and using the following coordinates as the internal symmetric coordinates, i.e.,

$$\boldsymbol{R}^{\mathrm{I}}=\begin{pmatrix}(\Delta\theta+\Delta\theta'+\Delta\theta'')/\sqrt{3}\\ (2\Delta\theta-\Delta\theta'-\Delta\theta'')/\sqrt{6}\\ (\Delta\theta'-\Delta\theta'')/\sqrt{2}\end{pmatrix}, \qquad (3.34)$$

the secular equation, $|\boldsymbol{G}^{\mathrm{I}}\boldsymbol{F}^{\mathrm{I}}-\lambda^{\mathrm{I}}\boldsymbol{E}|=0$ is derived. Then solving the equation, λ is given. V is expressed by

$$2V=\tilde{\boldsymbol{R}}\boldsymbol{F}\boldsymbol{R}$$
$$=f_1((\Delta\theta+\Delta\theta'+\Delta\theta'')/\sqrt{3})^2$$
$$+f_2((2\Delta\theta-\Delta\theta'-\Delta\theta'')/\sqrt{6})^2$$
$$+f_2((\Delta\theta'-\Delta\theta'')/\sqrt{2})^2$$

$$=2V_1+2V_2+2V_3. \qquad (3.35)$$

As considering symmetric deformation vibration in this study, the potential energy curve calculated is V_1 and $\Delta\theta=\Delta\theta'=\Delta\theta''$. Then correponding G element, g_1, is given by

$$g_1=2(1/m_y+(1-\cos\theta)/m_x)/l^2 +2((1-\cos\theta)^3\cos\theta/\sin^2\theta/m_x+\sin^2\theta/m_x +(1-\cos\theta)\cos\theta/m_y/\sin^2\theta)/l^2. \qquad (3.36)$$

3.4 Results and Discussion

3.4.1 Potential Energy Curves

The potential energy curves calculated for the neutral and cationic state are shown in Figs. 3.4 and 3.5. The potential energy V used in this study is referred to the minimum of the total energy for the neutral state. In Figs. 3.4 and 3.5a are shown one side of double-minimum potential energy curves for the neutral state and one side of single-minimum potential energy curves for the cationic state. Potential energy curves shown in Fig. 3.4 are obtained by varying ψ under C_s symmetry and those in Fig. 3.5a by varying ϕ under symmetry of C_{3v} for ammonia and trimethylamine and C_3 for triethylamine.

It has been found that equilibrium geometry of ethylamine for the neutral state can take either gauche (G) or trans (T) conformation.[21] Thus the potential energy

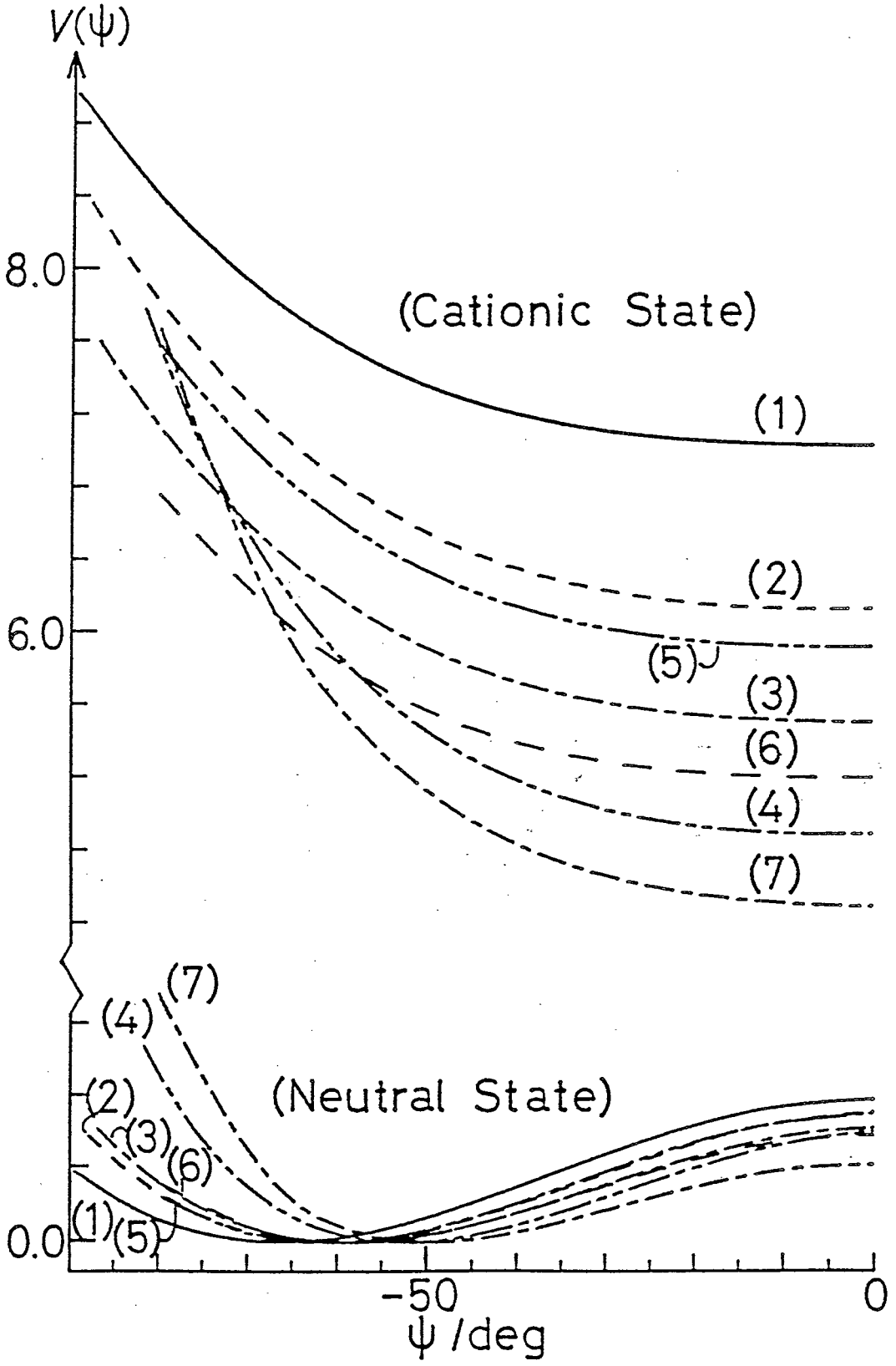

Fig. 3.4. Potential energy curves for ammonia and several alkylamines, against ψ under Cs symmetry. The notations 1 to 8 are the same as in Fig. 3.1. The molecular symmetry of (5) is C_1.

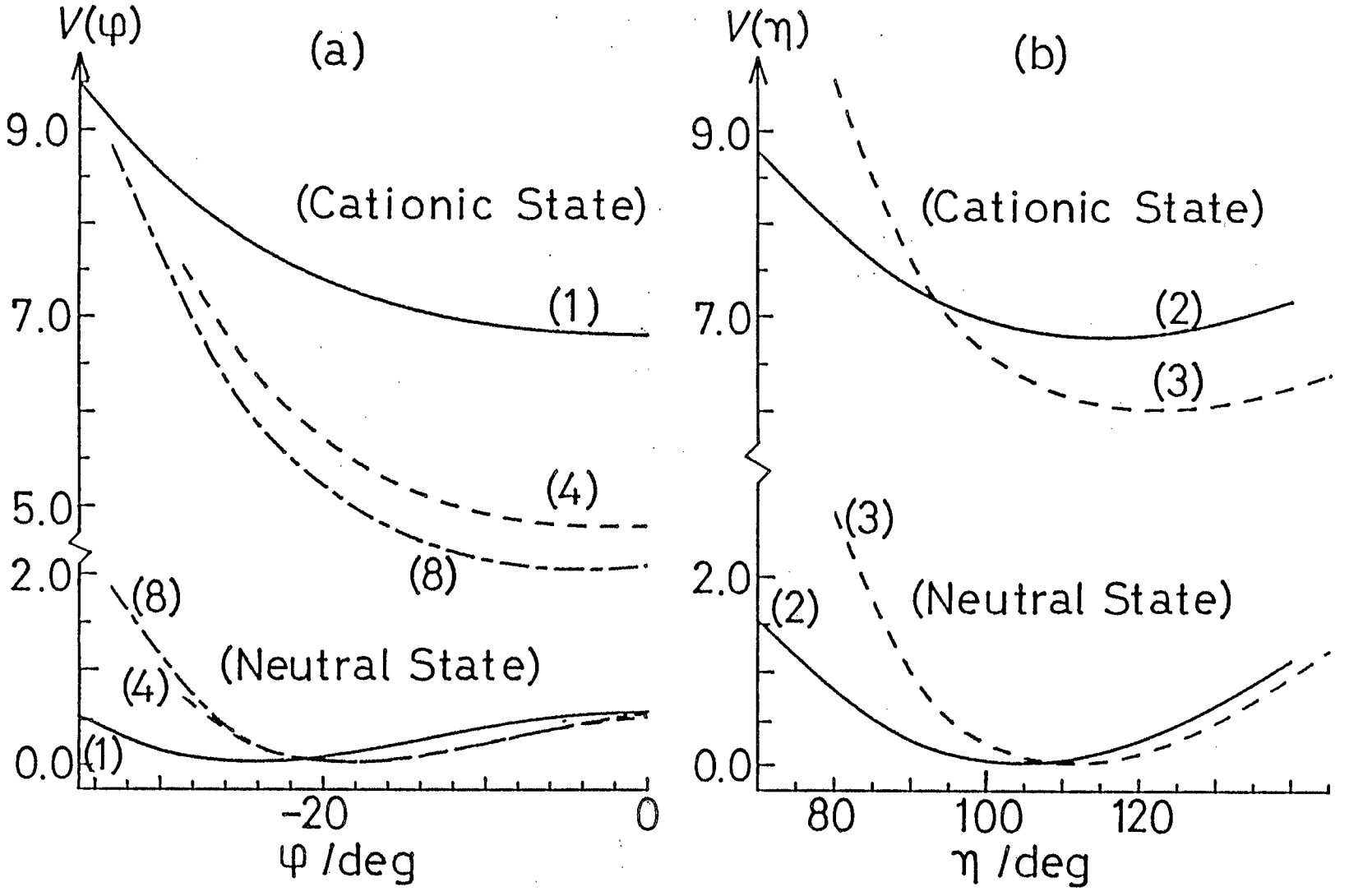

Fig. 3.5. Potential energy curves for several alkylamines, against ϕ under C_{3v} or C_3 symmetry (a), and against η under C_s symmetry (b). The notations are the same as in Fig. 3.1.

curves for ethylamine have been calculated taking both conformations. For the neutral state the T conformation gives somewhat steeper potential energy curve than G conformation. On the contrary, for the cationic state G conformation gives steeper curve than T. The cation with T conformation at $\psi=0°$ is stabler in total energy than that with G conformation. This was regarded as the result caused by repulsion between ethyl group and nitrogen lone-pair at $\psi=0°$, which arises from fixing all the structural parameters except ψ for the calculation.

Though the potential energy curves for neutral methylamine and ethylamine almost overlap as shown in Fig. 3.4, the curve for ethylamine cation is steeper than that for methylamine cation, and this is also due to the fixed geometry within the ethyl group. Same trend is seen in the case of dimethylamine and diethylamine.

As can be seen in Fig. 3.4 trimethylamine (4) and dimethylethylamine (7) have steeper curves ever the larger $|\psi|$ for both the neutral and the cationic state. This is considered to owe to the steric hindrance of the bulky substituent group.

The geometries optimized for neutral ammonia and the methyl amines with planar nitrogen skeleton are included in Table 3.1. Obvious difference in CN and/or HN bond lengths exists between the molecules with the pyramidal and the

planar nitrogen skeleton. These bonds are longer in the pyramidal form than in the planar form. The differences in total energy between the pyramidal and the planar form for the neutral state are 0.48, 0.45, 0.42, and 0.45 eV for ammonia, methylamine, dimethylamine, and trimethylamine, respectivery. The differences corresponding to the amino inversion barrier are larger than those previously reported.[3,53] The barriers determined from Figs. 3.4 and 3.5a are even higher because the geometries at ψ or ϕ=0° are not energetically optimized.[54] Furthermore neglect of configuration interaction (CI) and lack of superior basis sets may well make the potential energy curves calculated here different from the actual ones. However, the fact that the ionization induces drastic change on ψ or ϕ coordinate mainly, suggest that the intrinsic characters of the vibration induced by photoionization are describable with the present potential energy curves.

Potential energies as a function of the angle η are also calculated for methylamine and dimethylamine and are given in Fig. 3.5b. Although the values of η for the geometries of the most stable cations in the figure are different by about 10 degrees from those for the optimized geometries of neutral molecules, the curves for cation and neutral molecule are similar indicating that the deformation in η after the photoionization is small.

3.4.2 Band Shape of the Theoretical Photoelectron Spectrum

In order to obtain the theoretical photoelectron band from the potential energy curves, the following simple approach has been carried out. ψ or ϕ are connected with an internal coordinate θ. A harmonic oscillator approximation on $V(\theta)$ gives a force constant and a vibrational frequency by use of Willson's *GF* matrix method, summarized in the section 3.3. A wave-function Ψ for the harmonic vibration is calculated from the force constant. Although it is well known that the unharmonicity exists in the deformational vibration of amine mainly due to the large amplitude of the vibration, the unharmonic terms has been neglected because of the simplicity of the calculation. Assuming a Boltzmann distribution at 320 K which is the temperature of the ionization chamber, population p_i is obtained on each vibrational state i. The calculated frequencies and the populations are collected in Table 3.2 together with the experimental frequencies for ammonia and the methylamines. Calculated frequencies are not always in agreement with experimental ones. However, the following facts indicate that the essential property of molecular vibration in alkylamines concerned remains in the present potential energy curves; both experiment and the calculation concluded that the NH_2 wagging frequency is lower than the symmetric NH_2 deformational frequency for methylamine and that the CNC

Table 3.2. Vibrational Frequencies(cm^{-1}) and Population(%) on Each Vibrational Level(Populations are in Parenthesis)

state	experiment	calculation
	ammonia	
neutral	933[a)]	1450
	(v"=0; 99), (v"=1; 1)	(v"=0; 99), (v"=1; 1)
cationic	900	1690
	methylamine	
neutral	780[b,c,d)]	1370[e)]
	(v"=0; 97), (v"=1; 3)	(v"=0; 100)
	875[f)]	
	(v"=0; 98), (v"=1; 2)	
	1623[b,c,d)]	2740[g)]
	(v"=0; 100)	(v"=0; 100)
cationic	880	1330
	dimethylamine	
neutral	383[b,d)]	670[g)]
	(v"=0; 84),(v"=1; 14),(v"=2; 2)	(v"=0; 95),(v"=1; 5)
	735[b,d)]	1130[e)]
	(v"=0; 96), (v"=1; 4)	(v"=0; 99), (v"=1; 1)
cationic	∿520	1050

Table 3.2. (*continued.*)

	trimethylamine	
neutral	366[b,d,h]	580
	(v"=0; 88), (v"=1; 16), (v"=2; 2)	(v"=0; 92), (v"=1; 7), (v"=2; 1)
cationic	∿400	660

Experimental values for the cationic state are collected in this work. a) Refs. 2 and 22. b) Ref. 55. c) Ref. 56. d) Ref. 57. e) Vibrational mode corresponding to ψ. f) Observed in Raman spectrum, taken from Ref. 58. g) Vibrational mode corresponding to η. h) Ref. 35.

skeletal deformation frequency is lower than the a' N-H deformation frequency for dimethylamine.

Now the theoretical photoelectron band f shown in Fig. 3.6 is obtained as follows. The curve c, Ψ_0^2, is projected on the potential energy curve a for cation and weighted with p_0 for the v"=0 state. This gives us the photoelectron spectrum intensity corresponding to the ionization from v"=0. Then the photoelectron spectrum f is obtained as the accumulation of all the ionizations from the vibrational states whose population is larger than 1 %. In Fig. 3.7 are shown the theoretical photoelectron spectra for amines calculated in this work. In the figure, each spectrum is shifted in energy so that the maximum corresponding to I_{pv} comes on the same position on abscissa. It is assumed that the vibrational levels for the cationic state are continuous. The curve obtained in this manner should be comparable to the envelope of the experimental photoelectron spectrum. In Fig. 3.7 are also shown the theoretical photoelectron bands arising from the vibration on η for methylamine and dimethylamine. Both of them are sharp and I_{pth} is equal or close to I_{pv}. This indicates that this kind of vibration contributes less to the band shape.

The band width δ and threshold energy I_{pth} are determined from the theoretical photoelectron bands. The

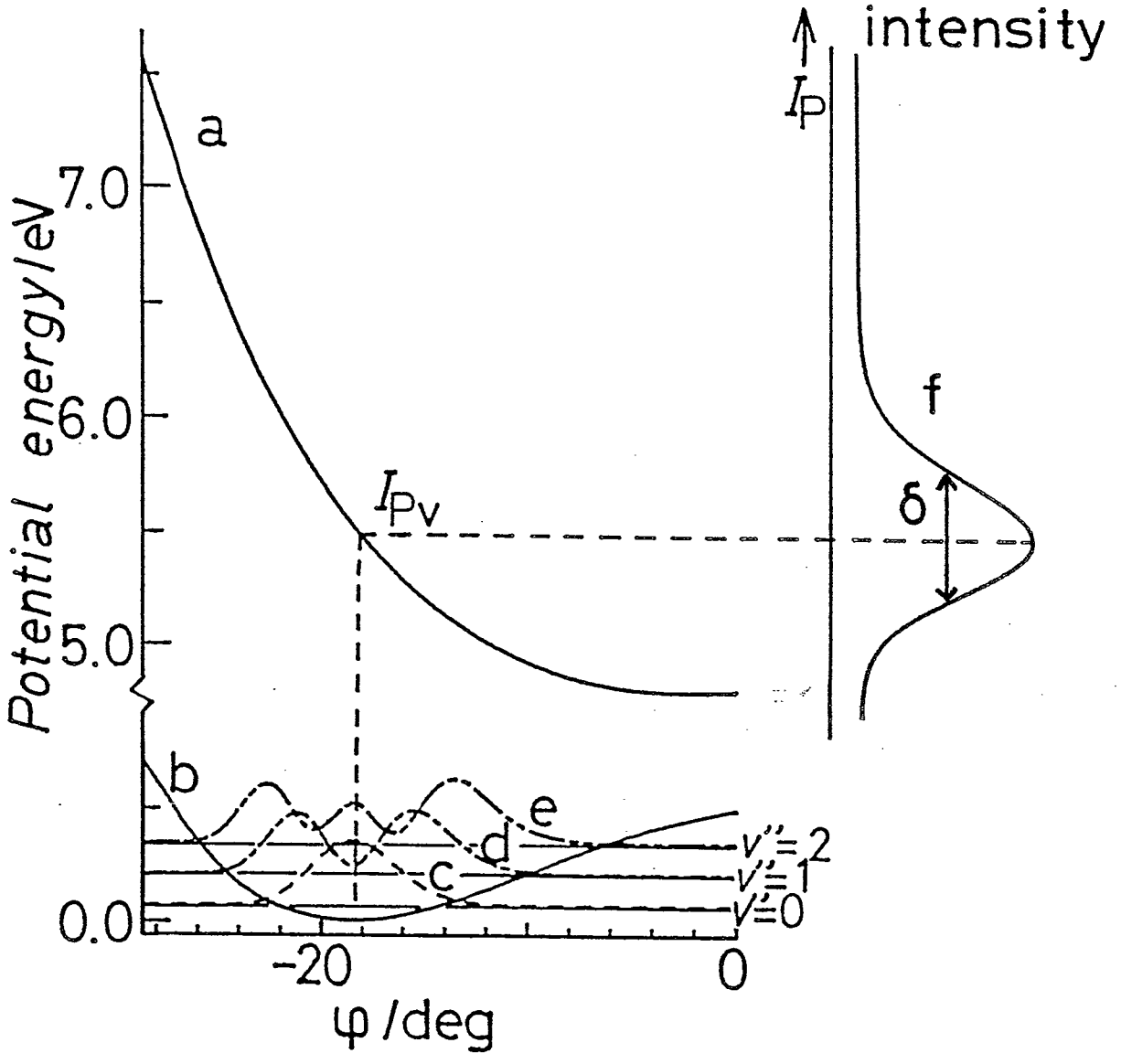

Fig. 3.6. Potential energy curves for the neutral (b) and the cationic (a) state of trimethylamine, the square of the wave function (Ψ_i^2) (c, d and e), and the photoelectron band (f) evaluated from them.

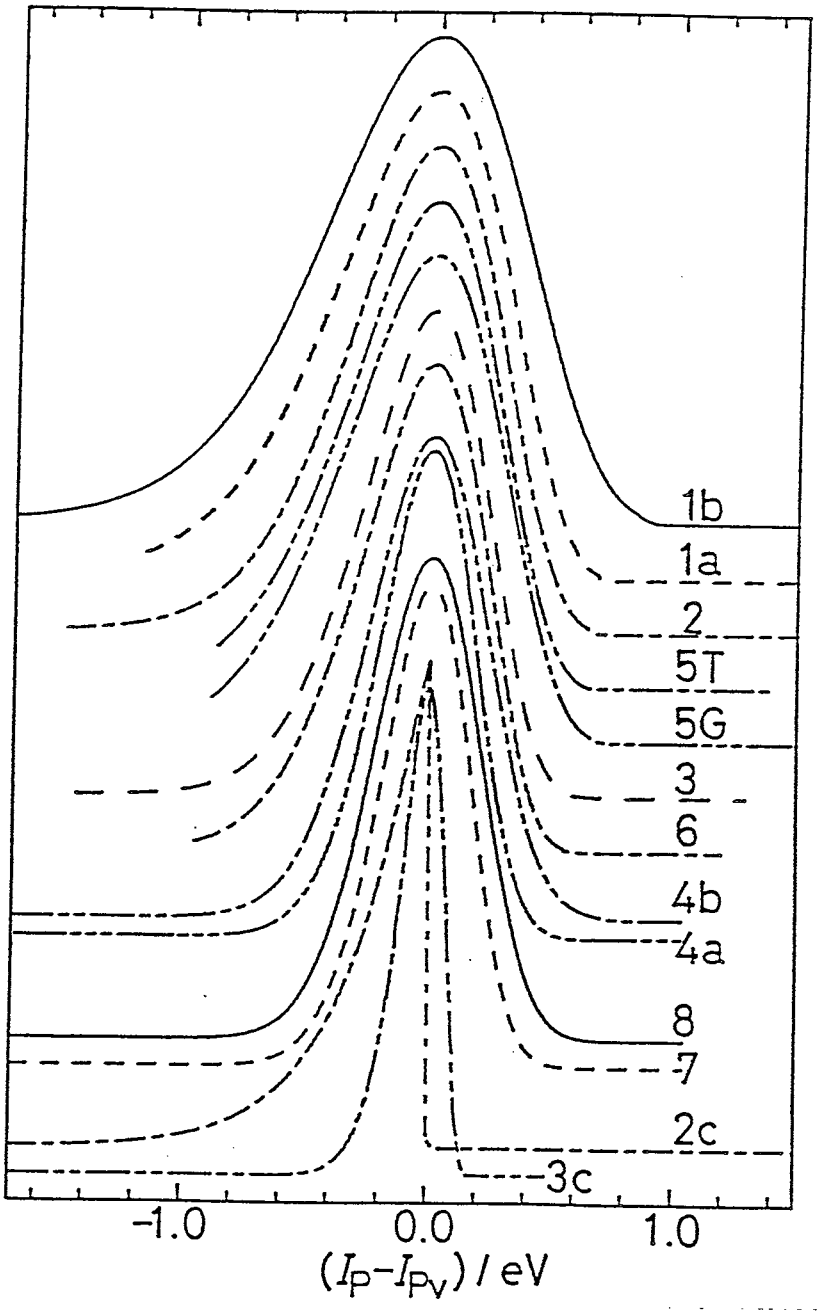

Fig. 3.7. Theoretical photoelectron band. The numerical notations are the same as in Fig. 3.1. a; calculated under C_s symmetry and b; calculated under C_{3v} symmetry. T; trans conformation, G; gauche conformation. c; the curves noted with c are band shapes calculated under the assumption that only the coordinate of η vibrates.

I_{Pth} is read at the onset whose intensity is 1 % of the band maximum. Table 3.3 contains the theoretical values for δ, I_{Pth}, I_{Pa}, and I_{Pv}, together with experimental ones. The I_{Pv}(ΔSCF) is defined as the difference in total energy between the neutral and the cationic state with the same geometry which is the most stable for the neutral state. I_{Pa} is defined as the difference in minimum total energy between the neutral and the cationic state each with the most stable geometry.

The calculated values of I_{Pth} are always larger than those of calculated I_{Pa}. This owes to the fact that I_{Pa} is the difference in total energy between optimized geometries for the neutral and cationic state, while I_{Pth} is evaluated by use of the potential energy curves as a function of only ψ or ϕ. That makes the total energy for cation at the minimum-energy point on the potential energy curve more unstable than that with the optimized geometry.[54] The theoretical values of I_{Pv}, I_{Pa}, and I_{Pth} are underestimated, and if a constant value of 3.1 eV is added to the theoretical values of I_{Pv}, they are in excellent agreement with the experimental ones.

3.4.3 Band Width

As can be seen in Fig. 3.8, δ's evaluated from the theoretical photoelectron band correlates well with the

Table 3.3. Experimental and Theoretical Ionization Potentials and Bandwidth (δ) (in eV)

	I_{Pv}		I_{Pa} [a]	I_{Pth}		δ		$\Delta I_{Pv,a}$	$\Delta I_{Pv,a}$ [b]	I_{Pa} [c]	I_{Pa} [d]
	exp	calc	calc	exp	calc	exp	calc	calc	corr	corr	corr
1) ammonia	10.90	7.79	6.76	10.08	6.91	0.95	0.95	1.03	-	-	-
2) methylamine	9.64	6.86	5.88	8.95	6.19	0.90	0.74	0.98	0.68	8.96	8.95
3) dimethylamine	8.94	6.15	5.19	8.18	5.55	0.79	0.60	0.96	0.66	8.28	8.27
4) trimethylamine	8.51	5.54	4.64	7.79	4.84	0.70	0.56	0.90	0.60	7.91	7.89
5) ethylamine	9.46	6.67	5.68	8.78	5.98	0.87	0.75	0.99	0.69	8.77	8.78
6) diethylamine	8.67	5.80	4.86	7.99	5.25	0.78	0.60	0.94	0.64	8.03	8.08
7) dimethylethylamine	8.39	5.11	4.36	7.61	4.61	0.73	0.42	0.75	0.45	7.49	7.71
8) triethylamine	8.09	5.02	4.16	7.37	4.42	0.72	0.51	0.86	0.56	7.53	7.47

a) The difference in total energies of the neutral molecule and the cation each with equilibrium geometry. b) Corrected $\Delta I_{Pv,a}$. c) $I_{Pv}^{exp} - \Delta I_{Pv,a}^{corr}$. d) Determined by adding the energy of a vibrational quanta to I_{Pth}^{exp}, see text.

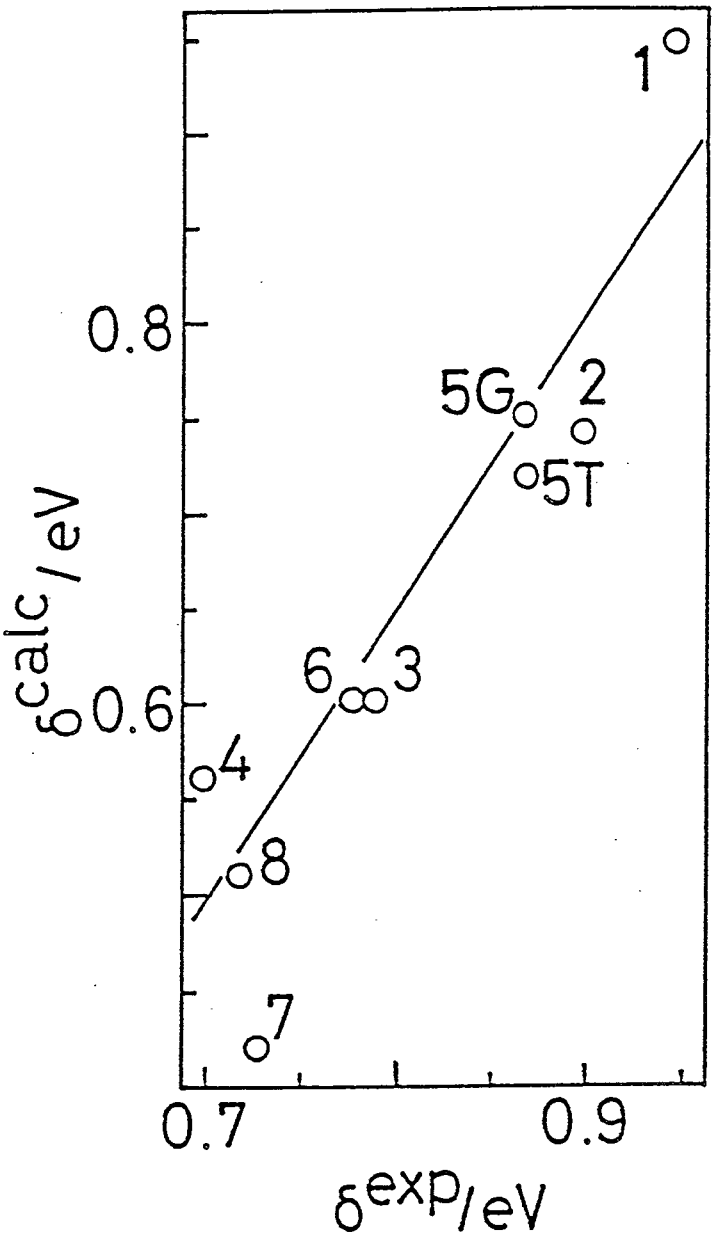

Fig. 3.8. Comparison between experimental and calculated δ. The notations are the same as in Fig. 3.1. G; gauche conformation. T; trans conformation.

experimental δ except dimethylethylamine (7).

The band width and the band shape depend on the following factors: (i) The difference of equilibrium geometries between the neutral and cationic state; (ii) the vibrational wave-function for the neutral state which is based on the feature of the potential energy curve for the neutral state; (iii) the slope of the potential energy curve for the cationic state.

The calculated δ must be under-estimated because the potential energy at minimum on the potential energy curve for cation is higher than that for the cation with the optimized geometry,[54] i.e., the potential energy curve for cation should be steeper. For ammonia and trimethylamine the theoretical photoelectron band has been obtained by two methods. One is the use of the potential energy curve for C_{3v} symmetry and the other is the use of C_s symmetry, i.e., the potential energy curve obtained as a function of ψ, while fixing the angle η to the optimized geometry for the neutral state (1b and 4b in Fig. 3.7). δ's evaluated under the C_s symmetry are 0.83 and 0.46 eV for ammonia and trimethylamine and the differences between the values for the C_{3v} and the C_s symmetry are 0.12 and 0.10 eV for ammonia and trimethylamine, respectively. This instance can be explained as follws. The vibrational wave-function for the neutral state under the C_s symmetry resembles to that under

C_{3v} symmetry. However, the potential energy curve for the cationic state under the C_{3v} symmetry is steeper than that under the C_s symmetry due to the effect of fixed angle η in the C_s symmetry. Thus δ's under the C_s symmetry are smaller than those under the C_{3v} symmetry for ammonia and trimethylamine.

As stated previously the potential energy curve for ethylamine cation with G conformation is steeper than that with T conformation, while the vibrational wave-functions for G and T conformation are similar each other. Then δ for G conformation (5G) is larger than that for T (5T) by 0.03 eV. Both conformations are possibly present in vacuo, which is ensured by the similarity in total energy between both conformations.[21)]

As shown in Fig. 3.8 the deviation from the correlation line between experimental and calculated values is large for the case of dimethylethylamine. δ for this amine is quite under-estimated because of the fixed CNC skeleton just as the case of trimethylamine calculated under C_s symmetry. There is some limitation in the present method to estimate band width of the UPS, because the potential energy curve used is a cross section of potential energy hypersurface taken only on a single coordinate on which change accompanied by photoionization is greatest.

3.4.4 Threshold Ionization Potential and Potential Energy Curve.

The I_{Pth} mainly depends on the next three factors: (I) The difference in the equilibrium geometries of the neutral and the cationic states; (II) the population on each vibrational level for the neutral state; (III) the vibrational probability density Ψ_0^2 on the neutral state at the geometry which is similar to the equilibrium geometry of the cationic state. When the difference for (I) is large, I_{Pa} may well be smaller than I_{Pth} and intrinsically undetectable in the UPS. While the large population on higher vibrational level causes larger probability of hot band. When the value for (III) is large, I_{Pa} should be detectable. Note that even if the value for (I) is large, the large value for (III) makes I_{Pa} detectable.

As stated in the previous section, for ammonia and trimethylamine, potential energy curves of the cationic state under C_{3v} symmetry are steeper than those under C_s symmetry, so $\Delta I_{Pv,th}$'s in the C_{3v} symmetry are larger than those in the C_s symmetry. Under the same circumstances $\Delta I_{Pv,th}$ for ethylamine of T conformation is smaller than that for G conformation by 0.08 eV. The total energy for cation at the minimum energy point on the present potential energy curve greatly differs from that with the optimized geometry for dimethylamine or diethylamine.[54] This is due

to the fixed CNC skeleton. It is interesting that although it is impossible to predict the values of $\Delta I_{Pv,th}$ accurately from the theoretical potential energy curves, the values of δ are predicted excellently from the curves as shown in Fig. 3.8 (except dimethylethylamine). This implies that the present potential energy curve for cation is distorted only around the equilibrium geometry for cation. With respect to dimethylethylamine, both δ and $\Delta I_{Pv,th}$ deviate from the correlation between experimental and calculated values. Thus the slope on the calculated curve for dimethylethylamine cation is gentler than the actual curve.

As stated in chapter 2, while I_p and δ systematically vary in the order of primary, secondary and tertiary amine, $\Delta I_{Pv,th}$ does not. This can be interpreted as follows. The populations on the higher vibrational levels on the neutral state increase in the order of primary, secondary and tertiary amine, since the vibrational frequency decreases in the same order. On the other hand the probability density Ψ_0^2 at the most stable geometry of cation decreases in the order of primary, secondary and tertiary amine. The two opposing factors result in the unsystematic order of $\Delta I_{Pv,th}$ as shown in Fig. 2.9.

3.4.5 Determination of Adiabatic Ionization Potential

The first ionization peak 10.075 eV in the UPS of

ammonia, observed also by several other workers,[6,7,16] has been regarded as the hot band.[6,7] Population on v"=1 is, however, 1 % as listed in Table 3.2, and the ratio of Ψ_1^2 to Ψ_0^2 at the equibrium geometry of ammonia cation is very small. Thus 0←1 ionization peak, i.e., hot band, should be indiscernible in the UPS. If the first peak were the 0←1 ionization peak, intensity of the first peak should be a few hundredth of that of the second peak according to Boltzmann distribution, since ionization cross section for the same vibrational mode is similar. The ratio of the first peak height to the second in the UPS is 0.24 and is too large to assign the first peak to 0←1 ionization peak. Then it is concluded that the first peak is not the 0←1 but the 0←0 ionization peak, and that I_{Pa} is 10.08 eV. As for primary amines, the frequency of deformation vibration of ψ, viz., NH_2 wagging vibration, is in the range of 850-750 cm^{-1} from the infrared spectra of liquid phase,[58] so the population on v"=1 should be 2-4 %. Peak height of the first peak in the vibrational progression in the first band for methylamine and ethylamine, compared to that of the second peak, however, is too large to assign the first peak to 0←1 ionization peak. Therefore the first peaks for methylamine and ethylamine pertain to the 0←0 ionization peak and the I_{Pa}'s are 8.95 and 8.78 eV, respectively.

Now one can estimate I_{Pa}'s for the methylamines and the

ethylamines by use of $I_{Pa}{}^{calc}$ calculated here and experimental $I_{Pth}{}^{exp}$. $I_{Pa}{}^{calc}$ is largely under-estimated because of the neglect of CI and superior basis set. So is $I_{Pv}{}^{calc}$, but one expects that this is somewhat canceled out in the difference $\Delta I_{Pv,a}{}^{calc}$ ($=I_{Pv}{}^{calc} - I_{Pa}{}^{calc}$). $\Delta I_{Pv,a}{}^{corr}$ is obtained by adding 0.30 eV to $\Delta I_{Pv,a}{}^{calc}$. The correction of 0.30 eV gives $\Delta I_{Pv,a}{}^{calc}$ equal to $\Delta I_{Pv,th}{}^{exp}$ for methylamine and ethylamine. Finally I_{Pa} is estimated by subtracting $\Delta I_{Pv,a}{}^{corr}$ from $I_{Pv}{}^{exp}$. The values of I_{Pa} are included in Table 3.3 together with $\Delta I_{Pv,a}{}^{calc}$ and $\Delta I_{Pv,a}{}^{corr}$. The difference between I_{Pa} and $I_{Pth}{}^{exp}$ are 0.12 and 0.16 eV for trimethylamine and triethylamine, respectively. These values indicate that the hot band should be observable and that the hot band can be at least 0←2 ionization peak if considered that the frequency of the vibration of ϕ for neutral trimethylamine and triethylamine is about 0.05 eV.[58] For diethylamine the difference between I_{Pa} and $I_{Pth}{}^{exp}$ is 0.05 eV, and this indicates that the hot band may be observable, or that the difference is only the error produced in the calculation because the frequency of the vibration of ψ is about 0.09 eV.[58] The difference for dimethylamine is 0.09 eV, and the hot band, 0←1 ionization peak, may exist. However, the hot band should not be observable, if the population p_1 and probability density Ψ_1^2 of the neutral state at the

equilibrium geometry of the cation are considered. The hot band of dimethylamine may be due to the coupling of the vibration of ψ with other vibrations.

According to the discussions the thermodynamic I_{Pa} is estimated by combining photoelectron spectroscopic I_{Pth} and vibrational energy. Assuming that 0←1 and 0←2 ionizations are observable for the secondary and the tertiary amines, respectively, the values for I_{Pa} are obtained by adding 0.09 eV to I_{Pth} for the secondary and 0.10 eV for the tertiary amines and are listed in Table 3.3. By using the I_{Pa} obtained in this manner, one can obtain the values of $\Delta I_{Pv,a}{}^{exp}$, which are compared with the theoretical $\Delta I_{Pv,a}$'s in Fig. 3.9. The correlation indicates that 0.3 eV subtraction from the theoretical value predicts the experimental one excelently, except for ammonia, triethylamine and dimethylethylamine. This result also supports the present determination of the thermodynamic I_{Pa} for amines. According to the discussions I_{Pa}'s for all the alkylamines done measurements of the UPS in this study are listed in Table 3.4.

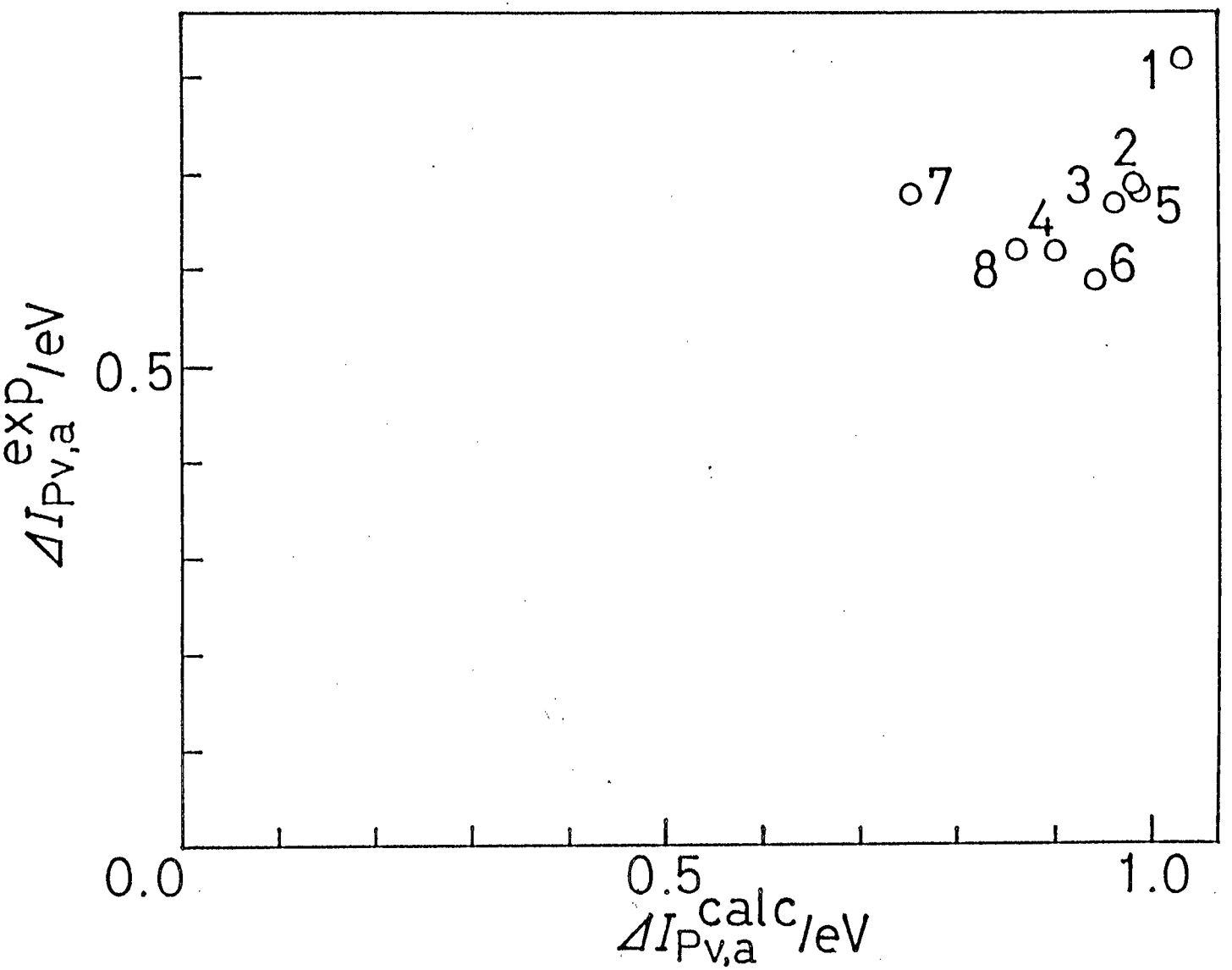

Fig. 3.9. Comparison between experimental and calculated $\Delta I_{Pv,a}$. The notations are the same as in Fig. 3.1.

Table 3.4. Photoelectron Spectroscopic I_{Pa} Estimated from I_{Pth}

(in eV)

	I_{Pth}	I_{Pa}		I_{Pth}	I_{Pa}
ammonia	10.08	10.08	*n*-butylamine	8.59	8.59
methylamine	8.95	8.95	di-*n*-butylamine	7.74	7.83
dimethylamine	8.18	8.27	tri-*n*-butylamine	7.15	7.25
trmethylamine	7.79	7.89	isobutylamine	8.63	8.63
ethylamine	8.78	8.78	diisobutylamine	7.73	7.82
diethylamine	7.99	8.08	triisobutylamine	7.14	7.24
triethylamine	7.37	7.47	*s*-butylamine	8.60	8.60
n-propylamine	8.68	8.68	*t*-butylamine	8.56	8.56
di-*n*-propylamine	7.80	7.89	amylamine	8.61	8.61
tri-*n*-propylamine	7.18	7.28	diamylamine	7.68	7.77
isopropylamine	8.66	8.66	triamylamine	7.11	7.27
diisopropylamine	7.73	7.82	dimethylethylamine	7.61	7.71

REFERENCES

[1] J. H. D. Eland, "Photoelectron Spectroscopy", Butterworth and Co., London (1974), Chap. 5.

[2] G. Hertzberg, "Infrared and Raman Spectra of Polyatomic Molecules II. Infrared and Raman Spectra of Polyatomic Molecules", D. Van Nostrand Co. New York (1945).

[3] R. A. Eades, D. A. Weil, D. A. Dixon and C. H. Douglass, Jr., *J. Phys. Chem*, **85**, 976 (1981)

[4] S. Profeta, Jr. and N. L. Allinger, *J. Am. Chem. Soc.*, **107**, 1907 (1985).

[5] A. D. Walsh and P. A Warsop, *Trans. Faraday Soc.*, **57**, 345 (1961).

[6] A. W. Potts and W. C. Price, *Proc. R. Soc. London, Ser. A*, **326**, 181 (1972).

[7] D. H. Aue, H. M. Webb and M. T. Bowers, *J. Am. Chem. Soc.*, **97**, 4136 (1975).

[8] M. E. Wocks, *J. Chem. Phys.*, **41**, 930 (1964).

[9] T. E. Sharp and H. M. Rosenstock, *J. Chem. Phys.*, **41**, 3453 (1964).

[10] M. Halmann and I. Laulicht, *J. Chem. Phys.*, **43**, 1503 (1965).

[11] P. M. Dehmer and J. L. Dehmer, *J. Chem. Phys.*, **69**, 125 (1978).

[12] P. M. Dehmer and J. L. Dehmer,*J. Chem. Phys.*, **68**, 3462

(1978).

[13] W. R. Harshbarger, *J. Chem. Phys.*, 53, 903 (1970).

[14] W. R. Harshbarger, *J. Chem. Phys.*, 56, 177 (1972).

[15] P. Avouris, A. R. Rossi, and C. Albrecht, *J. Chem. Phys.*, 74, 5516 (1981).

[16] J. W. Rabalais, L. Karlsson, L. O. Werme, T. Bergmerk, and K. Siegbahn, *J. Chem. Phys.*, 58, 3370 (1973).

[17] S. Tomoda and K. Kimura, *Chem Phys.*, 82, 215 (1983).

[18] S. Tomoda and K. Kimura, *Chem. Phys. Lett.*, 111, 434 (1984).

[19] S. Tomoda and K. Kimura, *Chem. Phys. Lett.*, 121, 159 (1985).

[20] K. Morokuma, S. Kato, K. Kitaura, I. Ohmine, S. Sakai, and S. Obara, IMS Computer Center Library, Institute for Molecular Science, No. 0372 (1980).

[21] The calculated bond lengths and angles for ammonia, and the methylamines agree with the experimental values[2,24-35] within a few hundredths of an angstrom and within a few degrees. The structural parameters for ethylamine are similar to those used in Ref. 36. For the ethylamines, the calculated conformations of the neutral state are in agreement with the result of experiment as follows. The most stable conformation of ethylamine has been reported to be either G (gauche) conformation with respect to the lone-pair of the nitrogen,[36,37] or T (trans) conformation.[38,39]

It has been found by the present calculations that the G conformation is the most stable. However, the energy difference between these two conformations is only 8 meV which is less than the noise level of the computational technique, which is also stated in Ref. 4. Diethylamine takes TT (trans-trans) conformation, i.e., each ethyl group has a methyl group at trans position with respect to the other ethyl group.[40] Triethylamine takes G'G'G' conformation, i.e., each of the methyl group comes to the gauche position against the lone-pair and other ethyl groups.[41] While another stable conformations were reported to be present,[41,42] the conformation of this molecule has been taken as G'G'G' which is the result of the present geometry optimization. The structural parameters for the neutral ammonia and the methylamines are in good agreement with those calculated by others.[3,4,43-50] The conformations calculated by L. Radom, et al.[51] for the neutral methylamine, dimethylamine and ethylamine are in reasonable agreement with the present results. For ethylamine cation the difference in total energy between T conformation and G conformation has been only 3 meV.

[22] E. B. Wilson, Jr., J. C. Decius, and P. C. Cross, "Molecular Vibrations", McGraw-Hill Inc., New York (1980).
[23] S. Mizushima and T. Shimanouchi, "Sekigai-Kyushu to Raman-Koka", Kyoritsu Zensho, Kyoritsu Shuppan, Tokyo

(1958).

[24] W. S. Benedict and E. K. Plyler, *Can. J. Phys.*, 35, 1235 (1957).

[25] Y. Morino, K. Kuchitsu and S. Yamamoto, *Spectrochim. Acta*, 24A, 235 (1968).

[26] K. Kuchitsu, J. P. Guillory, and L. S. Bartell, *J. Chem. Phys.*, 49, 2488 (1968).

[27] T. Nishikawa, T. Itoh, and K. Shimoda, *J. Chem. Phys.*, 23, 1735 (1955).

[28] D. R. Lide, Jr., *J. Chem. Phys.*, 27, 343 (1957).

[29] H. K. Higginbotham and L. S. Bartell, *J. Chem. Phys.*, 42, 1131 (1964).

[30] K. Takagi and T. Kojima, *J. Phys. Soc. Jpn.*, 30, 1145 (1971).

[31] J. E. Wollrab and V. W. Laurie, *J. Chem. Phys.*, 48, 5058 (1968).

[32] B. Beagley and T. G. Hewitt, *Trans. Faraday Soc.*, 65, 2565 (1968).

[33] D. R. Lide, Jr. and D. E. Mann, *J. Chem. Phys.*, 28, 572 (1958).

[34] J. E. Wollrab and V. W. Laurie, *J. Chem. Phys.*, 51, 1580 (1969).

[35] J. N. Gayles, *Spectrochim. Acta.*, 23A, 1521 (1967).

[36] P. J. Krueger and J. Jan, *Can. J. Chem.*, 48, 3229 (1970).

[37] A. S. Manocha, E. C. Tuazon, and W. G. Fateley, *J. Phys. Chem.*, **78**, 803 (1974).

[38] J. R. Durig and Y. S. Li, *J. Chem. Phys.*, **63**, 4110 (1975).

[39] M. Tsuboi, K. Tamagake, A. Y. Hirakawa, J. Yamaguchi, H. Nakagawa, A. S. Manocha, E. C. Tuzan and W. G. Fateley, *J. Chem. Phys.*, **63**, 5177 (1975).

[40] A. L. Verma, *Spectrochim. Acta, part A*, **27A**, 2433 (1971).

[41] C. H. Bushweller, S. H. Fleischman, G. L. Grady, P. McGoff, C. D. Rithner, M. R. Whalon, J. G. Brennan, R. P. Marcantonio, and R. P. Domingye, *J. Am. Chem. Soc.*, **104**, 6224 (1982).

[42] K. Kamur, *Chem. Phys. Lett.*, **9**, 504 (1971).

[43] A. Rauk, L. C. Allen, and E. Clementi, *J. Chem. Phys.*, **52**, 4133 (1970).

[44] W. A. Lathan, W. J. Hehre, L. A. Curtiss, and J. A. Pople, *J. Am. Chem. Soc.*, **93**, 6377 (1971).

[45] D. J. Defrees, B. A. Levi, S. K. Pollack, W. J. Hehre, J. S. Binkley and J. A. Pople, *J. Am. Chem. Soc.*, **101**, 4085 (1979).

[46] W. R. Rodwell and L. Radom, *J. Chem. Phys.*, **72**, 2205 (1980).

[47] P. Puley, G. Forarasi, F. Pang and J. E. Boggs, *J. Am. Chem. Soc.*, **101**, 2550 (1979).

[48] P. Pulay and E. Török, *J. Mol. Struct.*, **29**, 239 (1975).

[49] E. Flood, P. Puley and J. E. Boggs, *J. Am. Chem. Soc.*, **99**, 5570 (1977).

[50] S. Skaarup, L. L. Griffin and J. E. Boggs, *J. Am. Chem. Soc.*, **98**, 3140 (1976).

[51] L. Radom, W. J. Hehre, and J. A. Pople, *J. Am. Chem. Soc.*, **94**, 2371 (1972)

[52] A. D. Baker, D. Betteridge, N. R. Kemp, and R. E. Kirby, *Anal. Chem.*, **43**, 375 (1971).

[53] J. M. Lehn, *Fortchr. Chem. Forsch.*, **15**, 311 (1970).

[54] Because of the fixed structural parameters except ψ or ϕ, minimum total energies of the cations on the present potential energy curves are higher than those with the optimized geometries by the following values; 0.04 eV for ammonia, 0.23 eV for methylamine, 0.29 eV for dimethylamine, 0.14 eV for trimethylamine, 0.22 eV for ethylamine both with G and T conformations, 0.32 eV for diethylamine, 0.12 eV for dimethylethylamine, and 0.18 eV for triethylamine.

[55] G. Dellepine and G. Zerbi, *J. Chem. Phys.*, **48**, 3573 (1968).

[56] A. Y. Hirakawa, M. Tsuboi and T. Shimanoushi, *J. Chem. Phys.*, **57**, 1236 (1972).

[57] From infrared spectra for the methyl amines, of Refs. 55 and 56, the bond angle deformation frequencies about nitrogen skeleton are as follows: for methylamine,

780 cm^{-1} corresponding to mainly θ and partly to η, and 1623 cm^{-1} corresponding to mainly η and partly to θ; for dimethylamine 383 cm^{-1} corresponding to mainly η and partly to θ and to torsional angle around C-N axis, and 735 cm^{-1} corresponding to mainly θ and partly to C-N bond length; for trimethylamine 366 cm^{-1} dominantly corresponding to θ. In Raman spectra similar vibrations have also been reported.[58)]

[58] F. R. Dollish, W. G. Fateley, and F. F. Bentley, "Characteristic Raman Frequencies of Organic Compounds", Wiley-Interscience, N. Y. (1973).

Chapter 4. UPS for several Deuteralkylamines and Adiabatic Ionization Potentials for Ammonia, Methylamine, and Ethylamine

4.1 Introduction

Band shape for alkylamines has been well predicted by the potential energy curves for both the neutral and the cationic state in the preceding chapter, and then it is important whther this treetment is useful in other case. In order to verify this, it has been carried out whether the curves also predict band shape for their deuterium derivatives or not under an assumption that the electronic energies of the neutral state for hydrogen derivative and deuterium derivative are equa and those of the cationic state are also equal. As for band width, the inverse dependence of band width on $\mu^{\frac{1}{4}}$ (μ is the reduced mass) was stated to be observable as an effect of isotopic substitution,[1] however, an experimental verification of the idea has not been executed yet. Therefore the present discussion should be valuable.

As mentioned in the previous chapter, threshold ionization potential in the UPS is not always adiabatic ioniozation potential. Therefore in the preceding chapter adiabatic ionization potential has been determined by

considering the vibrational frequency, and then, in this chapter it is determined by comparing I_p's of vibrational progressions of hydrogen derivative with those of the deuterium derivative. Furthermore the whole vaibrational frequencies for ammonia cation are determined.

4.2 Experimental

4.2.1 Preparation

Preparation of deuteramine has been carried out by exchange of amine with deuterium oxide and it is done by modifying the method descrived in Refs. 2-4. The modified point is what D_2O is reacted with amine instead of amine hydrochloride because of dispatching the exchange rapidly.

Amine hydrochloride was recrystallized three times from ethanol, distilled as described in Ref. 5, and dried over CaO in a vacuum desicator. The apparatus used in carrying out the exchange is shown in Fig. 4.1. A quantity of 99.8 % pure D_2O (Commissariat a L'Energie Atomique), was poured into the tube *A*. Amine hydrochloride with CaO, heated under a running vacuum at 720 K for several days to remove $Ca(OH)_2$, was introduced into *E*, which was attached to the apparatus by a ground joint. The mixture was heated at 420-470 K in a vacuo. The amine evolved was collected in the tube *D*, which was cooled in liquid nitrogen. Approximately

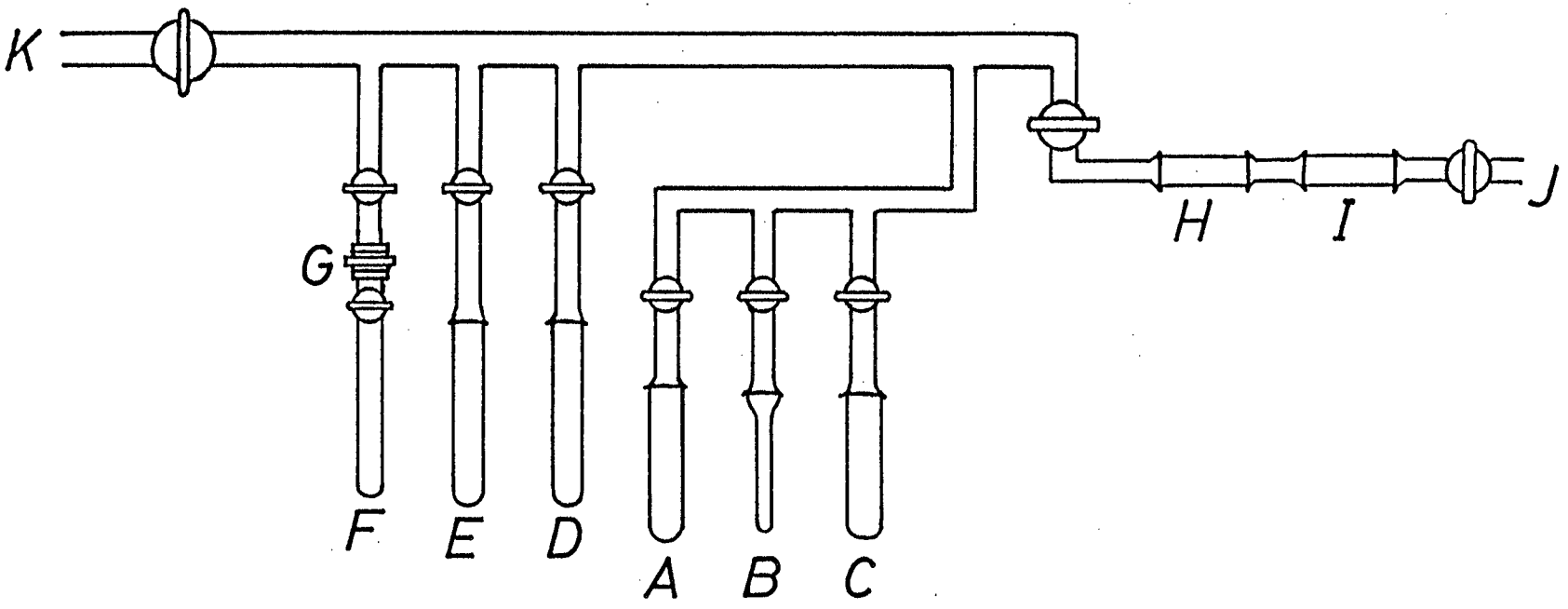

Fig. 4.1. Vacuum apparatus used for preparation of deuteramines. *A-F*; glass tube with a ground joint. *G*; diflon connector. *H*; P_2O_5. *I*; NaOH. *J*; air inlet. *K*; attached to vacuum pump.

three moles per a mole of amine of D_2O were then measure out in the graduated tube *B* from *A*, and distilled into the *D*. The mixture, which consists of amine and D_2O, was allowed to melt in the tube with the tap closed, and was warmed at 300 K-310 K for 30 minutes to exchange, after which the amine was collected over the CaO in tube *E*, which was cooled in liquid nitrogen. The mixture was allowed to melt in the tube with the tap closed, and was warmed at 300 K for 30 minutes in order to dry, after which the amine was collected in the *D*, cooled in liquid nitrogen. After the exchange-process was recycled by three times, the amine was collected in the *E*, contained a further quantity of the CaO, and so left overnight. Finally the amine was distilled into tube *F* with tap, which is attached with diflon-connector *G*. Tube *C* was used when the preparation was done according to the methods descrived in Refs.2-4. The isotopic purity of the deuteramines was checked by H-nmr and in the spectra the deuteramines had no peak in the area where amino-hydrogen should have appeared.

4.2.2 UPS Measurement

The experimental setup and conditions for the UPS measurement have been similar descrived in the previous chapter except the followings. That is to say that sample was colled by thermomodules to lower the vapor pressure, and

that preceding the measurement, D_2O was flowed by 2.7 mPa more than 6 hours. Then the first band of D_2O was measured and no presence of H_2O was confirmed.

4.3 Valence Force Field Calculation for Plane XY_3 Molecule

4.3.1 General Considerations

In order to obtain the values of the potential constatnts of a polyatomic molecule on a theoretical basis and predict the vibrational frequencies one must solve the secular equation and compare them with the experimental values. At present one can done the calculation by the use of a established computer-program, e.g., Gauss80, or the IMSPACK[6]. Another customary way is to make certain specific assumptions about the forces in the molecules such that the number of force constants to be determined is reduced.[7]

One of assumptions is the assumption of valence forces.[7] The assumption is that there is a strong restoring force in the line of every valence bond if the distance of the two atoms bound by this bond is changed. In addition there is a restoring force opposing a change of the angle between two valence bonds connecting one atom with two others. Here, often not all normal frequencies are necessary for a calculation of the force constants and

therefore a valuable check on the assignment of the frequencies is possible.

4.3.2 Plane XY_3 Molecule

A force that tends to restore the angle θ between each pair of XY bond is assumed in the valence force treatment. In addition, a force that tends to bring the angle between X-Y and the plane back to zero is assumed. Thus the potential energy is

$$2V=k_1(Q_{12}^2+Q_{13}^2+Q_{14}^2)+k_\delta(\delta_{23}^2+\delta_{24}^2+\delta_{34}^2)+k_\Delta(\Delta_{12}^2+\Delta_{13}^2+\Delta_{14}^2), \quad (4.1)$$

where, Q_{12}, Q_{13}, and Q_{14} are the change of the XY distances, where the δ_{ik}'s are the changes of the angles between the lines XY_i and XY_k, and where Δ_{12}, Δ_{13}, and Δ_{14} are the deviations of the lines XY from the Y_3 plane. k_1, k_δ, and k_Δ are the force constants.

Expressing the Q_{ik}, δ_{ik}, and Δ_{ik} in terms of the internal symmetry coordinates and solving the secular equation, the following equations for the normal frequencies are obtained:

$$\lambda_1=k_1/m_y, \quad (4.2)$$

$$\lambda_2=(1+3m_y/m_x)k_\Delta/m_y/l^2, \quad (4.3)$$

$$\lambda_3+\lambda_4=(1+3/2m_y/m_x)(k_1/m_y+3k_w/m_y/l^2), \quad (4.4)$$

$$\lambda_3\lambda_4=3(1+3m_y/m_x)k_1k_\delta/m_y^2/l^2, \quad (4.5)$$

in which λ_i is defined by

$$\lambda_i=4\pi^2c^2M_1\nu_i^2, \quad (4.6)$$

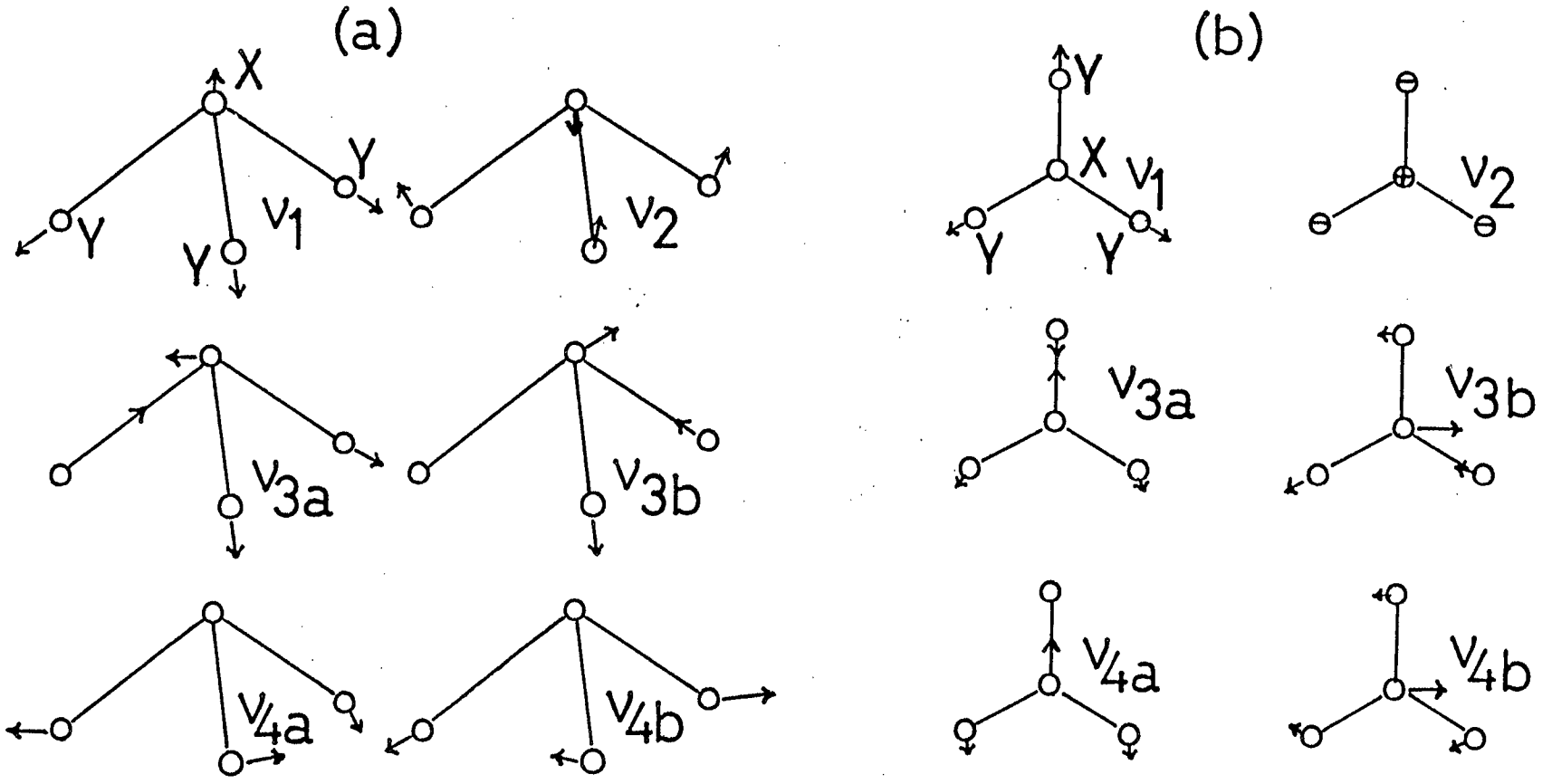

Fig. 4.2. Vibrational mode for XY_3 molecule. (a) pyramidal. (b) planne. As for ν_2 (+) denotes replacement from the upper side of the paper to the down side; (-) the opposite form.

where M_1 is 1/16 of the mass of the O^{16} atom. If all four frequencies are observed thus four equations for the three unknown force constants k_1, k_{δ/l^2}, and k_{Δ/l^2} can be acquired.

4.4 Results and Discussion

4.4.1 Spectra Observed and Band widths

In Fig. 4.3, the first band of the UPS for ND_3[8-10] is presented and so are the first bands for CH_3ND_2, $(CH_3)_2ND$, and $C_2H_5ND_2$ in Fig. 4.4. General spectral features are similar to those of NH_3, CH_3NH_2, $(CH_3)_2NH$, and $C_2H_5NH_2$, respectively. While as for ammonia, peaks corresponding to the stretching vibration observed for NH_3 is hard to be detected for ND_3 and shifted to lower I_p. The decrease of vibrational frequency by deuterium substitution may cause the phenomenon. By the same reason, spectra for CH_3ND_2 and $C_2H_5ND_2$ are less complicated than those for H-species.

I_p's and δ are tablated with δ calculated in Table 4.1. I_p's for deuterium derivatives are a few dozens of meV larger than those for hydrogen derivatives. As for I_{pv} this owes to the difference in zero-point energy for the neutral state between those derivatives and the difference in total energy of the cationic state at the vibrational quanta, at which I_{pv} arises, between those derivatives. As to I_{pth} the

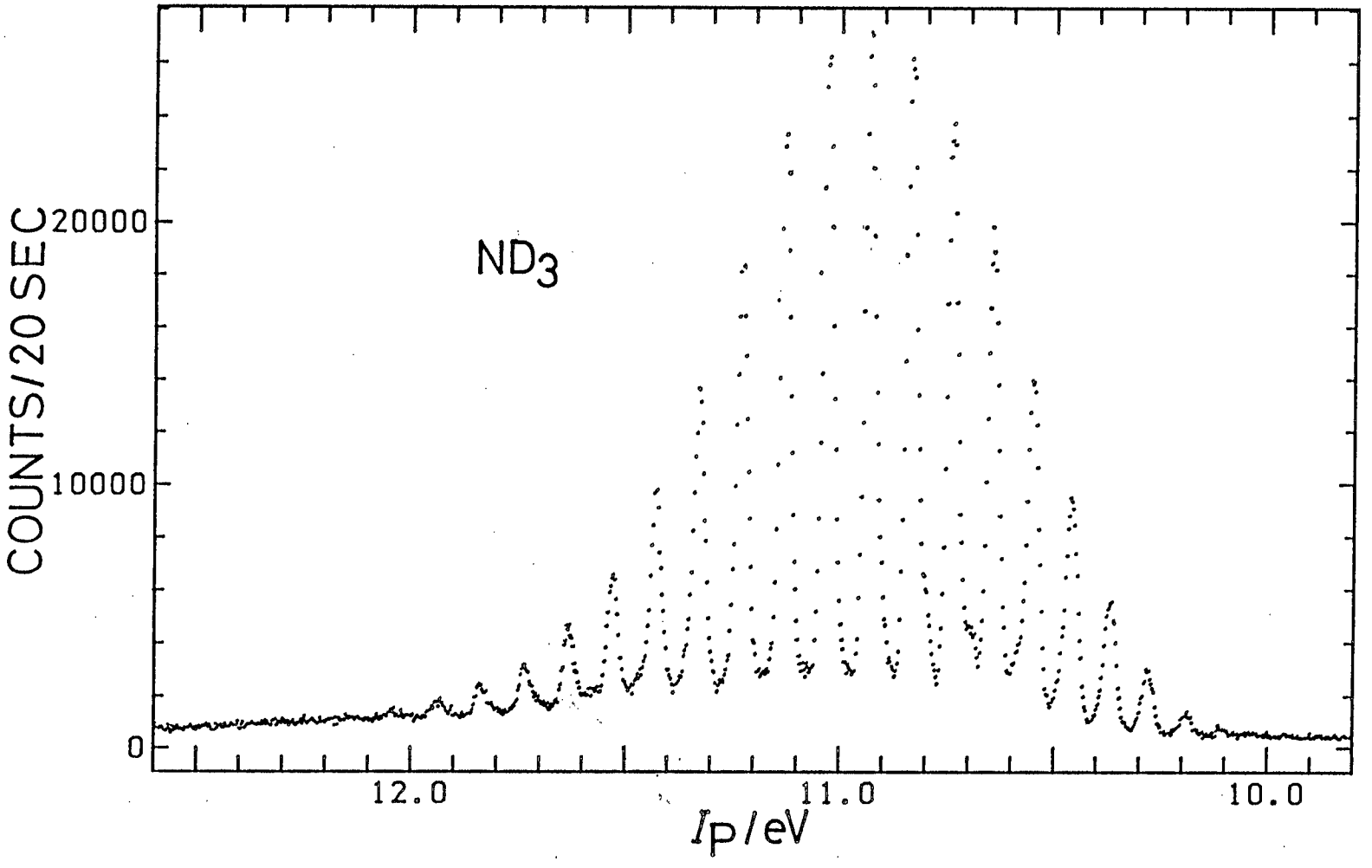

Fig. 4.3. First band of the UPS for ND_3.

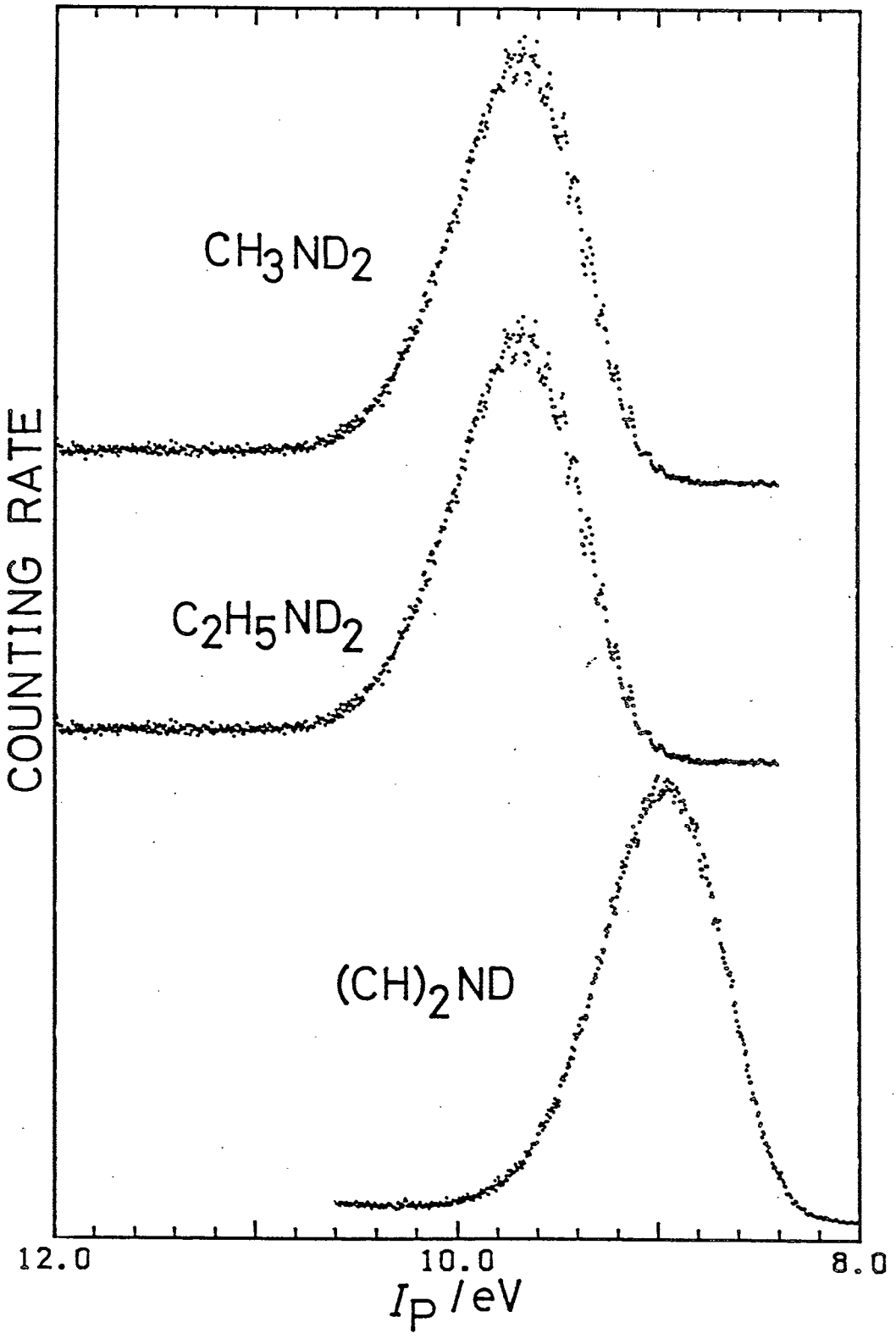

Fig. 4.4. First bands of the UPS for CH_3ND_2, $C_2H_5ND_2$, and $(CH_3)_2ND$.

instance will be discussed in the following section. For the ab initio MO calculations the zero-point energy is not ordinary taken into consideration when I_p is calculated since it is often within the error of calculations. Then I_p for the deuterium derivative was not calculated in this study, too. The calculations to estimate band shape of the UPS have been executed by the method descrived in the previous chapter and resultant photoelectron band shapes are similar to that seen in Fig. 3.7. As estimated by the calculations, δ's for D-species are smaller than those for H-species, listed in table 4.1. The instatnce is a verification that the present calculations are valuable to estimate the band shape of the UPS.

4.4.2 Vibrational Progressions and Determination of Adiabatic Ionization Potential for ammonia

As stated before, I_{pth} is not always equal to I_{pa}. Both I_p's are influenced by deuterium substitution. The difference in I_{pa} is defined as the difference in zero-point energy for both the neutral and the cationic state between H-species and D-species, however, that in I_{pth} is more complicated and is not able to be defined by uniform words. Since I_{pth} is influenced by not only the difference in total energy between the neutral and the cationic state but the Boltzmann distribution as stated in the previous chapter.

Table 4.1 Vertical I_{Pv} and Threshold I_{Pth} Ionization Potentials, Band width δ , Vibrational Frequencies, ν, and Ratio of Vibrational Frequencies and Ratio of Band Widths between the hydrogen and deuterium derivatives for the First Band of the UPS

Compound	I_{Pv}/eV	I_{Pth}/eV	δ/eV		ν/cm^{-1}		$h\nu^{D+}/h\nu^{H+}$		δ^D/δ^H	
			exp	calc	exp	calc	exp	calc	exp	calc
ND_3	10.93	10.10	0.76	0.85	728	1300	0.81	0.76	0.80	0.89
CH_3ND_2	9.68	8.98	0.78	0.64	605	1000	0.69	0.76	0.87	0.85
$C_2H_5ND_2$	9.51	8.82	0.76	0.63	725	970	0.85	0.76	0.84	0.84
$(CH_3)_2ND$	8.95	8.24	0.73	0.53	524	830	1.00	0.79	0.92	0.88

The following data are ionization potentials determined by othr workers. I_{Pa}'s are in parenthesis. ND_3; 10.8 (10.15),[8] (10.17),[9] 10.95 (10.21).[10]

In this section I_{Pa} is decided by comparing vibrational peaks between H-species and D-species.

Table 4.2 presents I_P of each peak of vibrational progression for NH_3 and ND_3. The vibrational spacings increase with increasing quantum number for both molecules, thus indicating a negative anharmonicity. In last column of Table 4.2 the difference in the I_P's of D-speacies and H-speacies, $I_P^D - I_P^H$, for each peak is listed and decreases with increasing quantum number. The instance can be interpreted as follows.

I_P for j←i ionization, $I_{Pj\leftarrow i}$, for the k-th normal vibration is defined by

$$I_{Pj\leftarrow i} = (E_T' - E_T'') + \sum_k (\varepsilon'_k - \varepsilon''_k) + 2j\varepsilon'_k - 2i\varepsilon''_k, \qquad (4.7)$$

where E_T and ε_k are the total energy and the zero-point energy, respectively, and the prime and double prime indicate the cationic and the neutral state, respectively. If the electronic energies of NH_3 and ND_3 are equal and if those of NH_3^+ and ND_3^+ are equal, then $I_{Pj\leftarrow i}^D - I_{Pj\leftarrow i}^H$ is given by

$$I_{Pj\leftarrow i}^D - I_{Pj\leftarrow i}^H = \Sigma(\varepsilon_k^{D'} - \varepsilon_k^{H'}) - \Sigma(\varepsilon_k^{D''} - \varepsilon_k^{H''}) + 2j(\varepsilon_k^{D'} - \varepsilon_k^{H'}) - 2i(\varepsilon_k^{D''} - \varepsilon_k^{H''}). \qquad (4.8)$$

If all the frequencies for both the neutral and the cationic state are known, $I_{Pj\leftarrow i}^D - I_{Pj\leftarrow i}^H$ is evaluated easily, by taking the zero-point energies for a given normal mode to

Table 4.2 Ionization Potentials of the First Band for Ammonia (in eV)

I_P		$I_P^D - I_P^H$
NH_3	ND_3	
10.073	10.102	0.029
10.182	10.190	0.008
10.290	10.279	-0.011
10.411	10.369	-0.042
10.527	10.460	-0.067
10.654	10.550	-0.104
10.785	10.587	-0.395
10.909	10.642	-0.143
10.982	10.696	-0.415
11.036	10.738	-0.171
11.111	10.835	-0.201
11.167	10.932	-0.235
.....	.....	.....

be one-half of the fundamental energies according to the harmonic oscllator approximation. Those frequencies for both NH_3 and ND_3 are obtained from the Raman or infrared spectra[7,11,12], however, only part of those frequencies for NH_3^+ and ND_3^+ have been known. In order to estimate the remainder frequencies, the force constants were calculated acording to the valence force field approximation (Eqs. 4.2-4.5). As for ammonia cation, ν_1 and ν_2 are observable in the UPS, however, ν_3 and ν_4 are not detected. Therefore by Eqs. 4.2 and 4.3 the force constants k_1 and k_{Δ/l^2} are able to be calculated from λ_1 and λ_2, while k_{δ/l^2} cannot be obtained directly. Varying the quantities k_{δ/l^2} from zero to 1.0 in order, frequencies ν_3 and ν_4 were calculatred. Comparing ν_1 and ν_2 between the neutral and the cationic state, ν_3 and ν_4 for the cationic state should be smaller than those for the neutral state, so it is expected that values of k_{δ/l^2}'s are within the range of 0.01-0.48. k_{δ/l^2} for ND_3^+, k^D_{δ/l^2}, is estimated to be 10% larger or smaller than that for NH_3^+, k^H_{δ/l^2}, comparing both k_1 and k_{Δ/l^2} between NH_3^+ and ND_3^+, i.e., k_1's are 4.15 and 3.989 mdyne/Å for NH_3^+ and ND_3^+, respectively, and k_{Δ/l^2}'s are 0.385 and 0.428 for NH_3^+ and ND_3^+, respectively. The value of $I^D_{P0\leftarrow0}$-$I^H_{P0\leftarrow0}$ is expected to be 29 meV or 8 meV according to the previous discussions. So testing each k_{δ/l^2} under the above-mentioned conditions, it has been concluded that only

$I_{P0\leftarrow0}^{D}-I_{P0\leftarrow0}^{H}$ of 29 meV is possible and that at that situation $k_{\delta/1^2}$'s are 0.40 and 0.44 for NH_3^+ and ND_3^+, respectively. Thus all the frequencies for NH_3^+ and ND_3^+ have been evaluated and listed with those for NH_3 and ND_3 in Table 4.3.

In Table 4.3 is presented the values of $I_{Pj\leftarrow i}^{D}-I_{Pj\leftarrow i}^{H}$, and by comparing those values between experiments, shown in Table 4.2, and calculations, it may be concluded that I_{Pa}' are 10.073 and 10.102 for NH_3 and ND_3, respectively.

I_P's of vibrational progression for CH_3NH_2 and CH_3ND_2 are listed in Table 4.4. Unfortunately all the frequencies for methylamine cation have not known yet and the calculations to estimate the values are more complicated than for ammonia. Furthermore, as for amino wagging vibration, which is observed remarkabley in the UPS, difference in I_P between 0←1 and 0←0 ionization is equal to that between 1←0 and 0←0 ionization, so I_{Pa}'s have not been confirmed by this method. Then according to the discussion of previous chapter, I_{Pa}'s are chosen to be 8.950 and 8.978 eV for CH_3NH_2 and CH_3ND_2, respectively. As for ethylamine, I_P's are listed in Table 4.5 and same discussions were done. It was concluded that I_{Pa}'s are 8.874 and 8.815 eV for $C_2H_5NH_2$ and $C_2H_5ND_2$, respectively, since difference in I_P between 0←1 and 0←0 ionization is 22 meV and that between 1←0 and 0←0 ionization is 10 meV. Further, as for $C_2H_5ND_2$ ionization peak of 8.715 eV is 0←1,

Table 4.3 The Energies of the Fundamental Vibrations for ammonia and the Calculated Energy Difference $I_P^D - I_P^H$

(in meV)

	$h\nu_1$	$h\nu_2$	$h\nu_3$	$h\nu_4$
NH_3	414	118	428	202
	328	110	345	160
ND_3	300	93	304	148
	227	89	251	117

$I_{Pj}^{D \leftarrow i} - I_{Pj}^{H \leftarrow i}$

j←i	$h\nu_1$	$h\nu_2$
0←2	257	79
0←1	143	54
0←0	143	29
1←0	-72	8
2←0	-173	-13
3←0	-274	-34
4←0	-375	-55
5←0	-476	-76
...	...	...

Table 4.4 Ionization Potentials of the First Band for Methylamine (in eV)

I_P CH_3NH_2	I_P CH_3ND_2	$I_P^D - I_P^H$
8.950	8.978	0.028
9.045	9.053	0.008
9.140	9.128	-0.012
9.231	9.201	-0.031
9.316	9.272	-0.044
9.411	9.342	-0.069
9.501	9.413	-0.088
9.573	9.473	-0.100
9.665	9.547	-0.118
9.748	9.618	-0.130

Table 4.5 Ionization Potentials of the First Band for Ethylamine (in eV)

I_P $C_2H_5NH_2$	I_P $C_2H_5ND_2$	$I_P^D - I_P^H$
-	8.715	-
8.784	8.815	0.031
8.883	8.903	0.020
8.983	8.985	0.002
9.085	9.070	-0.015
9.190	9.135	-0.055

i.e., hot band. Thus determination of I_{Pa} shown in the previous chapter is found to be reasonable and the judgement of hot band by considering Boltzmann distribution is found to be adequite.

According to the discussion of the previous chapter, I_{Pa} for $(CH_3)_2ND$ is estimated to be 8.31 eV by adding vibrational frequency of the neutral state, 0.07 eV[13,14], to I_{Pth}, 8.24 eV. I_{Pa} could not be decided by the method descrived in this chapter because vibrational peak was not separated clearly in the UPS for both $(CH_3)_2NH$ and $(CH_3)_2ND$. Thus I_{Pa}'s for both dimethylamine were taken to values decided by method descrived in the previous chapter.

References

[1] J. H. D. Eland, "Photoelectron Spectroscopy", Butterworth and Co., London (1974), Chap. 5.

[2] H. J. Emeléus and H. V. A. Briscoe, *J. Chem. Soc.*, 1937, 127.

[3] E. R. Roberts, H. J. Emeléus, and H. V. A. Briscoe, *J. Chem. Soc.*, 1939, 41.

[4] A. P. Gray and R. C. Lord, *J. Chem. Phys.*, 26, 690 (1957).

[5] P. A. Leighton, *J. Am. Chem. Soc.*, 53, 3017 (1931).

[6] K. Morokuma, S. Kato, K. Kitaura, I. Ohmine, S. Sakai, and S. Obara, IMS Computer Center Library, Institute for Molecular Science, No. 0372 (1980).

[7] G. Herzberg, "Molecular Spectra and Molecular Structure II. Infrared and Raman Spectra of Polyatomic Molecules", Van Nostrand, New Tork (1945), Chap. 2.

[8] G. R. Branton, D. C. Frost, F. G. Herring, C. A. McDowell, and I. A. Stenhouse, *Chem. Phys. Lett.*, 3, 581 (1969).

[9] G. R. Branton, D. C. Frost, T. Makita, C. A. McDowell, and I. A. Stenhouse, *Phil. Trans. R. Soc. Lond.*, A268, 77 (1970).

[10] A. W. Potts and W. C. Price, *Proc. R. Soc. Lond.*, 326A, 181 (1972).

[11] M. V. Migeotte and E. F. Barker, *Phys. Rev.*, 50, 418

(1936).

[12] W. S. Benedict and F. K. Plyler, *Can. J. Phys.*, 35, 1235 (1957).

[13] W. G. Fateley and F. A. Miller, *Spectrochim. Acta*, 18, 977 (1962).

[14] G. Dellepine and G. Zerbi, *J. Chem. Phys.*, 48, 3573 (1968).

Chapter 5. Correlation Between Electrochemical and Photoelectron Spectroscopic Data

5.1 Introduction

A certain molecule deforms so significantly after ionization of the HOMO electron that the equilibrium or ground-state molecular geometries are quite different for the reactant and the product cation. For such a molecule one expexts the first band of the UPS to have a large difference between the vertical I_p's, or no observable adiabatic I_p and only a broad structureless band, and the electrochemical oxidation to behave totally irreversibly because of the large activation energy needed to rearrange the molecular geometry for the oxidation to occur through a thermal electron transfer process. This implies that, if, the intramolecular reorganization energy contributes most of the total reorganization energy for the oxidation reaction, the band shape in the UPS should be correlate with the parameter for electron transfer kinetics for the irreversible electrode reaction. As for the electrode kinetics, discussion by means of the potential energy curve has been a few and limited to hydrogen generation at the platinum electrode[1,2] or theoretical ones.[3] So it is meaningful to discuss about the electrode kinetics by both

the experiment and the theory by the use of the potential energy curve.

Alkylamines undergo a large geometrical change with ionization, and give a broad first band in the UPS, and an irreversible oxidation wave on a cyclic voltammogram.[4-6] In Refs. 4 and 6, the potential sweep rate was slower than 11 volts per second. So In this chapter, the cyclic voltammograms of higher potential sweep rate have been presented and correlation between the electrochemical and the photoelectron spectroscopic data is presented on the basis of the previous potential energetic considerations.

5.2 Experimental

5.2.1 Reagents

The amines used were prepared by heating the aminehydrochloride with CaO to 420-470 K in a vacuo. As descrived in the chapter 4, the aminehydrochloride were recrystallized three times from ethanol, and Cao had been heated under a running vacuum at 720 K for several days. The apparatus used in the preparation was the same one descrived in Fig. 4.1. The acetonitrile was purified by methods descrived as follows: Method 1; (1) degassing by a series of freeze-pump-thraw cycles; (2) dehydrating by stirring with P_2O_5 for a few hours; (3) interchanging P_2O_5 by

moving acetonitrile by a vacuum-distillation technique; (4) repeating (2) and (3) for a few times; (5) distillating acetonitrile to the cell vessel by the vacuum-distillation: Method 2; dehydrating by stirring with P_2O_5 overnight and distillating at 353.5-355 K under the atmospheric pressure. Difference of the methods of purification was not detected and measurements were almost done using acetonitrile distilled by the method 2. The $NaClO_4$ for supporting electrolyte used was recrystallized from water and dehydrated at the temperature over 400 K under the running vacuum and was stored over $Mg(ClO_4)_2$.

5.2.2 Apparatus

A schematic diagram of the apparatus is shown in Fig. 5.1. Voltammograms were obtained with a three-electrode operational amplifier arrangement. The potential sweep was a staircase wave form[4,7] by the out-put of the digital-analog(D/A) convertor controlled by the CPU and the current, converted to the voltage, was stored to the memory through the analog-digital(A/D) convertor. The use of the staircase wave form makes enable to eliminate the effects of charging current since the electrode double layer charging current decays more rapidly than faradaic current.[7] The sweep form was either a one-cycle triangle, positive going, then negative going, or multi-cycle sweeps. The sweep rates

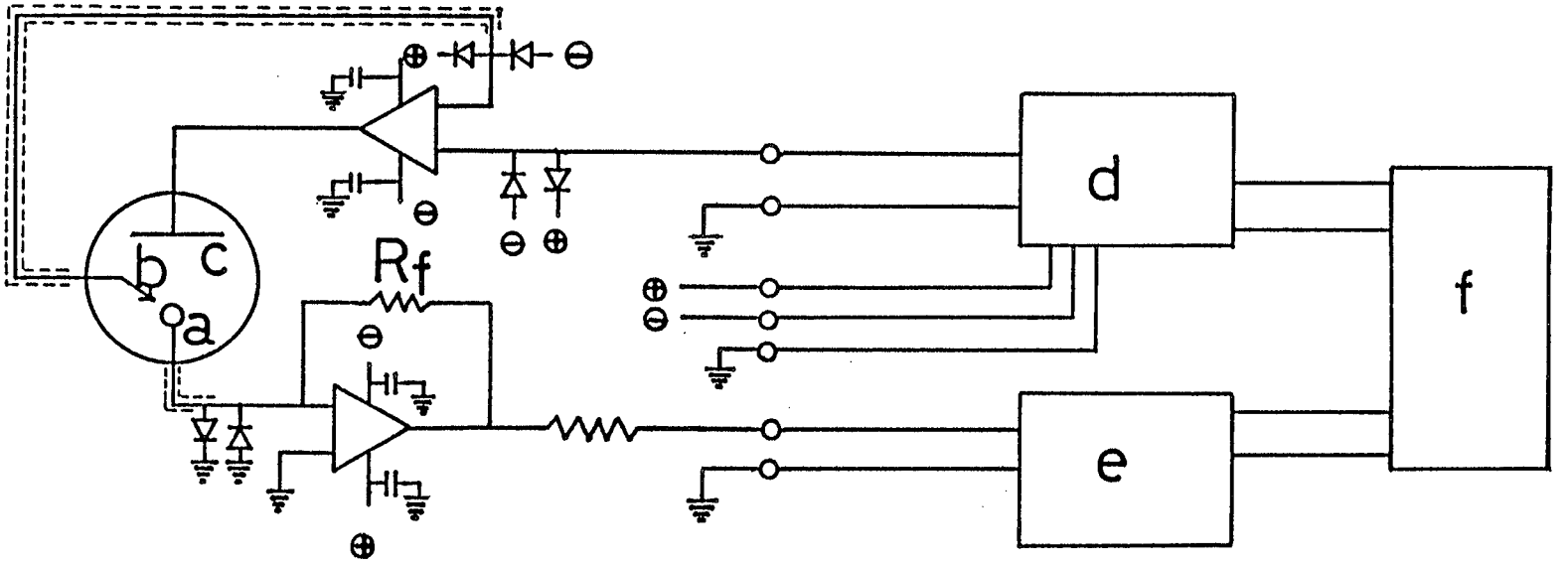

Fig. 5.1. Schematic digram of apparatus. a;working electrode. b;reference electrode. c;counter electrode. d;D/A convertor. e;A/D convertor. f;CPU.

used were the range of 6-50 volts per second. In order to sweep at high speed, FET input operation amplifier, μA356 was used in the circuits of both the potentiostat and the current transducer. The highest rate to be used pratically was limited by the speed of D/A or A/D conversion, i.e., the D/A conversion needs 300 μs at least and the A/D conversion does 130 μs. The sweep wave form was adjusted to give steps having risers varying from 5 to 30 mV, and flats varying from 50 to 300 μs. The D/A and A/D convertor were calibrated by a digital voltmeter and the input of the A/D convertor was calibrated with a known resistor every a few hours.

The working electrode was consisted of a 0.1 mm diameter platinum wire embeded in a glass. That was made as follows: Glass tube of 8 mm external diameter was heated and its internal diameter was made to be about 0.1 mm. Then inserting platinum wire into the glass tube, the glass was sealed under a running vacuum. Cutting the glass at a proper spot, it was polished by two kind of sand papers, i.e., one was coarse grained and the other was fine, and was finally polished with alminum powders. The counter electrode was a 0.5 mm platinum spiral of about 8 mm external diameter. The reference electrode was $Ag/AgNO_3$ (0.10 mol/dm^{-3}) in acetonitrile, which was separated from sample solutions by a cracked glass. In

order to minimize stray capacitance, no switches were used, and the magnitude of the current gain was adjusted by replacing the feedback resistor, R_f. In addition, the lead from the working electrode to the current transducer was ca. 5 cm, so were that from the potentiostat out-put to both the counter electrode and the reference electrode, and all the lead used were shielded wires. All experiments were conducted in a metal box grounded to earth.

5.2.3 Cyclic Voltammogram Measurements

The following procedure was used to obtain the voltammograms. 0.100 mol/dm^{-3} $NaClO_4$ in acetonitrile (20 cm^3) was placed in the cell and a blank was recorded. 5 cm^3 of 0.01 mol/dm^{-3} amine in acetonitrile solution was then added and after mixing, a voltammogram was recorded. Following the measurement, 2 cm^3 of 0.01 mol/dm^{-3} ferrocene in acetonitrile solution was added and after mixing, a voltammogram was recorded again. In this concentration R_f used was 1MΩ. The electrode pretreatment used was to polish with alumina powders. The potential of the ferrocinium/ferrocene couple ($E°$=0.400 V vs. NHE)[8] was used as the internal reference.[9]

5.3 Some Equations on the Cyclic Voltammogram

5.3.1 Reversible Electrode Reaction

Supposing a reversible reaction

$$O_x + ne \rightleftharpoons R, \tag{5.1}$$

the following equations describing current-voltage-relationships for stationary electrode voltammetry have been given by Matsuda and Ayabe[10] and Nicholson and Shain[11] and are repeated here.

$$E^\circ = E_{\frac{1}{2}} - RT/nF \ln(\gamma_O D_R^{\frac{1}{2}} / \gamma_R / D_O^{\frac{1}{2}}), \tag{5.2}$$

then

$$E_{\frac{1}{2}} = E_p \pm 1.1 RT/nF, \tag{5.3}$$

and

$$E^\circ = (E_{Pa} + E_{Pc})/2. \tag{5.4}$$

Where $E_{\frac{1}{2}}$ is the half wave potential; E° the formal electrode potential; γ the activity coefficient in which subscript O and R denote oxidized and reduced form; D diffusion coefficient in cm^2/s; n the total number of electrons per mole of reactant; E_{Pa} and E_{Pc} the anodic peak potential and the cathodic peak potential, respectively. Thus at 302 K,

$$|i_{Pa}| = |i_{Pc}| = 269 A n^{3/2} D_R^{\frac{1}{2}} C_R^b v^{\frac{1}{2}}, \tag{5.5}$$

$$E_p = E_{\frac{1}{2}} + 0.0285/n, \tag{5.6}$$

$$\Delta E_p = E_{Pa} - E_{Pc} \cong 0.060/n. \tag{5.7}$$

Where i_p is peak current in A; A the electrode area in cm^2; C_R^b the bulk concentration of the reduced form in mol/dm^{-3}; v the sweep rate in V/s.

5.3.2 Irreversible Electrode Reaction

Supposing an irreversible oxidation reaction,

$$O_x + ne \underset{}{\overset{k}{\longleftarrow}} R, \tag{5.8}$$

the following equations have been given by Matsuda and Ayabe[10] and Nicholson and Shain,[11]

$$k=k_s\exp[(-\beta n_a F/RT)(E-E^\circ)], \tag{5.9}$$

where k_s is the constant independent of the potential; βn_a the number of electrons per mole of reactant in the rate determinimg step times symmetry factor, whose physical meaning is one of subjects of discussion in this study. Thus

$$i=nFAC_R{}^b D_R{}^{\frac{1}{2}}\pi^{\frac{1}{2}}\chi(bt), \tag{5.10}$$

where
$$b=\beta n_a Fv/RT, \tag{5.11}$$

and
$$bt=(\beta n_a F/RT)(E_i-E). \tag{5.12}$$

$$i_P=299n(\beta n_a)^{\frac{1}{2}}AD_R{}^{\frac{1}{2}}C_R{}^b v^{\frac{1}{2}}, \tag{5.13}$$

$$E_P=E_{\frac{1}{2}}+RT/(\beta n_a F)(0.780+\ln(D_R{}^{\frac{1}{2}}/k_s)+\ln b^{\frac{1}{2}}). \tag{5.14}$$

Then the following equation is derived as,

$$\Delta E_P=E_{P/2}-E_P=0.048/\beta n_a, \tag{5.15}$$

in which, the constant is adjusted for 302 K.

The symmetry factor β is also appeared in the well-known Butler-Volmer electrodic equation

$$i=i_0[\exp[(1-\beta)F\eta/RT]-\exp[-\beta F\eta/RT]], \tag{5.16}$$

with

$$i_0=F\vec{k}C_R{}^b\exp(-\beta F\Delta\phi_e/RT)=F\overleftarrow{k}C_O{}^b\exp((1-\beta)F\Delta\phi_e/RT), \tag{5.17}$$

where i is the drift-current density (or simply current density) and i is given by the difference between the

oxidation $\vec{i}$ and the reduction $\overleftarrow{i}$ current; $\Delta\phi_e$ the equilibrium potential; η the overpotential; C_R^b and C_O^b the bulk concentration of the reduced and the oxidized forms, respectively. $\beta F\eta$ is argued crudely as the ammount by which the energy barrier for the molecule-to-electrode transfer is lowered and this argument will be transformed later in this chapter to a quantum-mechanical one. Furthermore in terms of the transfer coefficients, $\vec{\alpha}$ and $\overleftarrow{\alpha}$, Eq. 5.16 can be rewritten thus,

$$i=i_0[\exp[\vec{\alpha}F\eta/RT]-\exp[-\overleftarrow{\alpha}F\eta/RT]]. \qquad (5.18)$$

Equation 5.18 is the most general form of the Butler-Volmer equation and Eq. 5.16 is used in the case of a one-step, single-electron transfer reaction.

5.4 Results and Discussion

5.4.1 Electrochemical Data

The experiments presented here involved $PrNH_2$, Pr_2NH, and Pr_3N. (Pr denotes propyl group here.) All of these gave oxidation peaks in acetonitrile and the reaction products were completely soluble under the conditions of these experiments. In Fig. 5.2 cyclic voltammograms are shown and Table 5.1 presents the electrochemical data obtained with various sweep rate. (As for the electrochemical oxidation of alkylamines in acetonitrile n_a is known to be equal to

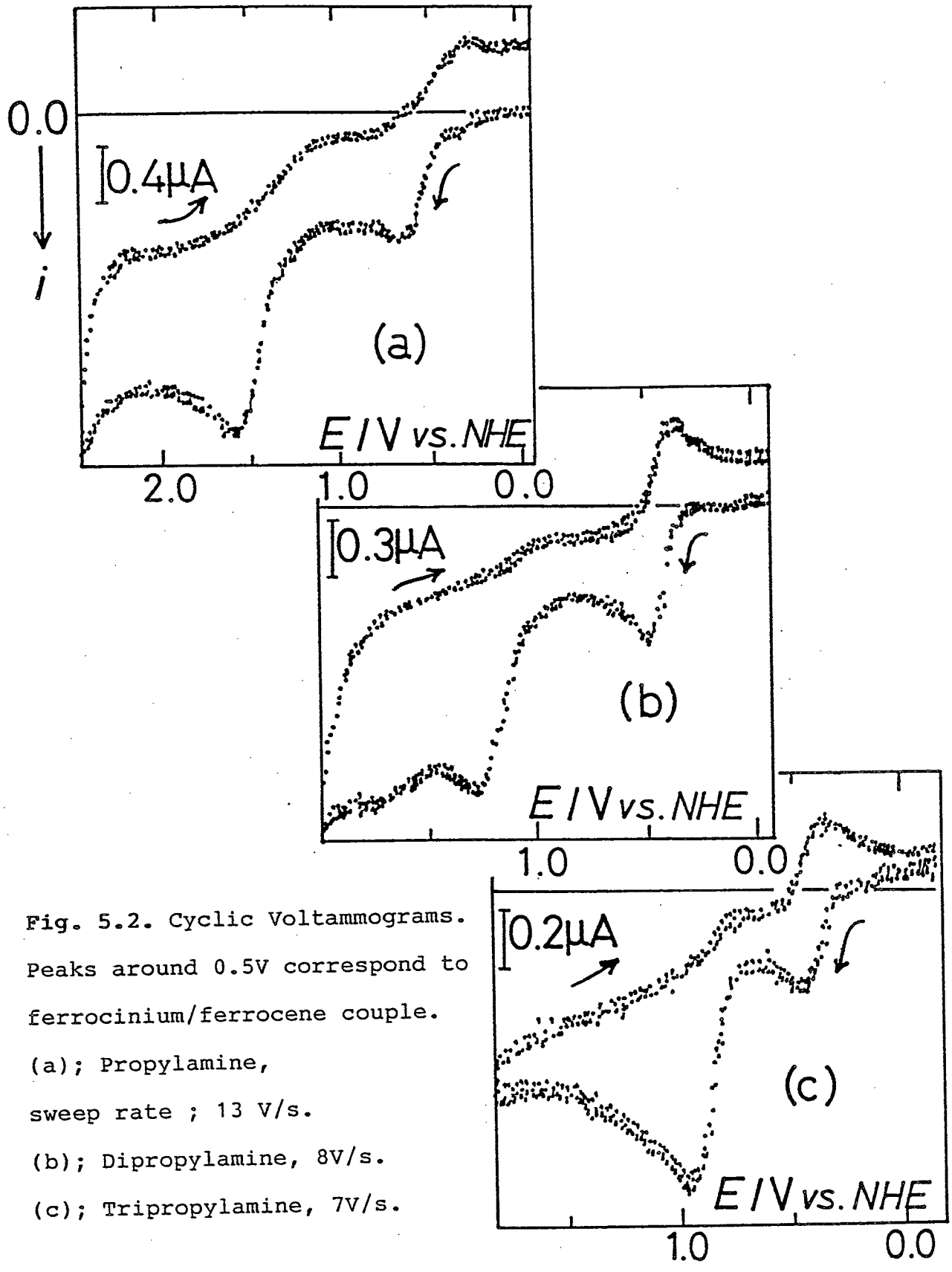

Fig. 5.2. Cyclic Voltammograms. Peaks around 0.5V correspond to ferrocinium/ferrocene couple.
(a); Propylamine,
sweep rate ; 13 V/s.
(b); Dipropylamine, 8V/s.
(c); Tripropylamine, 7V/s.

Table 5.1 Peak Potential, E_p, Anodic Peak Current, i_{Pa}, and Symmetry Factor, β on Several Sweep Rate, v

	v/Vs^{-1}	E_{Pa} a)/V	E_{Pc} a)/V	i_{Pa}/μA	β
$PrNH_2$	14	1.53	1.27	2.1	0.14
	15	1.61	1.16	2.3	0.13
	18	1.58	1.18	2.5	0.11
Pr_2NH	8	1.29	1.19	0.7	0.20
	17	1.28	1.17	1.3	0.16
	33	1.37	-	1.8	0.12
Pr_3N	7	0.97	0.88	0.9	0.32
	17	0.97	(0.93)	1.2	0.28
	33	1.07	-	2.0	0.22
	50	1.06	-	2.5	0.19

a) *vs. NHE.*

one,[4] so only β is used in this study.) Mann reported that in no case could any indication of reduction of the amine or of its reaction products be detected,[4] however, that seems to have been slightly observed as shown in Fig. 5.2.

There may well be some tendency that the E_{Pa}'s increase with increasing sweep rate. And the i_p's increase with increasing sweep rate, while the β's slightly decrease. It is derived from Eq. 5.14 that the E_p varies only 30 meV when the sweep rate, v, becomes ten times at 300 K, however, E_p's obtained both in this study and in Ref. 4 varied more than 30 meV when v changes within about a few times. The phenomenon should be necessary to be discussed further. The value of E_{Pa}-E_{Pc} is about 60 mV if the electrode reaction is reversible,[11] however, these values for the present molecules are far larger, so the reactions are able to be concluded not to be reversible. Further the cathodic peak is still ambiguous, so the phenomenon is disputable yet. In fact it is known that the elimination of hydrogen is followed after the electron transer,[12-15] and so the E_{Pc} cannot be seen at slower sweep rate or should be ambiguous peak.

5.4.2 Correlation between the Electrochemical and the Photoelectron Spectroscopic Data

Figs. 5.3 and 5.4 shows the correlation between E_{Pa},

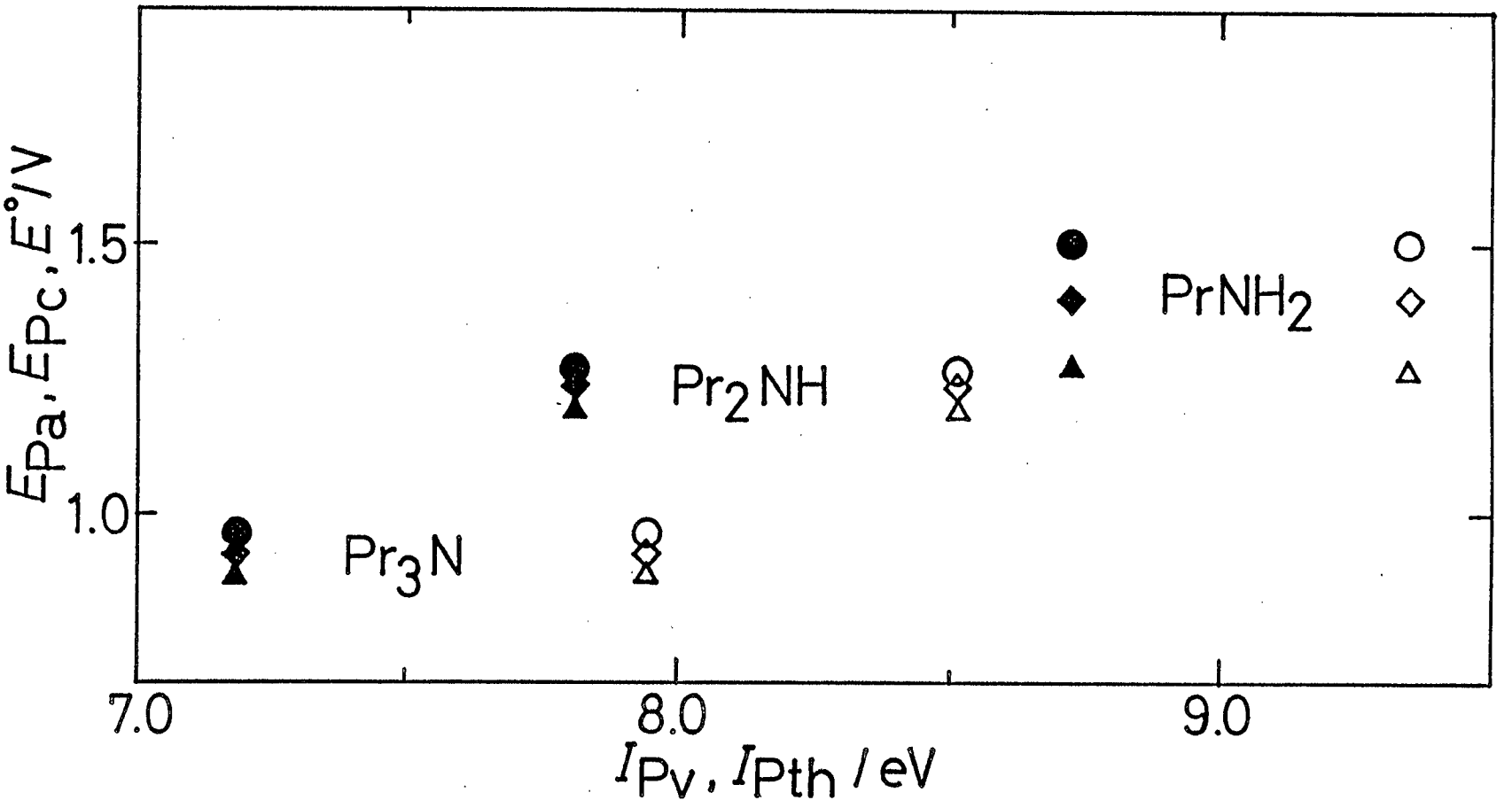

Fig. 5.3. Plots of electrochemical data, E_{Pa} (○), E_{Pc} (△), and $E°$ (◇) vs. ionization potentials, I_{Pv} (open marks) and I_{Pth} (closed marks)

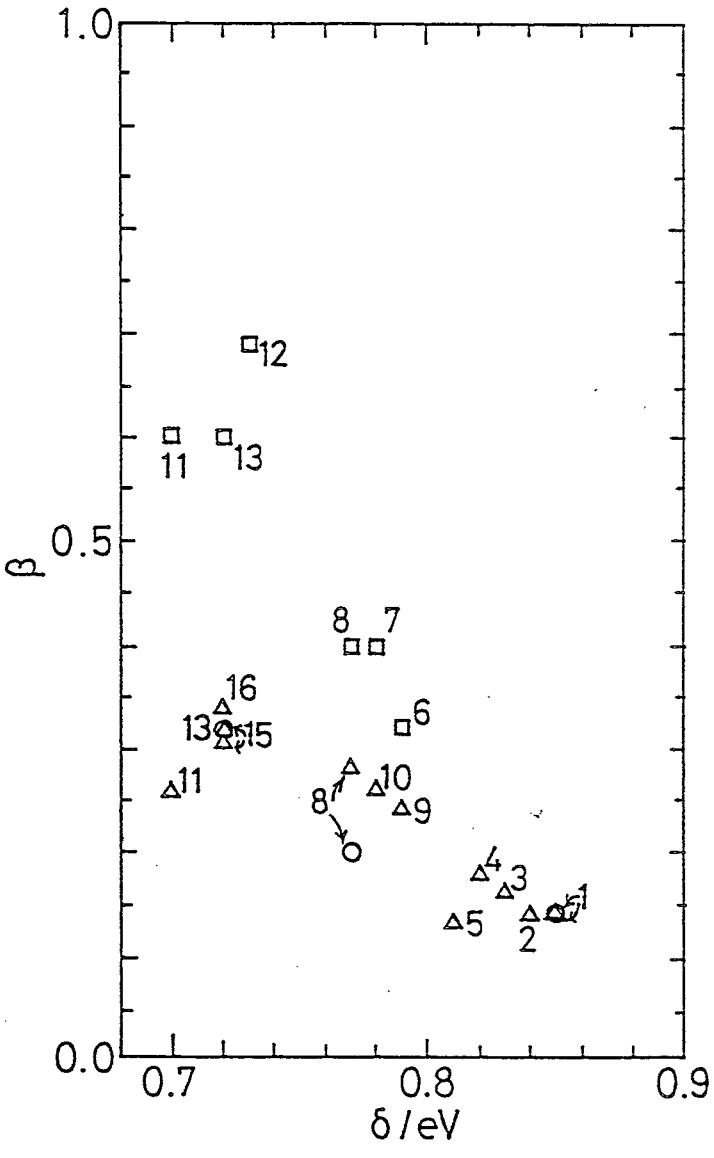

Fig. 5.4. Plots of symmetry factor, β, vs. band width, δ. (△) and (□) are taken from Refs.4 and 6. (1);Propylamine, (2);butylamine, (3);*i*-butylamine, (4);*t*-butylamine, (5);amylamine, (6);dimethylamine, (7);diethylamine, (8);dipropylamine, (9);dibutylamine, (10);diamylamine, (11);trimethylamine, (12);dimethylethylamine, (13);triethylamine, (14);tripropylamine, (15);tributylamine, (16);triamylamine.

E_{Pc}, or $E°$, calculated by means of Eq. 5.4, and I_{Pv} and the correlation between β and δ. The former has been checked for many compounds by many workers,[17-20] however, the latter has been done for the first time. The former has been understood by thinking that the first I_P for the UPS and the E_{Pa} correspond to both the release of the HOMO electron. While the latter can be understood by introducing potential energy diagrams for the amine and the amine cation in very crude way.

The geometrical structure of amines should change significantly after removal of the nitrogen lone-pair electron by either photoelectron emission or electrochemical oxidation at an electrode. Potential energy diagrams for the species involved in the photoionization or oxidation process are illustrated in Fig. 5.5. The configurational coordinated in Fig. 5.5 is the deformation angle ψ as defined in chapter 3. Since the nitrogen skeleton for a ground-state neutral amine molecule is pyramidal,[21-23] the potential energy curve for the neutral molecule M has a double minimum and a maximum (ψ=0°). The potential energy curve for an ion molecule M^+_{vac} has a single minimum at ψ=0° because the ground-state nitrogen moiety for the ion molecule is planar.[24-26] Now assuming that the shapes of potential energy curve for M in solution and in the gaseous phase are similar by neglecting the solvation effect and

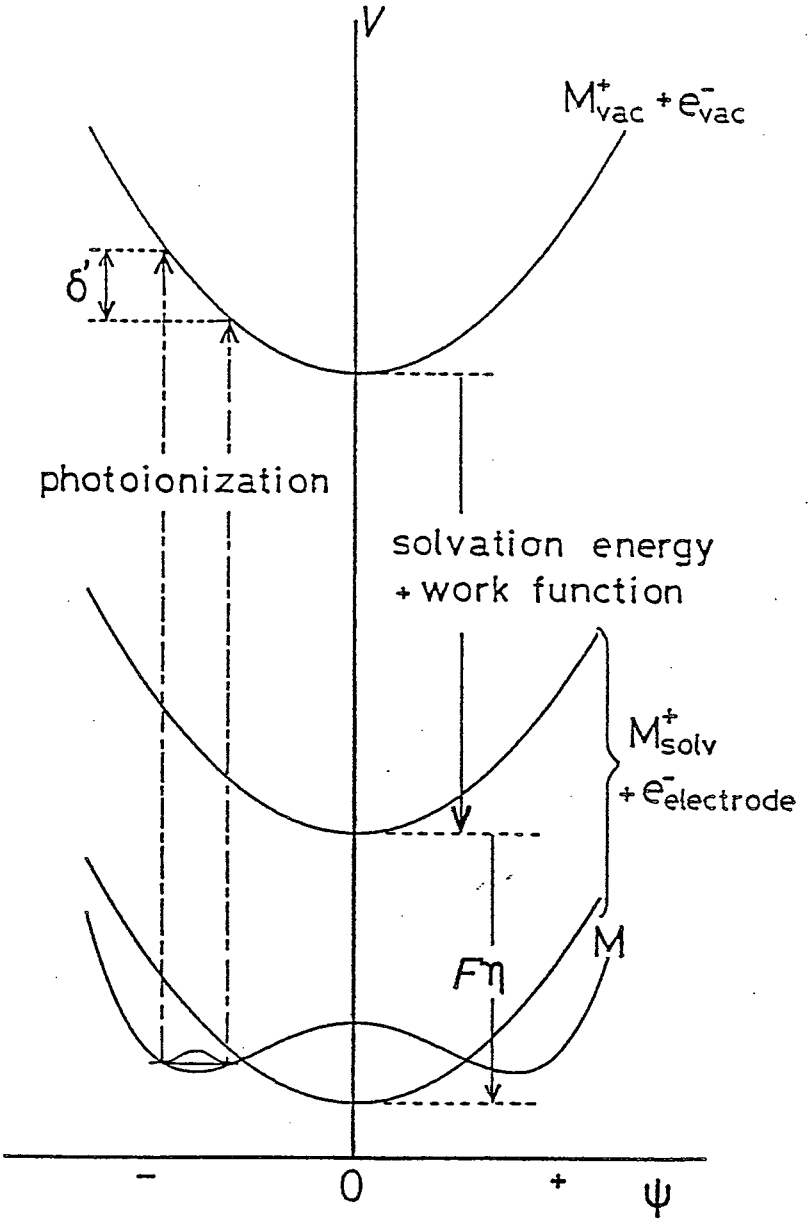

Fig. 5.5. Hypothetical potential energy curves for the neutral and the cation molecules which are involved in the photoionization and electrochemical processes. The potential energy curve for ($M^+_{vac}+e^-$) is stabilized by the solvation of the ion and the stabilization of an electron by moving into an electrode, and further by electrode potential $F\eta$. δ' represents full-band-width of the UPS.

that the potential energy curve for M^+_{solv} in solution, produced by electrolytic oxidation, is given by shifting the potential energy curve for M^+_{vac} in the gaseous phase downword by an amount equal to the solvation energy of M^+ and the work function of the electrode material. The potential energy curve for M^+_{solv} is further shifted vertically by an energy $F\eta$ when the electrode is positively charged by η. However, the potential of the neutral molecule M is not affected by the electrical potential. Since the absolute stabilization energy for each system is of no concern in the present discussion, the potential energy curves for both M_{vac} and M_{solv} are represented by the same curve M.

In order to make the diagram even simpler the potential energy barrier near the intersection point is made up of straight lines as shown in Fig. 5.6, which has been frequently used by Bockris[27] to interpret the symmetry factor β with regard to the potential energy profiles for the reactant and product. The electrical energy $F\eta$ introduced into the system decreases the activation energy for the oxidation reaction by $\beta F\eta$. When the slopes θ and γ of the potential energy curves for reactant M and product M^+, respectively, are used, the symmetry factor β is expressed as follows,[27]

$$\beta=\tan\theta/(\tan\theta+\tan\gamma). \qquad (5.19)$$

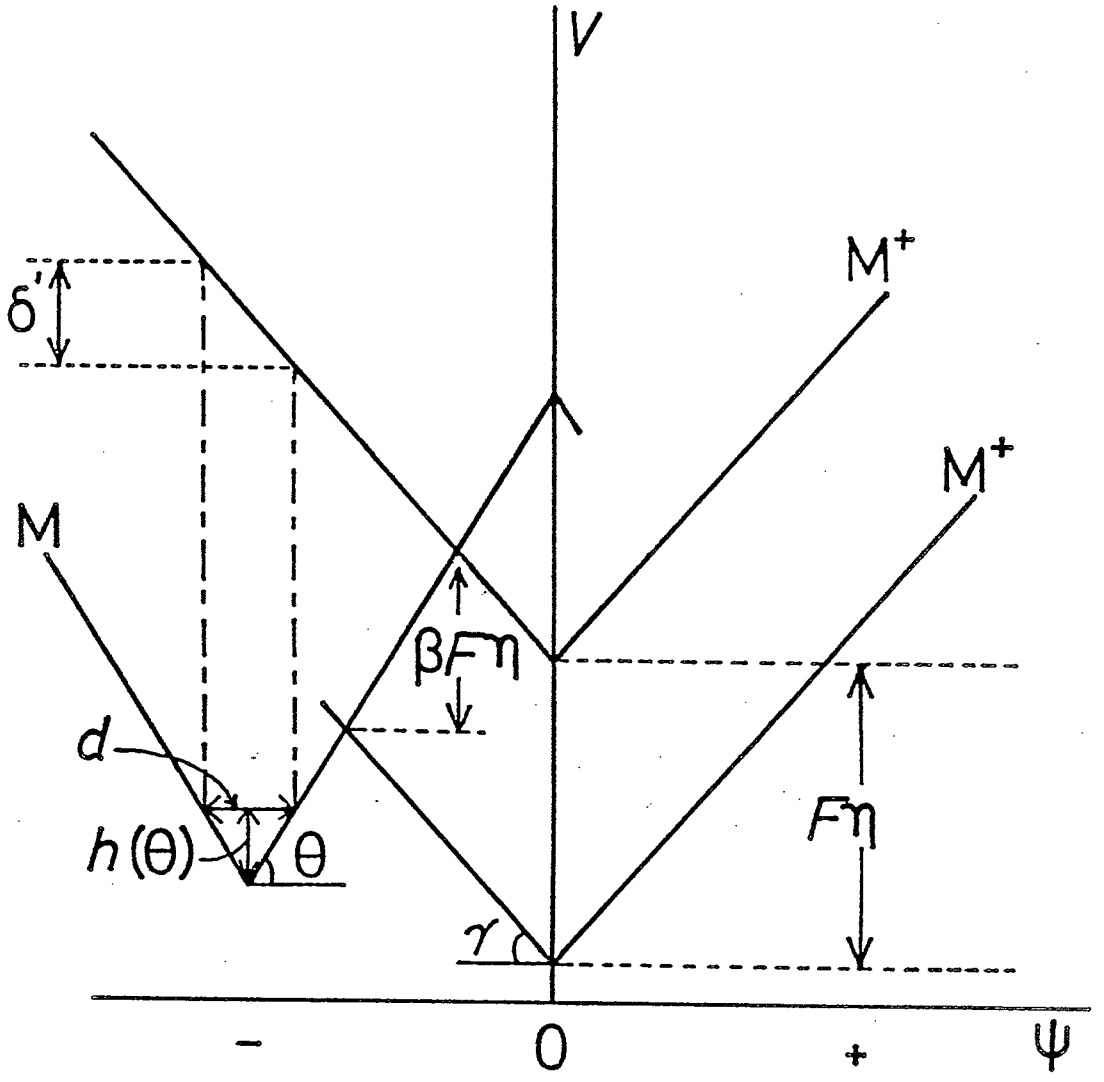

Fig. 5.6. Linearized potential energy curves for the neutral and the ion molecule. δ' represents full-band-width of the UPS.

By use of the diagram in Fig. 5.6, the origin of the band width in the UPS can also be interpreted. The full-band width δ' is equal to the length of the potential energy curve of ion molecule M^+ corresponding to the breadth d of the potential energy curve of neutral molecule M in the ground state. Here, δ' is about twice δ because of the linearized curves. In order to estimate d the zero-point energy is necessary. The zero-point energy is a function of the force constant and the reduced mass, and therefore is closely related to the potential energy profile and to the slope θ. Thus the zero-point energy for M is defined here as $h(\theta)$. Now, the slopes θ and γ are given as

$$\tan\theta=2h(\theta)/d, \tag{5.20}$$

and

$$\tan\gamma=\delta'/d. \tag{5.21}$$

By substituting $\tan\theta$ and $\tan\gamma$ in Eq. 5.19, the symmetry factor β is giben as

$$\beta=h(\theta)/(h(\theta)+\delta'/2). \tag{5.22}$$

Hence if $h(\theta)$ should happen to be constant, or does not change much for molecule to molecule under study, a negative correlation must exist between the symmetry factor and the band width as shown in Fig. 5.7.

In the above discussions, however, some of the very important factors which critically control electron transfer reactions on the electrode in solution are completely neglected. Those factors, for example, are the

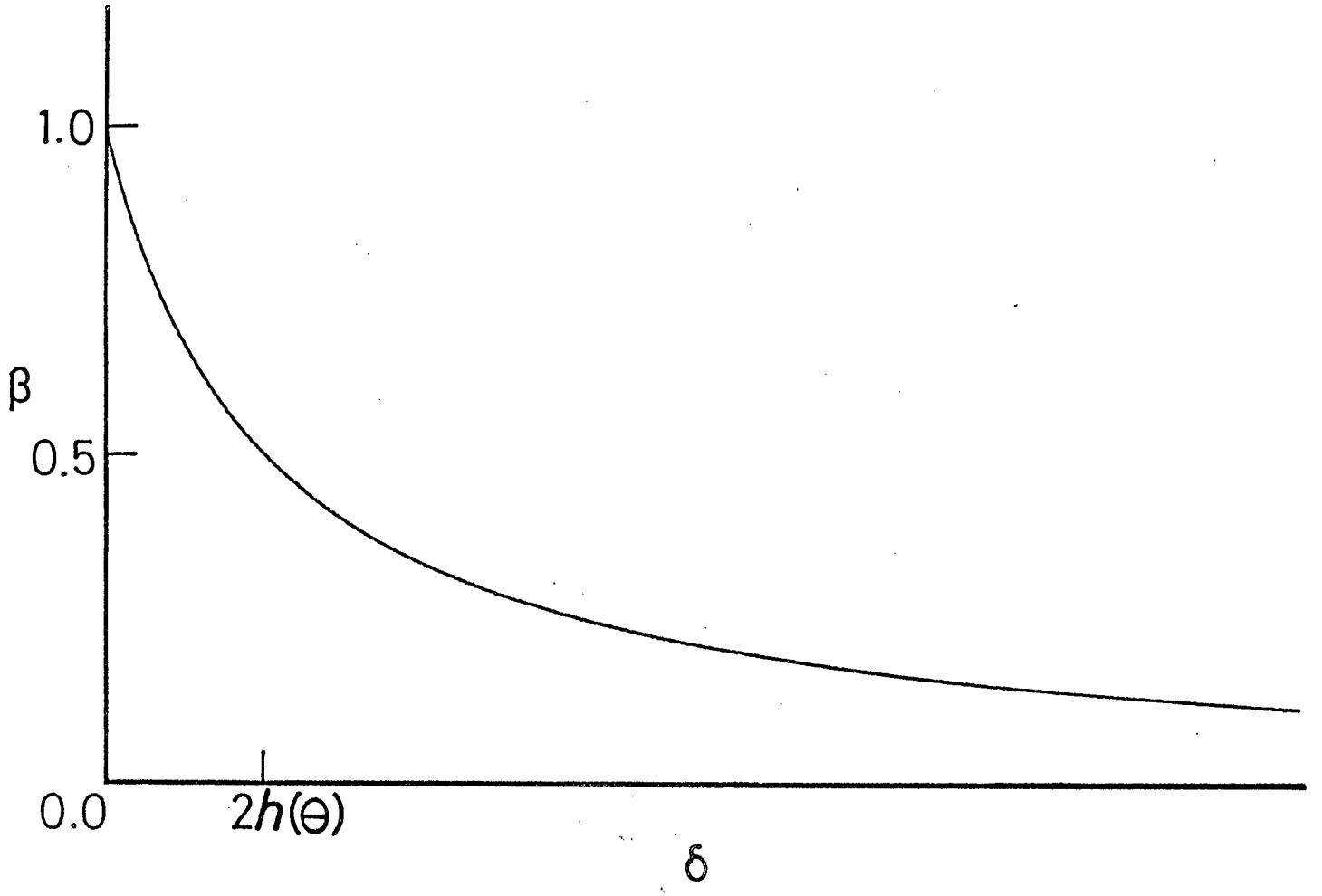

Fig. 5.7. The predicted correlation between the symmetry factor β and the band width δ, under the assumption that $h(\theta)$ is a constant.

reorganization energy in the solvation sphere and the effect of the double-layer structure which could be drastically affected by the nature of the elctrode material, supporting electrolyte, and adsorption of reactants or products. Those factors, however, seem to have a minor effect on the β-δn correlation for alkylamines because the same kind of correlation also exists with the symmetry factor taken at a glassy carbon electrode in an aqueous alkaline solution.[6] This fact indicates that most of the activation energy for the oxidation reaction of amines originates from the intramolecular reorganization energy. The system having a good β-δ correlation must have a HOMO which fixes the molecular geometry firmly and because of this fact it should have a broad first band in the UPS and a totally irreversible electrode reaction.

5.4.3 Estimation of the Symmetry Factor by Means of the Potential Energy Curve

In order to verify the idea descrived in the preceding section, calculations of the symmetry factor were done by using the foregoing potential energy curves. Since using the curve instead of the line, Eq. 5.22 is rewritten by,

$$\beta=-\partial E_a/\partial \Delta F\eta, \qquad (5.23)$$

where E_a is the activation energy for the oxidation reaction as shown in Fig. 5.8. Therefore β is calculated by the

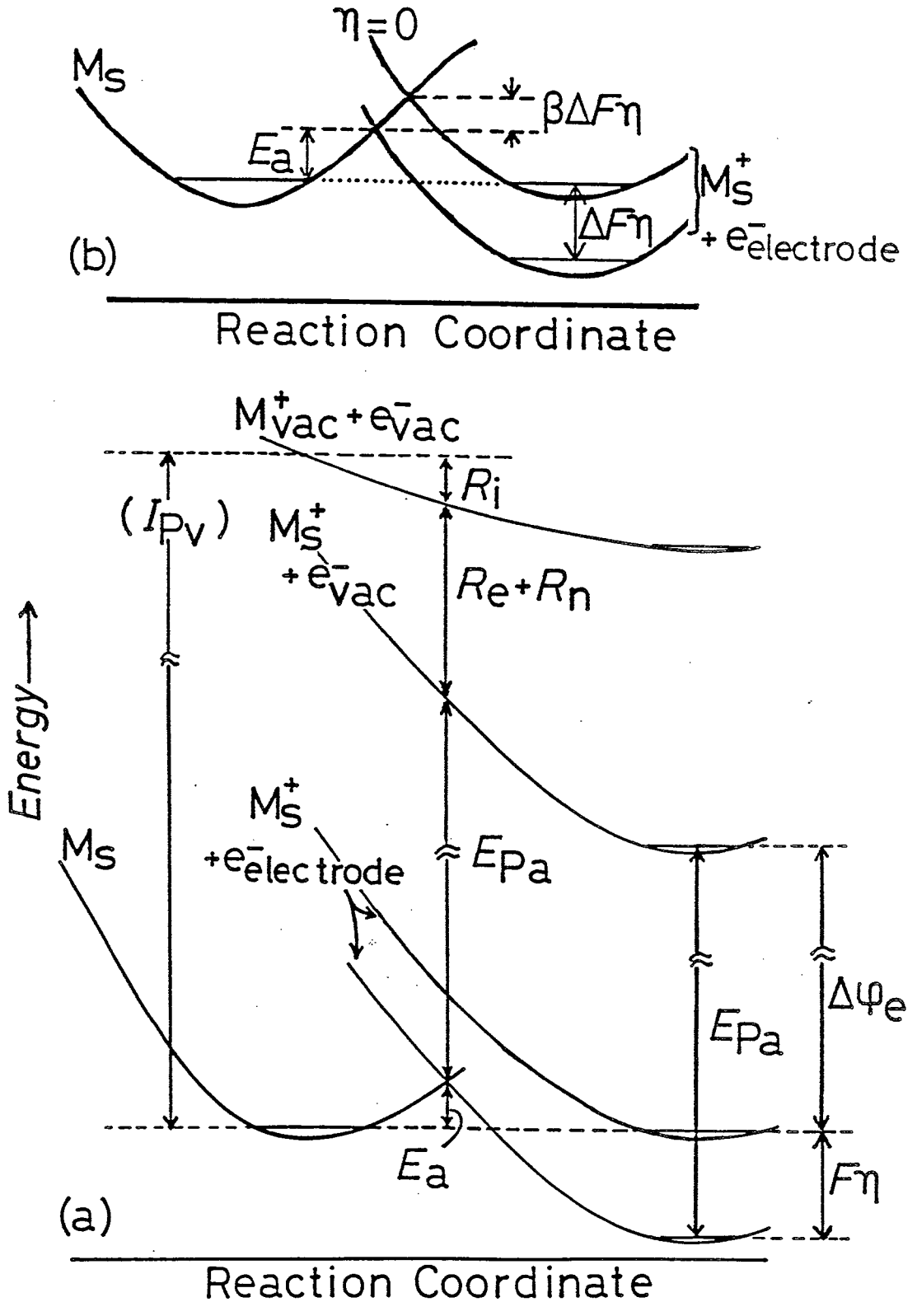

Fig. 5.8. The symmetry factor β and oxidation peak potential E_{Pa} on the potential energy curves.

differential of the curves for both the neutral and the cation molecule at the intersection point. Figure 5.8a shows the I_P and E_{Pa} on the potential energy curves. Now E_{Pa} is used in stead of the oxidation potential because the latter has never determinated yet and has been still ambiguous in this study. The peak potential is the potential at which a rate of transport of spcies is slower than the rate of oxidation or reduction of the species and then the potential is dependent on the sweep rate,v. The value is difficult to define thermodynamically, however on the curves, shown in Fig. 5.8, the point at which E_{Pa} is denoted is expressed where the activation energy is equal to E_a, and on that point reorganizations for the intramolecule, the electrons, and the solvent molecule, whose energies are shown by R_i, R_e, and R_n, respectively, partially occure. If M_{vac} is equal to M_s I_{Pv} is indicated as shown in Fig. 5.8a.

According to the preceding approximation, the shape of a potential energy curve for a cation does not change on solvated by a solvent, so R_e and R_n are constant. Thus the potential energy curve for M^+_{vac} was used as the curve for M^+_{solv} and β was calculated as follows; at first the curve for M^+_{solv} was shifted downword till the difference in energy for the ground state between the neutral and the cation molecule became to zero, i.e., the equilibrium potential, $E°$; furthermore the curve for M^+_{solv} shifted every 5 meV and

then β was calculated each time. The shifted values from E° are called the overpotential, η. Table 5.2 presents β calculated at a several η for ammonia, methylamine, dimethylamine, and trimethylamine. β's dcrease with the increase of η and the instance has not been generally confirmed yet. However, it has been slightly seen in also Table 5.1 and also observed for tetraalkylstannum.[28] It is the first time that the dependence of β on η has been discussed by the experiment and the calculation by using the potential energy curve.

As shown in Table 5.1 or Fig. 5.4, β's has increased in the order of primary, secondary, and tertiary, however, those calculated decreased in the same order or were about equal, as shown in Table 5.2 if E_a's are similar for all amines. This was concluded that effects of the solvation to potential energy curves must be considered.

Now plots E_{pa} obtained in this study together with those reported by other workers against I_{pv} are shown in Fig. 5.9. Thus,

$$E_{pa}=0.46I_{pv}+\text{const}, \tag{5.24}$$

for E_{pa} obtained in this study, and

$$E_{pa}=0.43I_{pv}+\text{const}, \tag{5.25}$$

and

$$E_{pa}=0.46I_{pv}+\text{const} \tag{5.26}$$

for E_{pa} reported in Ref. 4, and Ref. 6, respectively. These equations indicate that the value of E_{pa} for the tertiary

Table 5.2 Activation Energy, E_a, and symmetry factor, β, calculated by use of the potential energy curves at a several overpotentials

compound	$F\eta$/eV	E_a/eV	β
ammonia	0.0	0.24	0.46
	0.10	0.20	0.42
	0.20	0.16	0.38
	0.30	0.12	0.33
	0.40	0.09	0.29
	0.50	0.06	0.25
	0.60	0.04	0.21
	0.68	0.026	0.15
methylamine	0.0	0.22	0.53
	0.10	0.17	0.47
	0.20	0.12	0.41
	0.30	0.08	0.35
	0.40	0.05	0.28
	0.50	0.03	0.21
	0.51	0.026	0.19
dimethylamine	0.0	0.19	0.51

Table 5.2 (*continued.*)

(dimethylamine)	0.10	0.14	0.46
	0.20	0.10	0.41
	0.30	0.06	0.34
	0.40	0.03	0.25
	0.43	0.06	0.23
trimethylamine	0.0	0.17	0.44
	0.10	0.13	0.38
	0.20	0.10	0.33
	0.30	0.06	0.28
	0.40	0.04	0.72
	0.47	0.026	0.18

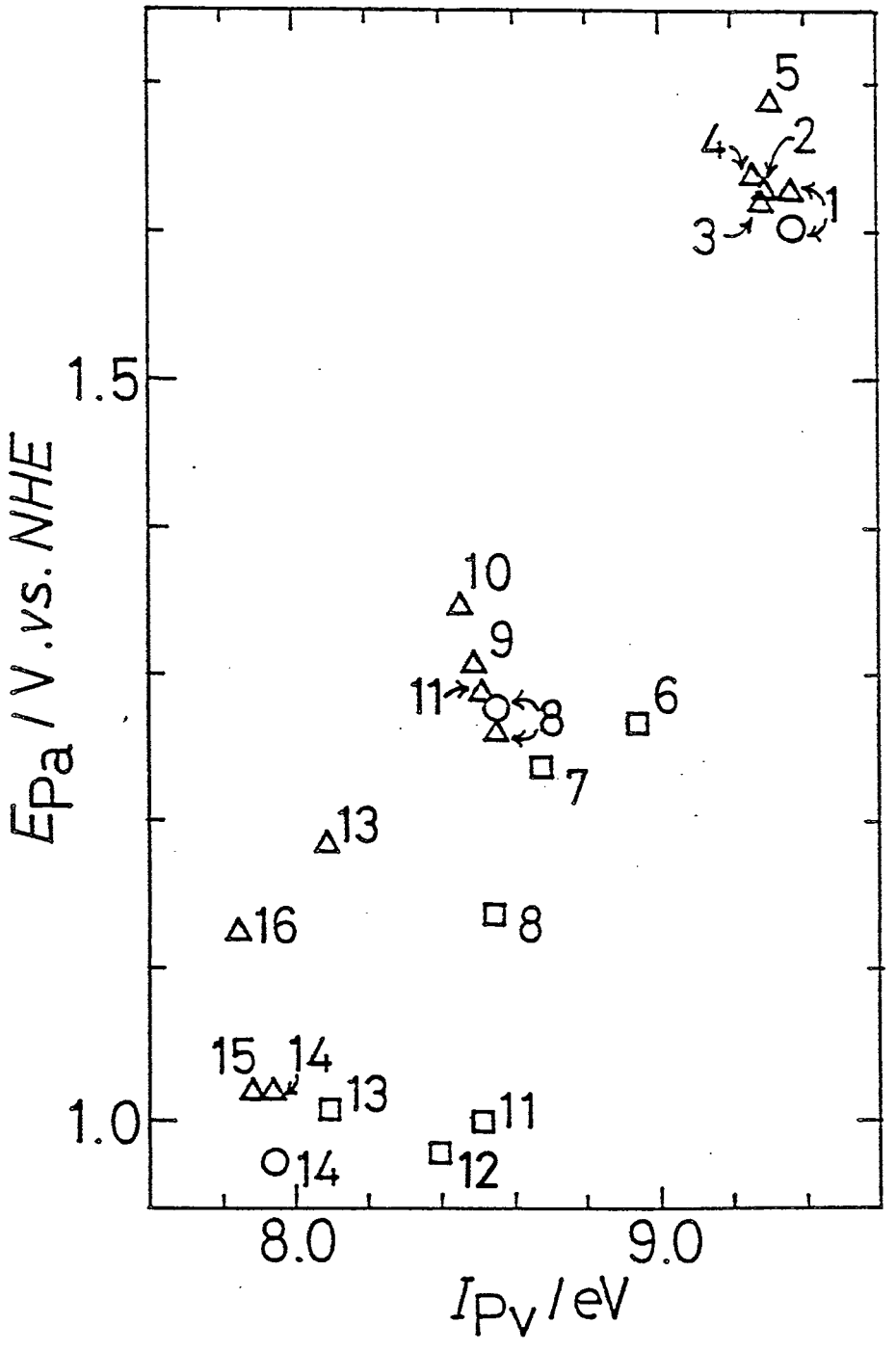

Fig. 5.9. Plots of E_{Pa} vs. ionization potentials, I_{Pv} . (△) and (□) are taken from Refs. 4 and 6, respectively. The numerical notaions are same as in Fig. 5.4.

alkylamine does not lower from that for the primary amine as compared with I_{Pv}, then the degree of the solvation effect for tertiary amine is smaller than that for primary amine.

In comparison with an energy required on the photoionization of a free molecule, I_P, an energy required on the photoionization of a solvated molecule has been acquired as a threshold energy, E_t, for several alkylamines.[29] I_P, E_t, and E_{Pa} are defined as

$$M^+_{vac}+e^-_{vac} \longleftarrow M_{vac} \qquad I_P, \qquad (5.27)$$

$$M^+_{solv}+e^-_{vac} \longleftarrow M_{solv} \qquad E_t, \qquad (5.28)$$

$$M^+_{solv}+e^-_{electrode} \longleftarrow M_{solv} \qquad E_{Pa}. \qquad (5.29)$$

E_t's are correlated with I_P and the following equation is obtained as,

$$E_t=0.76I_{Pv}+\text{const.} \qquad (5.30)$$

Comparing the slope of the E_t-I_{Pv} relation with that of the E_{Pa}-I_{Pv} relation, the degree of the solvation effect is found to depened on the geometry that the reaction is occured, and the degree at the point where E_t is observed is smaller than at the point where E_{Pa} is observed. On the other hand, the reorganization energy for the intramolecule is almost independent of the geometry, because I_{Pa}-I_{Pv} relation is expressed for both experiments and calculations as,

$$I_{Pa}=0.93I_{Pv}+\text{const}, \qquad (5.31)$$

and

$$I_{Pa}=0.94I_{Pv}+\text{const}, \qquad (5.32)$$

respectively. Furthermore it is considered that E_t is the middle energy between for the vertical transition and for the adiabatic transition.[29,30]. Thus E_t and E_{Pa} are expressed on the potential energy curves as shown in Fig. 5.10.

Considering about E_{Pa}-I_{Pv} relation and E_t-I_{Pv} relation, primary amines should receive the solvation effect more largely than tertiary amines. Then adopting this effect on the potential energy curve, the curve for the cationic state becomes steeper. This instance is larger in the primary amine than the tertiary amine, so β for the former becomes larger.

β observed in acetonitrile solution, which is acquired both in this study and in Ref. 4, is about twice larger than in basic aqueous solution.[6] Therefore the potential energy curve for the cation molecule solvated by acetonitrile is probably steeper than that solvated by basic aqueous solute, if both the curve for the neutral molecule are expressed to become similar. And according to the preceding calculations of β by using the potential energy curves, as shown in Table 5.2, E_{Pa} observed in acetonitrile is estimated to be larger than in basic aqueous solution. The tendency of experimental E_{Pa}'s is consistent with the latter, and the former cannot be said to be incorrect yet. Since the solvation effect to the neutral molecule is far smaller than

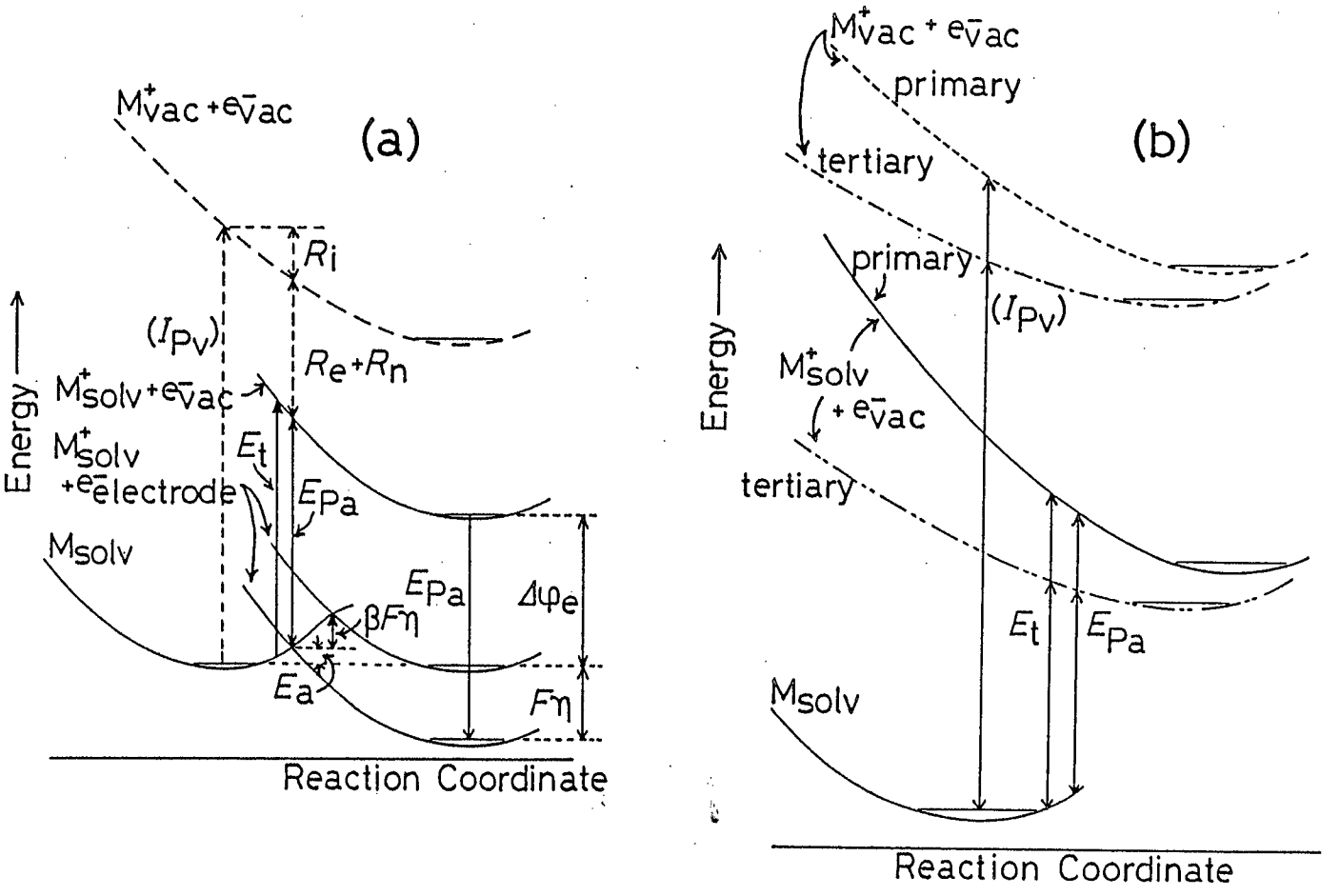

Fig. 5.10. E_t and E_{Pa} expressed on the potential energy curves. (a); E_{Pa} is defined the same point shown in Fig. 5.8. The point where E_t is expressed is nearer to the point where the vertical transition occures than where E_{Pa} is defined. (b); The difference of the solvation effect on the potential energy curves between primary amine and tertiary amine is also expressed.

that to the cation, this consideration may be reasonable. Thus it is found that β cannot be directly connected to δ without the solvation effect quantitatively, however, the intrinsic character for β is found to be represented by means of the expression using δ of the UPS and the present potential energy curves. As for the electrochemical oxidation of alkylamines in acetonitrile or basic aqueous solution, the reorganization energy about the intermolecule should be more striking than about the intramolecule, and the effect influences the shape of the potential energy curve of the cationic state and symmetry factor.

References

[1] J. A. V. Butler, *Proc. Roy. Soc.*, **157A**, 423 (1936).

[2] R. Parsons and J. O'M. Bockris, *Trans. Faraday. Soc.*, **46**, 914 (1951).

[3] P. Delahay, "Double Layer and Electrode Kinetics", John Wiley and Sons, Inc., New York, chapter 7 (1965).

[4] C. K. Mann, *Anal. Chem.*, **36**, 2424 (1964).

[5] K. K. Barnes and C. K. Mann, *J. Org. Chem.*, **32**, 1474 (1967).

[6] M. Masui, H. Sayo, and Y. Tsuda, *J. Chem. Soc(B).*, **1968**, 973.

[7] C. K. Mann, *Anal. Chem.*, **33**, 1484 (1961).

[8] H. M. Koepp, H. Wendt, and H. Strehlow, *Z. Elektrochem.*, **64**, 483 (1960).

[9] R. R. Gagné, C. A. Koval, and G. C. Lisensky, *Inorg. Chem.*, **19**, 2854 (1980).

[10] H. Matsuda and Y. Ayabe, *Z. Elektrochem.*,**59**, 494 (1955).

[11] R. S. Nicholson and I. Shain, *Anal. Chem.*, **36**, 706 (1964).

[12] P. J. Smith and C. K. Mann, *J. Org. Chem.*, **34**, 1821 (1969).

[13] L. C. Portis, J. T. Klug, and C. K. Mann, *J. Org. Chem.*, **39**, 3488 (1974).

[14] R. F. Dapo and C. K. Mann, *Anal. Chem.*, **35**, 677 (1963).

[15] M. Masui and H. Sayo, *J. Chem. Soc(B).*, 1971, 1593.

[16] L. L. Miller, G. D. Nordblom, and E. A. Maeda, *J. Org. Chem.*, 37, 916 (1972).

[17] E. S. Pysh and N. C. Yang, *J. Am. Chem. Soc.*, 85, 2124 (1963).

[18] S. F. Nelson, V. Peacock, and R. Weiman, *J. Am. Chem. Soc.*, 98, 5269 (1976).

[19] M. Fleischmann and D. Pletcher, *Tetrahedron Lett.*, 60, 6255 (1968).

[20] W. C. Neikam, G. R. Dimelver, and M. M. Desmond, *J. Electrochem. Soc.*, 111, 1190 (1964).

[21] G. Hertzberg, "Infrared and Raman Spectra of Polyatomic Molecules II. Infrared and Raman Spectra of Polyatomic Molecules", D. Van Nostrand Co. New York (1945).

[22] R. A. Eades, D. A. Weil, D. A. Dixon and C. H. Douglass, Jr., *J. Phys. Chem*, 85, 976 (1981).

[23] S. Profeta, Jr. and N. L. Allinger, *J. Am. Chem. Soc.*, 107, 1907 (1985).

[24] A. D. Walsh and P. A Warsop, *Trans. Faraday Soc.*, 57, 345 (1961).

[25] A. W. Potts and W. C. Price, *Proc. R. Soc. London, Ser. A*, 326, 181 (1972).

[26] D. H. Aue, H. M. Webb and M. T. Bowers, *J. Am. Chem. Soc.*, 97, 4136 (1975).

[27] J. O'M. Bockris and A. K. Reddy, "Modern

Electrochemistry", Plenum Press, New York, (1970) Chapter 8.

[28] R. J. Klinger, S. Fukuzumi, and J. K. Kochi, "Inorganic Chemistry: Toward the 21st Century", ed. by M. H. Chisholm, American Chemical Society, Washington, D. C. (1983), p. 117.

[29] I. Watanabe, K. Maya, Y. Yabuhara, and S. Ikeda, *Bull. Chem. Soc. Jpn.*, **59**, 907 (1986).

[30] K. Maya, I. Watanabe, and S. Ikeda, *J. Electron. Spectrosc. Relat. Phenom.*, in press.

Chapter 6. Further Consideration on the Band Shape of the UPS

6.1 Introduction

In the UPS, the band shape can be classified to three types[1] shown in Fig. 6.1. Type 1 bands may be roughly symmetrical and broad, i.e., the case of amines. In type 2 bands, the low I_p edge is sharp, which indicates that the 0←0 transition is still the strongest, or at least its intensity is substantial, e.g., the first band of benzene[2-10] as shown in Fig. 6.2. Bands of type 3 have envelopes that are distorted by the Jahn-Teller effect, e.g., the second band of ammonia.[11] In order to insight the band shape more generally, this chapter deals new value connected to the band shape and the value should reveal the chemical information included in the band shape of the UPS.

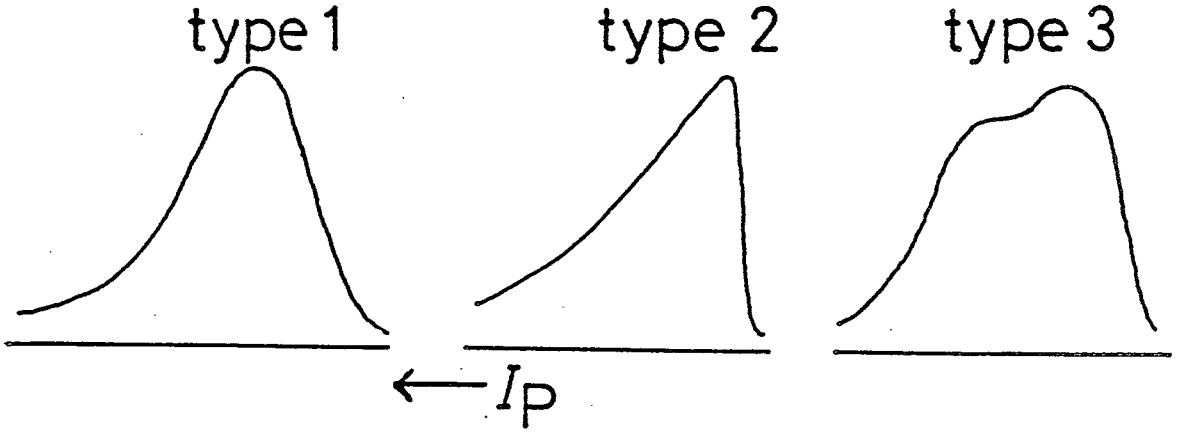

Fig. 6.1. Tipical band shapes observed in the UPS.

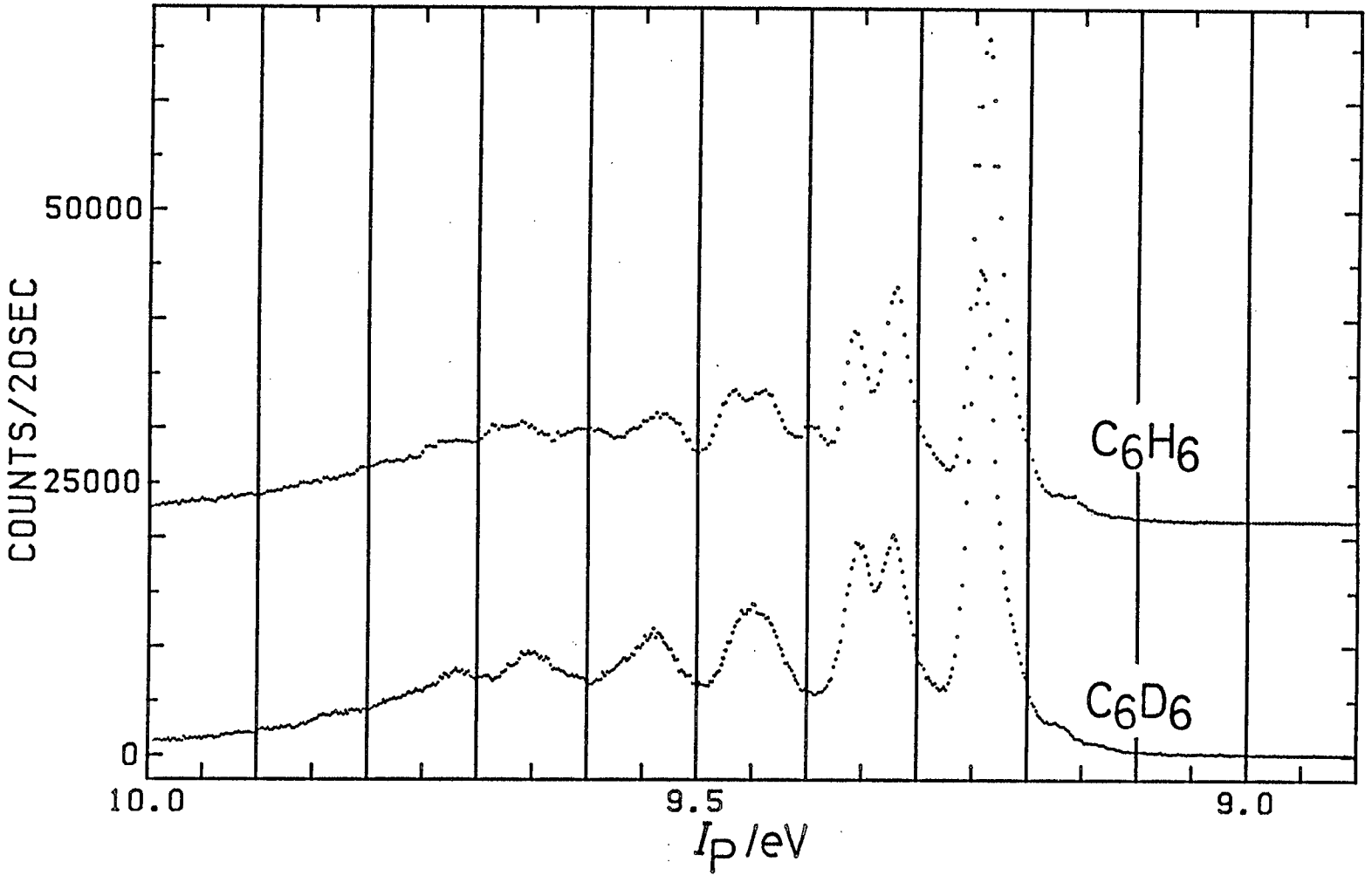

Fig. 6.2. First bands of the UPS for benzene.

6.2 Band Width Toword the Lower Ionization Potential

Band width δ has been found to concern itself with the potential energy curves for both the neutral and the cationic state and to include informations on the chemical reactivity, according to the preceding discussions. Although there are a possibility that δ for the type 1 band is equal to that for the type 2 band, the difference in the chemical properties included between these two bands should be remarkable. Therefore it is hard to consider the chemical reactivity by only values of δ if compared all together.

Now a new quantity should be introduced. That is band width toward the lower ionization potential, δ_l, and band width toward the higher ionization potential, δ_h(Fig. 6.3). For example the first band for benzene, whose band shape is type 2 band, δ_l is nearly zero and δ_h is almost equal to δ, while for the familiar first band for alkylamine both δ_l and δ_h are about one-half of δ, and the former is still smaller. Table 6.1. presents those obtained by experiment and calculation for a several alkylamines. The correlation is good, so δ_l and δ_h are interpreted as follows: δ_l is the energy difference in the potential energy for the cationic state between the geometry 1 and the geometry 2, and δ_h is the difference in that between the geometry 1 and the

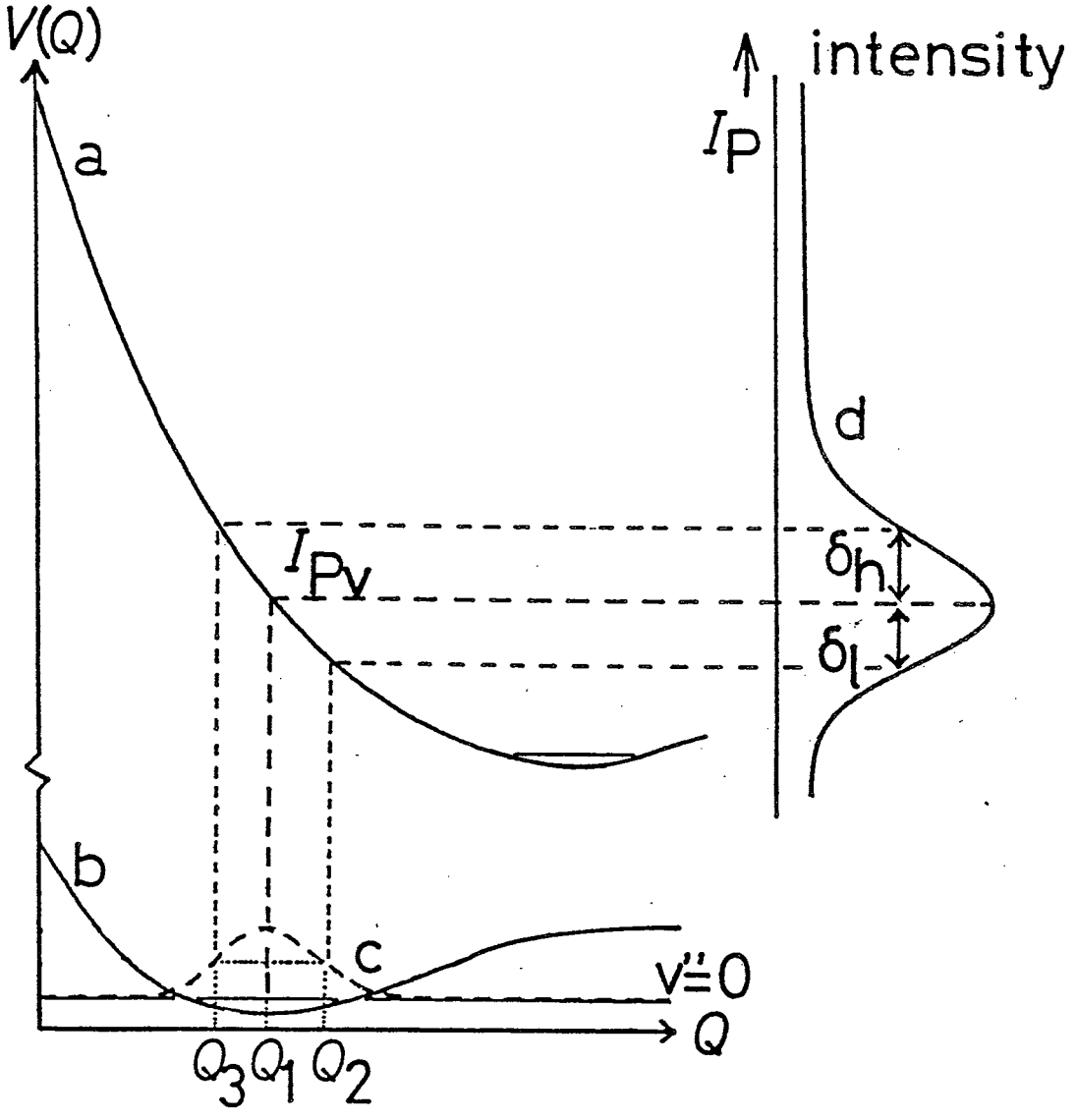

Fig. 6.3. Band width, δ_l and δ_h, on the potential energy curves for both the neutral and cationic state. a; The curves for the cationic state. b; The curves for the neutral state. c; The square of the vibrational wave-function. d; The photoelectron band. Q_i corresponds to the geometry i, see text.

Table 6.1 Experimental and Calculated δ_l and δ_h for a several alkylamines (in eV)

	δ_l		δ_h	
	exp	calc	exp	calc
NH_3	0.45	0.42	0.51	0.53
CH_3NH_2	0.41	0.32	0.49	0.42
$C_2H_5NH_2$	0.39	0.32	0.48	0.43
$(CH_3)_2NH$	0.36	0.26	0.43	0.34
$(C_2H_5)_2NH$	0.35	0.26	0.43	0.34
$(CH_3)_3N$	0.33	0.26	0.38	0.30
$(C_2H_5)_3N$	0.34	0.24	0.38	0.27
ND_3	0.37	0.38	0.38	0.47
CH_3ND_2	0.37	0.29	0.41	0.35
$C_2H_5ND_2$	0.37	0.28	0.40	0.36
$(CH_3)_2ND$	0.33	0.24	0.40	0.29

geometry 3. Where the geometry 1 gives the maximum of the vibrational probability density Ψ_0^2 on the neutral state and there are two geometries, which make the probability density Ψ_0^2 on the neutral state half-maximum. The geometry 2 is nearer geometry to the ground state for the cationic state between these two geometries, while the geometry 3 is the other geometry.

Thus δ_l mainly reflects both the geometrical change with ionization and the shape of the potential energy curve for the cationic state on the geometry 1 toward the geometry 2. While δ_h reflects the shape of the curve on the geometry 1 toward the geometry 3. As for type 1 band, both δ_l and δ_h are large and they represent that the geometrical change with ionization is large and that the potential energy curve for the cationic state is steeper than that for the neutral state. As to type 2 band, δ_l is small and δ_h is larger, and they represent that the geometrical change is small and that the curve for the cationic state is much steeper than that for the neutral state. On the other hand, if both δ_l and δ_h are small, the band is just like the band for rare-gas.

The difference of the equilibrium geometry between the neutral and the cationic state reflects on $\Delta I_{Pv,a}$, however, the determination of δ_l is easier than that of I_{Pa}. Therefore δ_l is valid to check the change of the geometry

with photoionization.

6.3 Application to Cyclohexanone and its Methyl Derivatives

Cyclohexanone is a cyclic ketone and its HOMO is expected to oxigen non-bonding orbital n_O, so substitution of methyl group causes change on the electronic structure. Figure 6.4 presents the first band for cyclohexanone and its methyl derivatives. The inductive effect of methyl group is obvious in the order of 2-, 3-, and 4- substitution. This order is same as the distance between oxgen and methyl group. Thus first band should be assurely assigned to n_O and HOMO should be effected by methyl group.

Band type for 2,6-dimethylcyclohexanone is type 1 and that for others is type 1. As for 2-methycyclohexanone δ_h is larger than cyclohexanone, while δ_l is still small. This instance indicates that the potential energy curve for the cationic state is steeper, and that the stretch vibration of C=O on the cationic state is intensely hindered by substitution on 2-position to C=O. While for 2,6-dimethylcyclohexanone, δ_l is larger and δ_h is still similar to others, and the phenomenon shows that the curve for the cationic state is still similar, while the geometrical change with ionization is large. This may be due to the large steric hindrance on 2-and 6-position to C=O for the

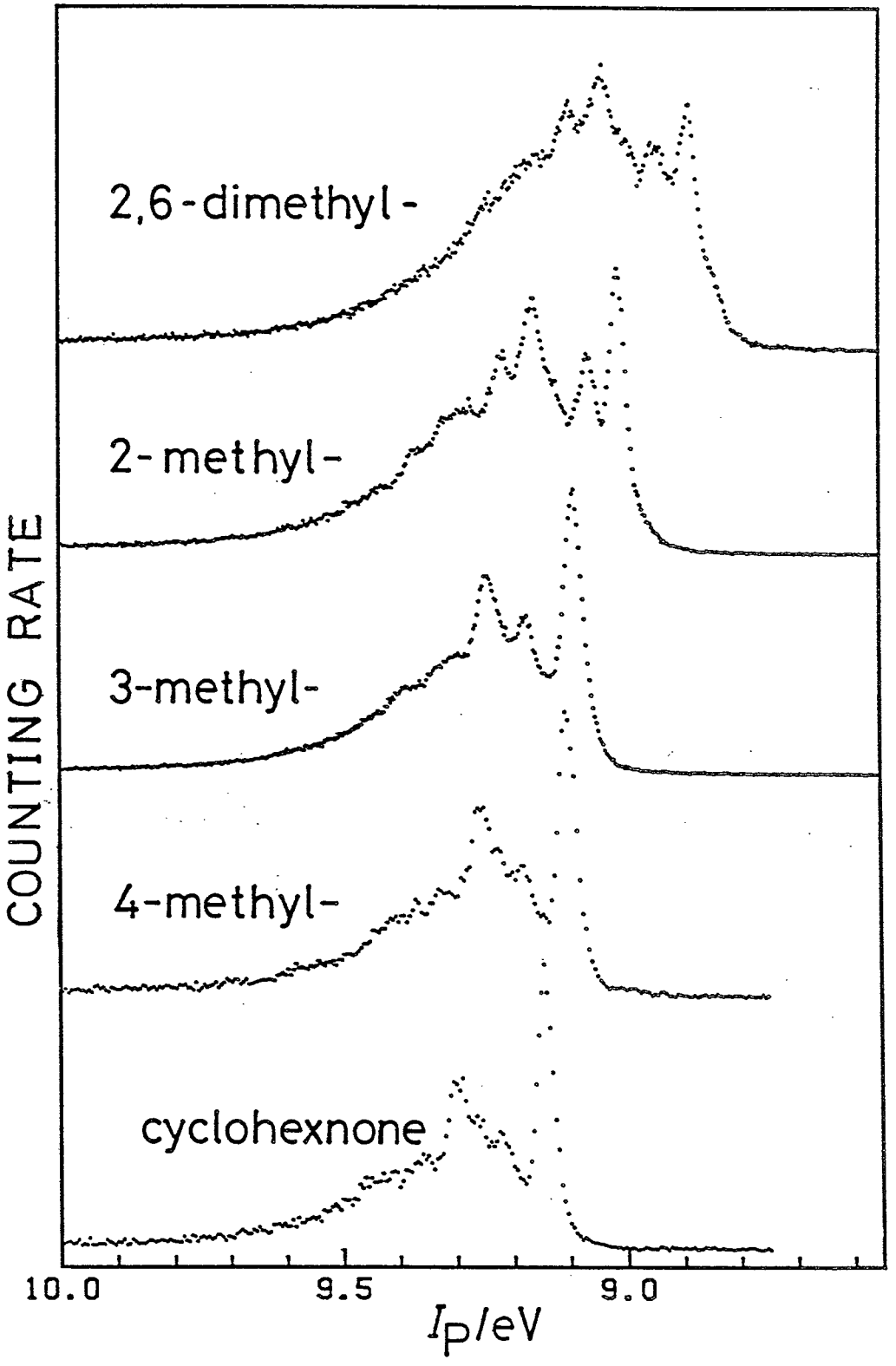

Fig. 6.4. First bands of the UPS for cyclohexanone and its methyl derivatives.

cation molecule.

6.4 Activation Energy of the Electrochemical Oxidation and the Band Width

According to the preceding discussions, if δ_1 is large, it points out that the potential energy curve on the cationic state is steep. Then the instance should cause the activation energy at the equilibrium potential on the electrode oxidation to be large, on the other hand that of the reverse reaction to be much larger. Therefore a molecule with large δ_1 gives intrinsically irreversible electrochemical oxidation reaction. The instance should make the positive correlation between δ_1 and $(E_{Pa}-E°)$. δ, which is about twice as δ_1 for alkylamine, correlates with $(E_{Pa}-E°)$ good as shown in Fig. 6.5, and it does better than δ_1. Thus in any case the band width should reflect intrinsic parts of the activation energy considered in this section. Further the energy cannot be obtained by the irreversible-voltammogram, so even if estimated only relatively, this idea should be valuable to analize the oxidation reaction at the electrode.

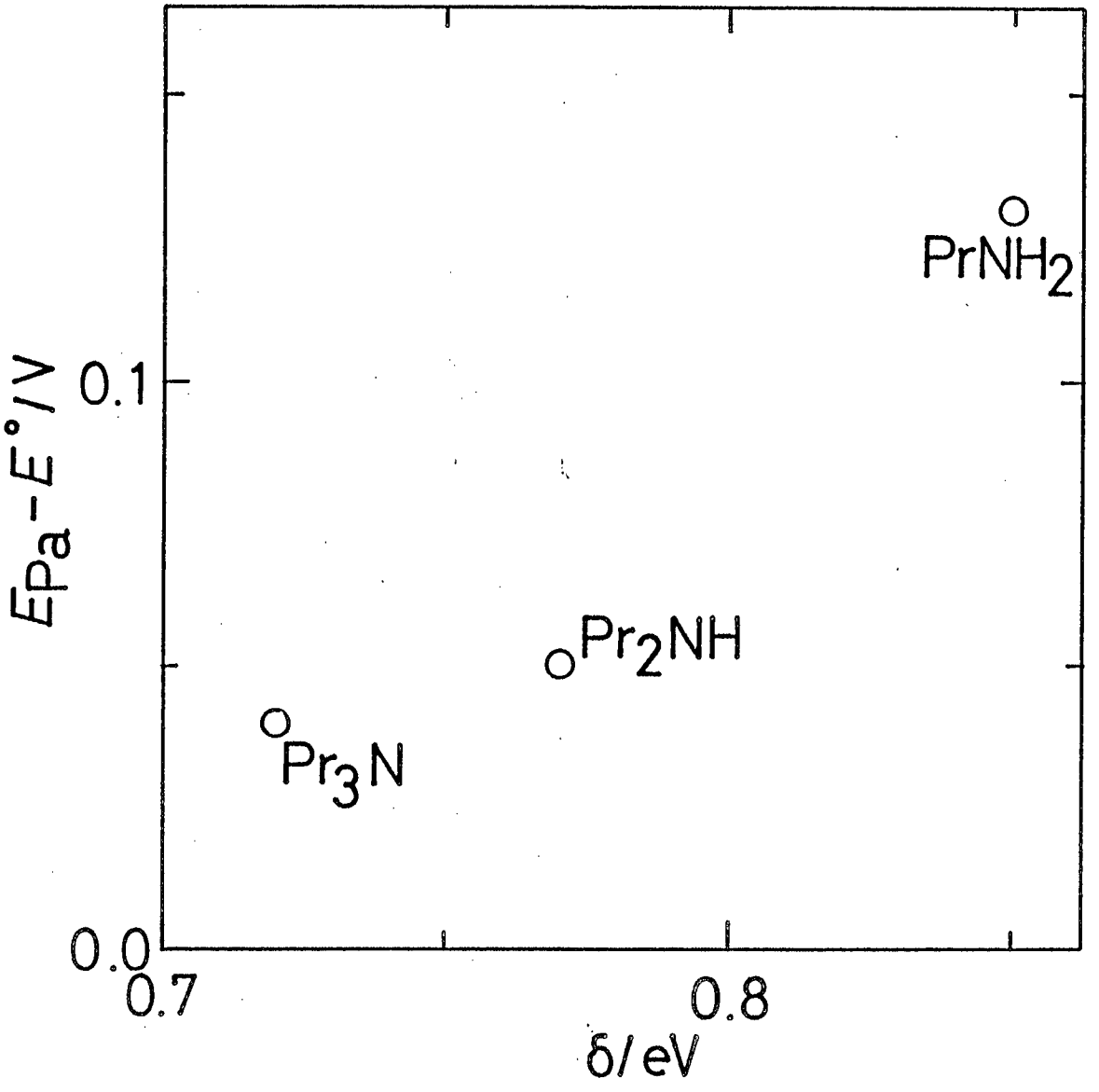

Fig. 6.5. Plots of the E_{Pa}-$E°$ vs. the band width δ.

References

[1] J. H. D. Eland, "Photoelectron Spectroscopy", Butterworth and Co., London (1974), Chap. 5.

[2] T. A. Carlson and C. P. Anderson, *Chem. Phys. Lett.*, **10**, 561 (1971).

[3] H. Bock and G. Wagner, *Angew. Chem. Int. Ed.*, **11**, 150 (1972).

[4] M. Klessinger, *Angew. Chem. Int. Ed.*, **11**, 525 (1972).

[5] P. K. Bischof, M. J. S. Dewar, D. W. Goodman, and T. B. Jones, *J. Organomet. Chem.*, **82**, 89 (1974).

[6] J. M. Behan, R. A. Jhonstone, and T. W. Bentley, *Org. Mass. Spectrom.*, **11**, 207 (1976).

[7] L. Mattsson, L. Karlsson, R. Jardny, and K. Siegbahn, *Phys. Scripta.*, **16**, 221 (1977).

[8] H. Bock, W. Kaim, and H. E. Rohwer, *J. Organomet. Chem.*, 135, C14 (1977).

[9] W. Schmidt, *J. Chem. Phys.*, **66**, 828 (1977).

[10] T. Kobayashi, *Phys. Lett.*, **69A**, 105 (1978).

[11] A. W. Potts and W. C. Price, *Proc. R. Soc. London*, **A326**, 181 (1972).

[12] J. W. Rabalais, L. Karlsson, L. O. Werme, T. Bergmerk, and K. Siegbahn, *J. Chem. Phys.*, 58, 3370 (1973).

Concluding Remarks

UPS is the technique that offers us informations on electronic states of the molecule directly. Frequently I_p has been observed when a new compound has synthesized like as ir, Raman, and nmr. Excepting I_p's, however, few data is utilized. For example, width of a photoelectron band is qualitatively considered to be related to change in geometry with ionization, but their quantitative treatment is limited to simple molecule.

In this study, in order to seek for any chemical informations included in band shape of the first band of the UPS which is related to HOMO the UPS for a series of alkylamines were measured precisely, and ab initio MO calculations for several amines were carried out. And then cyclic voltammograms were measured to obtain informations on the electrochemical oxidation of the HOMO electron of alkylamine. Then following conclusions were obtained.

Band shape of the UPS was estimated well by the simple Franck-Condon approach using potential energy curves calculated for both the neutral and cationic states. The band width and the threshold ionization potential were defined by use of the potential energy curves for both the neutral and cationic states. The threshold ionization potential observed in the UPS was found not to be always

thermodynamically adiabatic ionization energy, and the values of I_{Pa} for a series of alkylamines were evaluated by taking account of molecular vibrational frequency for the neutral state. While I_{Pa} of ammonia, methylamine, and ethylamine were decided by comparing vibrational progressions between these amines and those deuterium derivatives.

The instrument for measurements of cyclic-voltammogram(CV) at high sweep rate was constructed by using a mini-computer and CV for alkylamines were measured. Generally alkylamines were known to be irreversibly oxidized in a several solvents, however, it was concluded that they behave slightly reversibly at the high sweep rate. The correlation between one of the kinetic parameter, β, and band width of the UPS, δ, was found. In order to explain the correlation the potential energetic discussion on the electrode oxidation reaction was done and it was obtained that the solvation effects were found obviously on β. Considering molecules of the different type like as benzene, new quatity correponding to band width was introduced. Using both the redox potential and anodic peak potential obtained by the CV, the band width was found to be related to the activation energy at the equilibrium potential, which is difficult to acquire in the case of the irreversible reaction. Therefore one of the chemical informations

included in the band shape of the first band of the UPS was one related to the electrochemical oxidation. And the molecule with large δ was found to be irreversibly oxidized intrinsically.

Acknowledgement

The author would like to express his sincere gratitude to Professor Shigero Ikeda for his cordial guidance, discussion, and support in coordinating this work.

The author also wishes to express his heartful thanks to Dr. Iwao Watanabe for his helpful discussion and accurate instruction.

The author is also grateful to many members of Ikeda Labolatory for their helpful discussions and encouragement.

The author also thanks all his friends for their serviceable suggestions and encouragement.

List of Publications

1. "UV Photoelectron Spectroscopic Investigation and the DV-Xα MO Calculation of Tetrakis(2-methyl-2-propanethiolato)molybdenum(IV)"
   M. Takahashi, I. Watanabe, S. Ikeda, M. Kamata, and S. Otsuka
   Bull. Chem. Soc. Jpn., 55, 3757 (1982).
2. "Correlation Between the Symmetry Factor of the Electrode Reaction and the Band Shape of the Photoelectron Spectrum for Alkylamines"
   M. Takahashi, I. Watanabe, and S. Ikeda
   J. Phys. Chem., 87, 5059 (1983).
3. "He(I) Photoelectron Spectra of Various Alkylamines"
   M. Takahashi, I. Watanabe, and S. Ikeda
   J. Electron Spectrosc. Relat. Phenom., 37, 275 (1985).
4. "Band Shape of Photoelectron Spectrum and Potential Energy Curve for Alkylamine"
   M. Takahashi, I. Watanabe, and S. Ikeda
   Bull. Chem. Soc., in submitted.
5. "He(I) Photoelectron Spectra of Several Deuteralkylamines and Determination of Adiabatic Ionization Potentials"
   M. Takahashi, I. Watanabe, and S. Ikeda
   in preparation.
6. "He(I) Photoelectron spectra for a several amines"
   M. Takahashi, I. Watanabe, and S. Ikeda

in preparation

7. "Electrochemical Oxidation and Band Shape of the UPS for Alkylamines"

M. Takahashi, I. Watanabe, and S. Ikeda

in preparation.

Appendix

Data Bank

The full spectra of the UPS of amines and benzene are collected in the following figures.

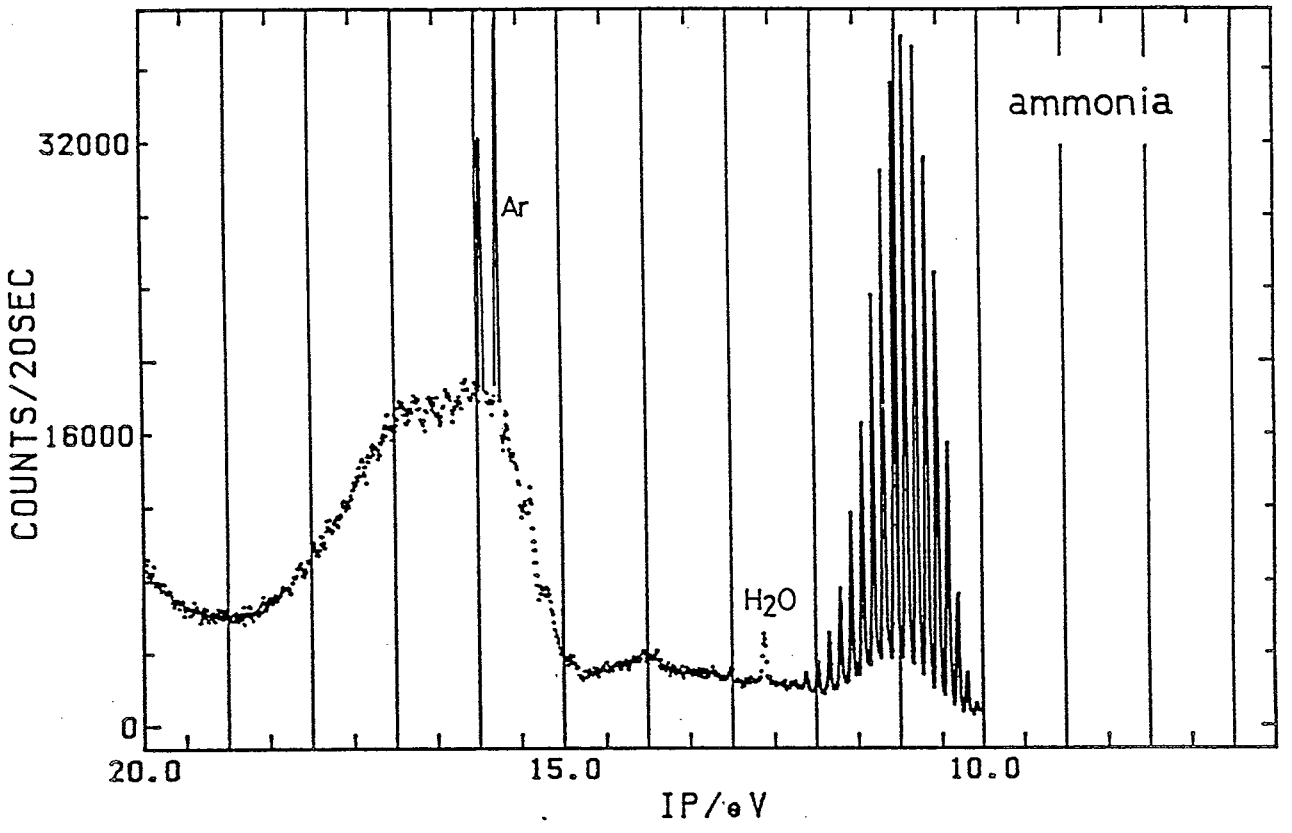
ammonia
32000
16000
0
COUNTS/20SEC
Ar
H2O
20.0
15.0
10.0
IP/eV

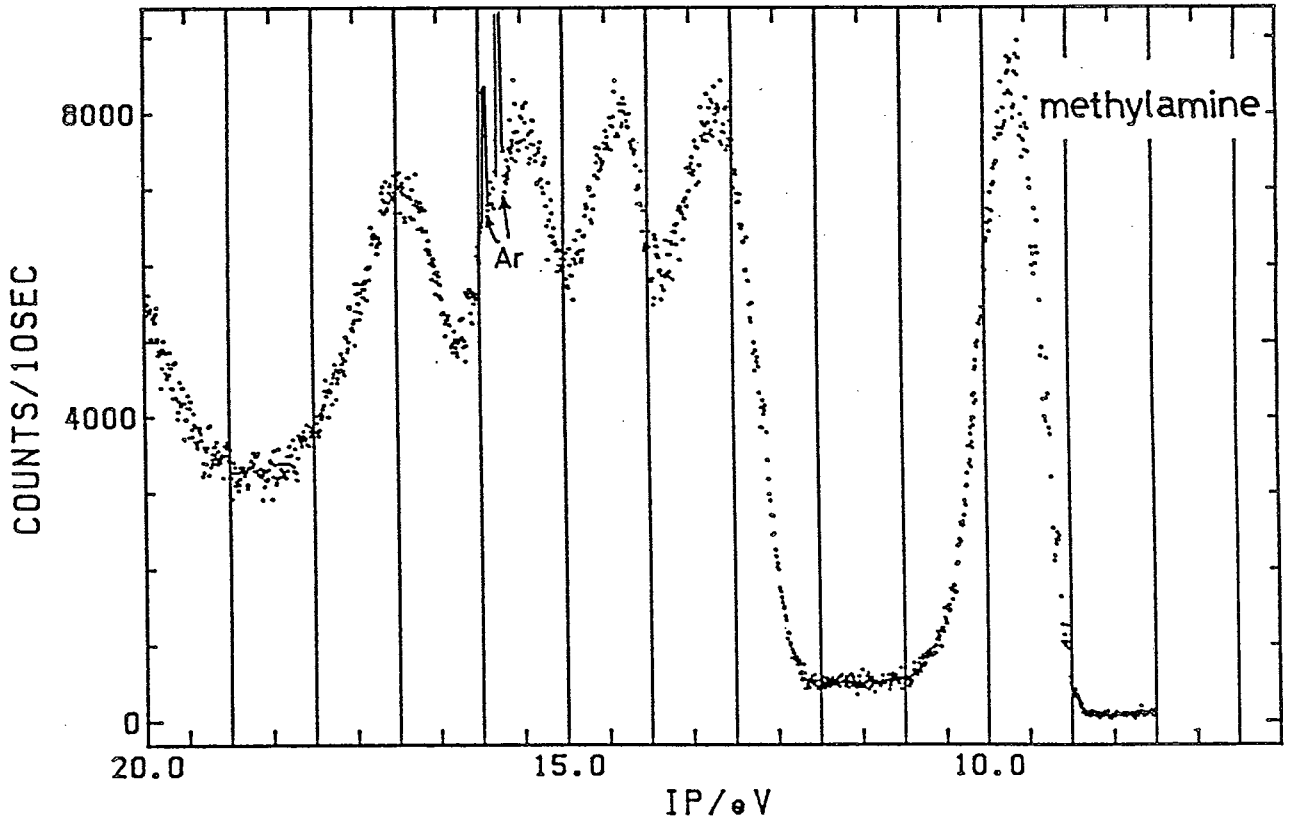
methylamine
8000
4000
0
COUNTS/10SEC
Ar
20.0
15.0
10.0
IP/eV

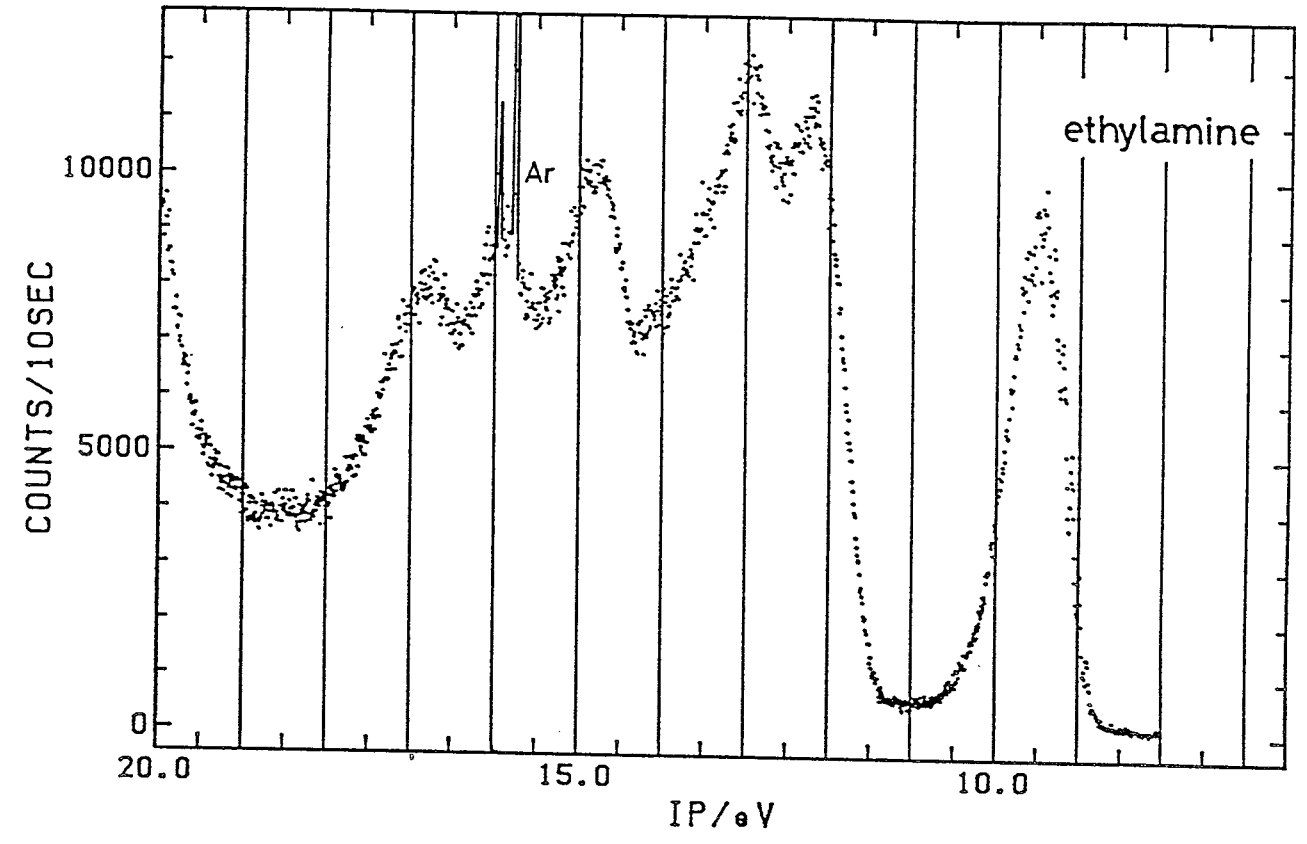
ethylamine
Ar
10000
5000
0
COUNTS/10SEC
20.0
15.0
10.0
IP/eV

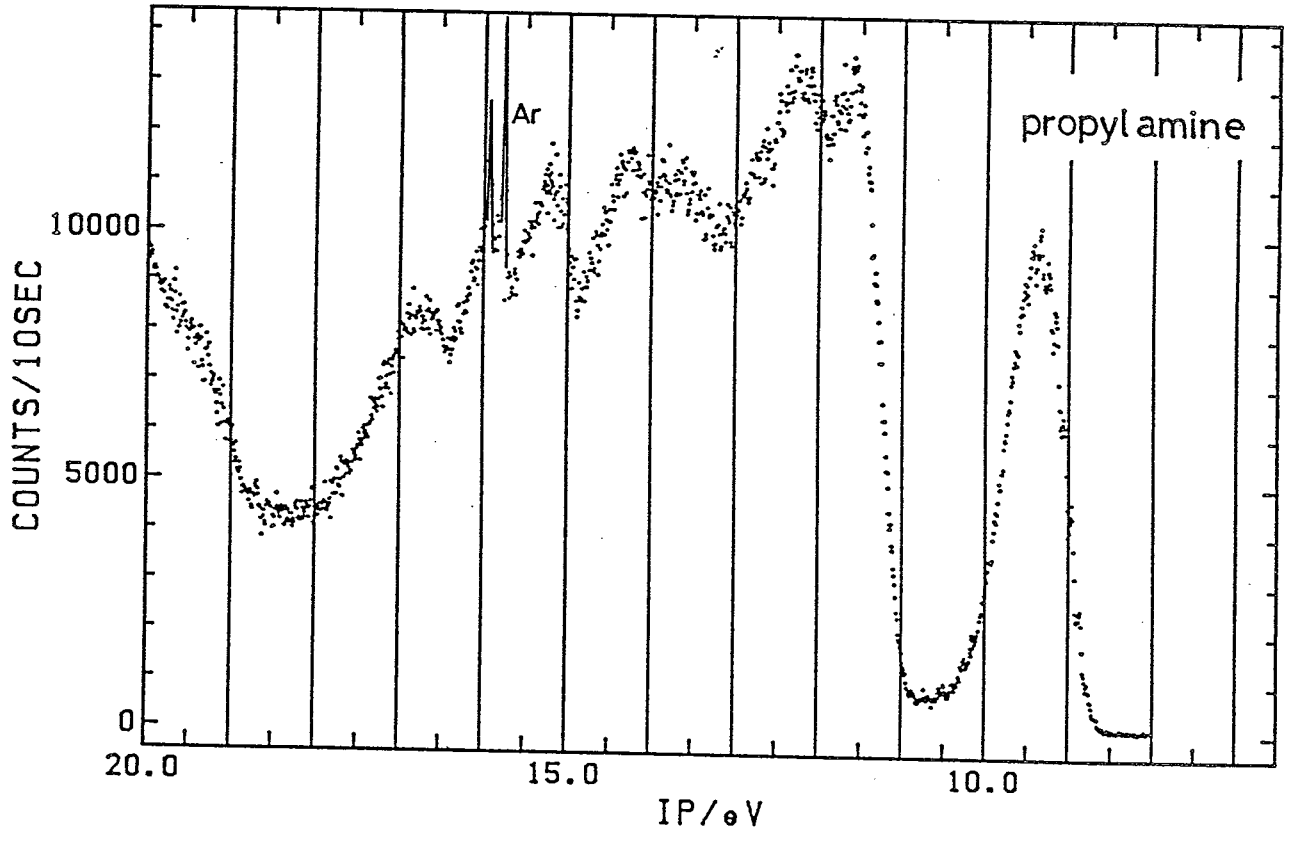
propylamine
Ar
10000
5000
0
COUNTS/10SEC
20.0
15.0
10.0
IP/eV

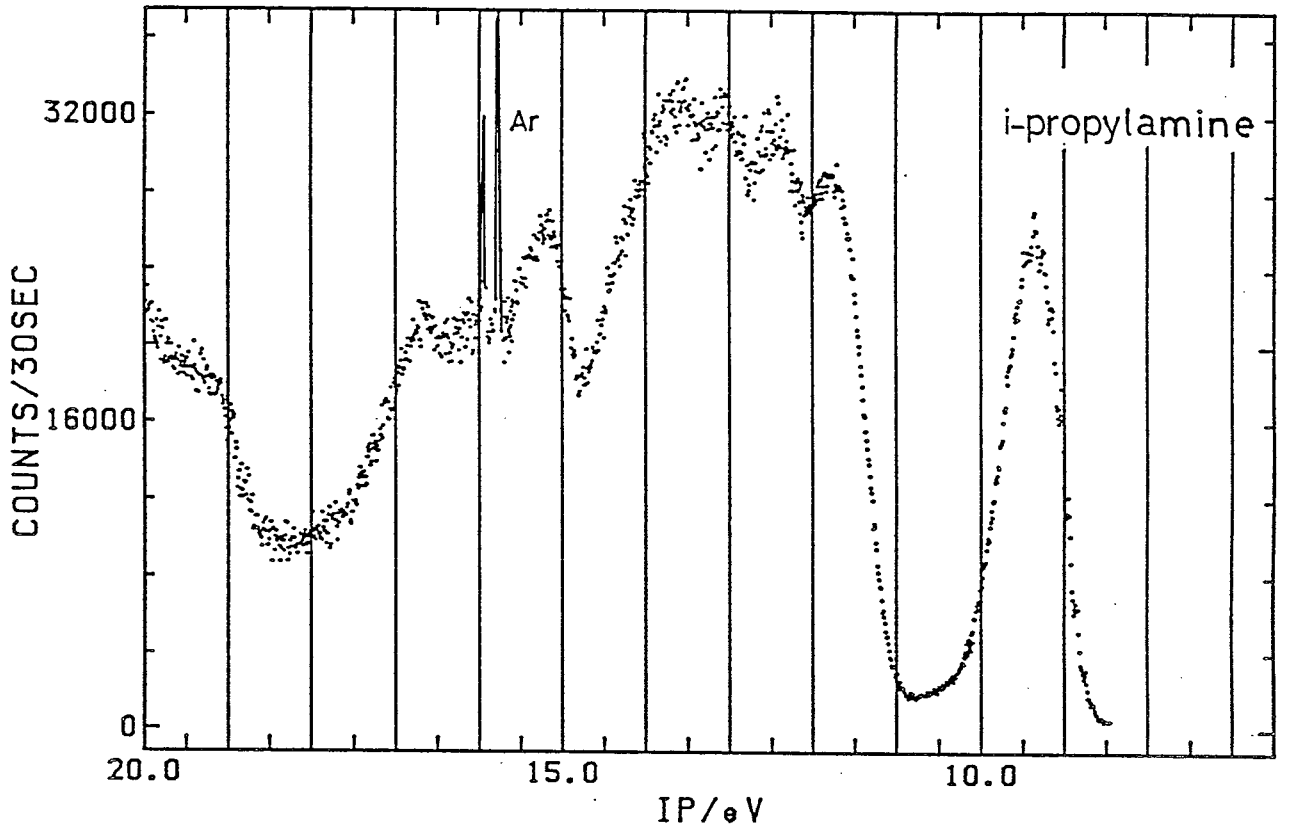
32000
16000
0
COUNTS/30SEC
Ar
i-propylamine
20.0
15.0
10.0
IP/eV

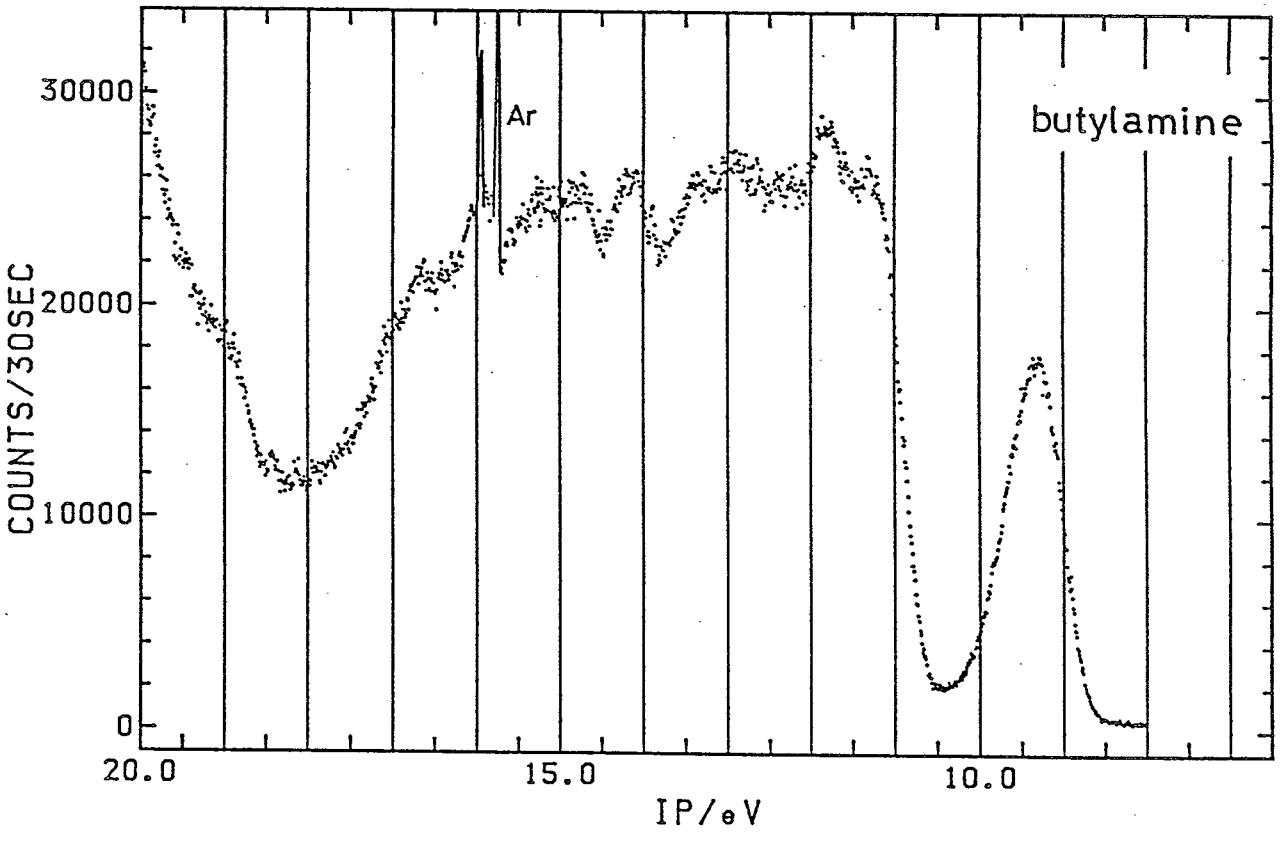
30000
20000
10000
0
COUNTS/30SEC
Ar
butylamine
20.0
15.0
10.0
IP/eV

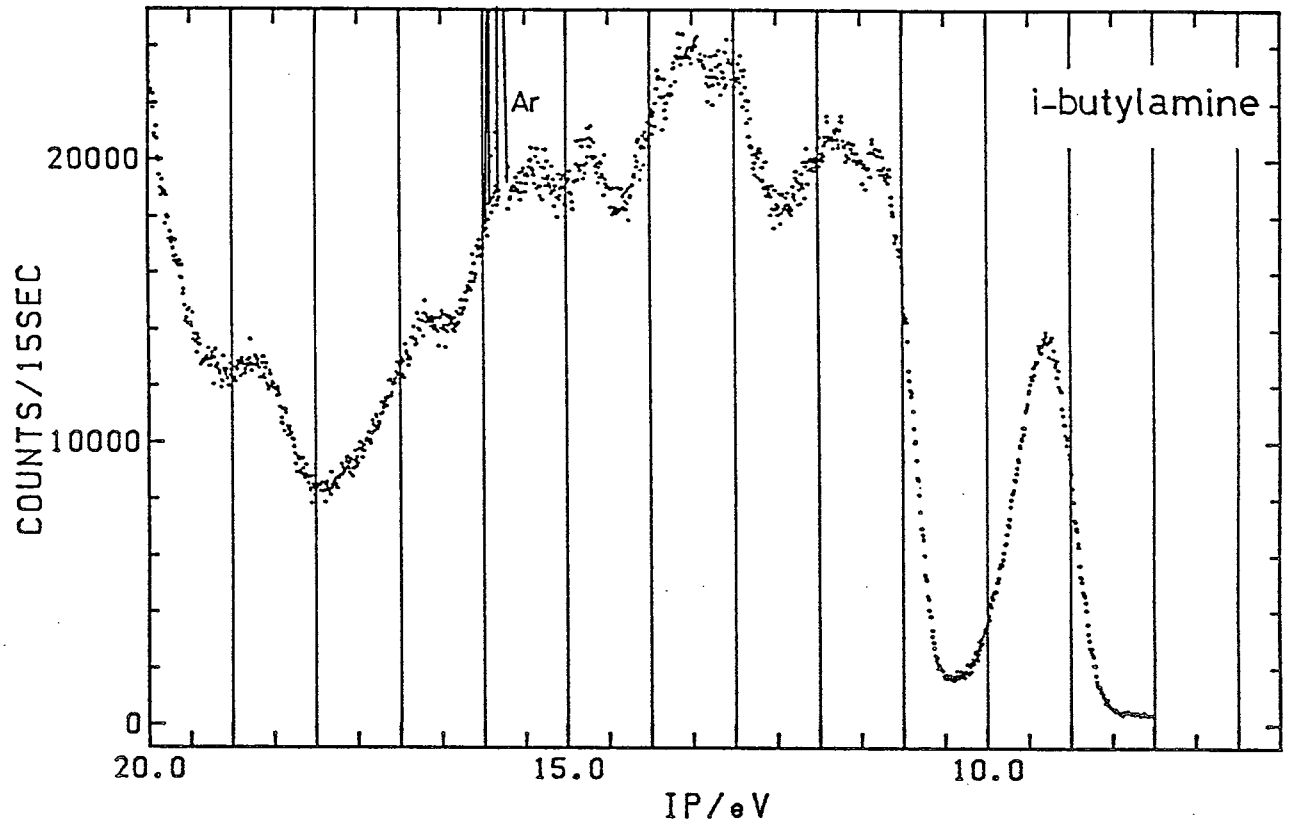
i-butylamine
Ar
20000
10000
0
COUNTS/15SEC
20.0
15.0
10.0
IP/eV

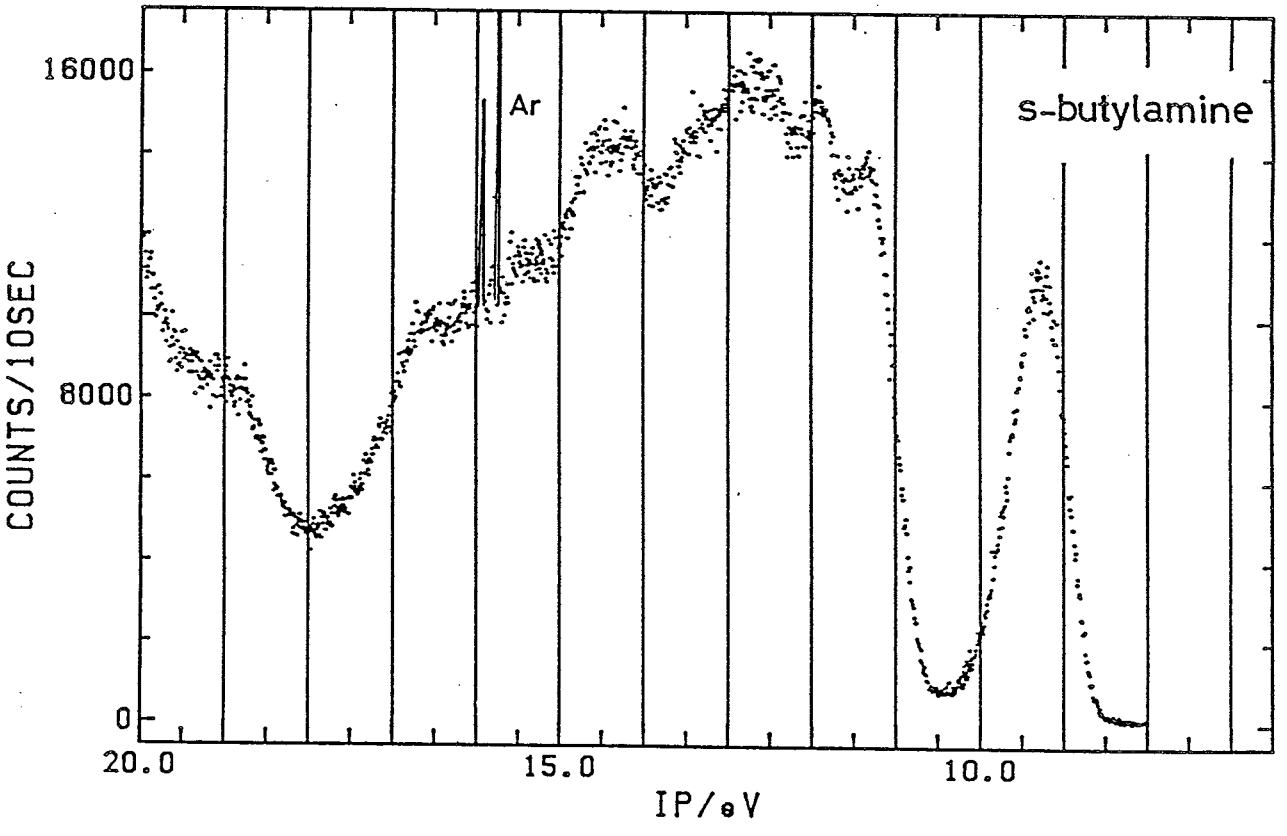
s-butylamine
Ar
16000
8000
0
COUNTS/10SEC
20.0
15.0
10.0
IP/eV

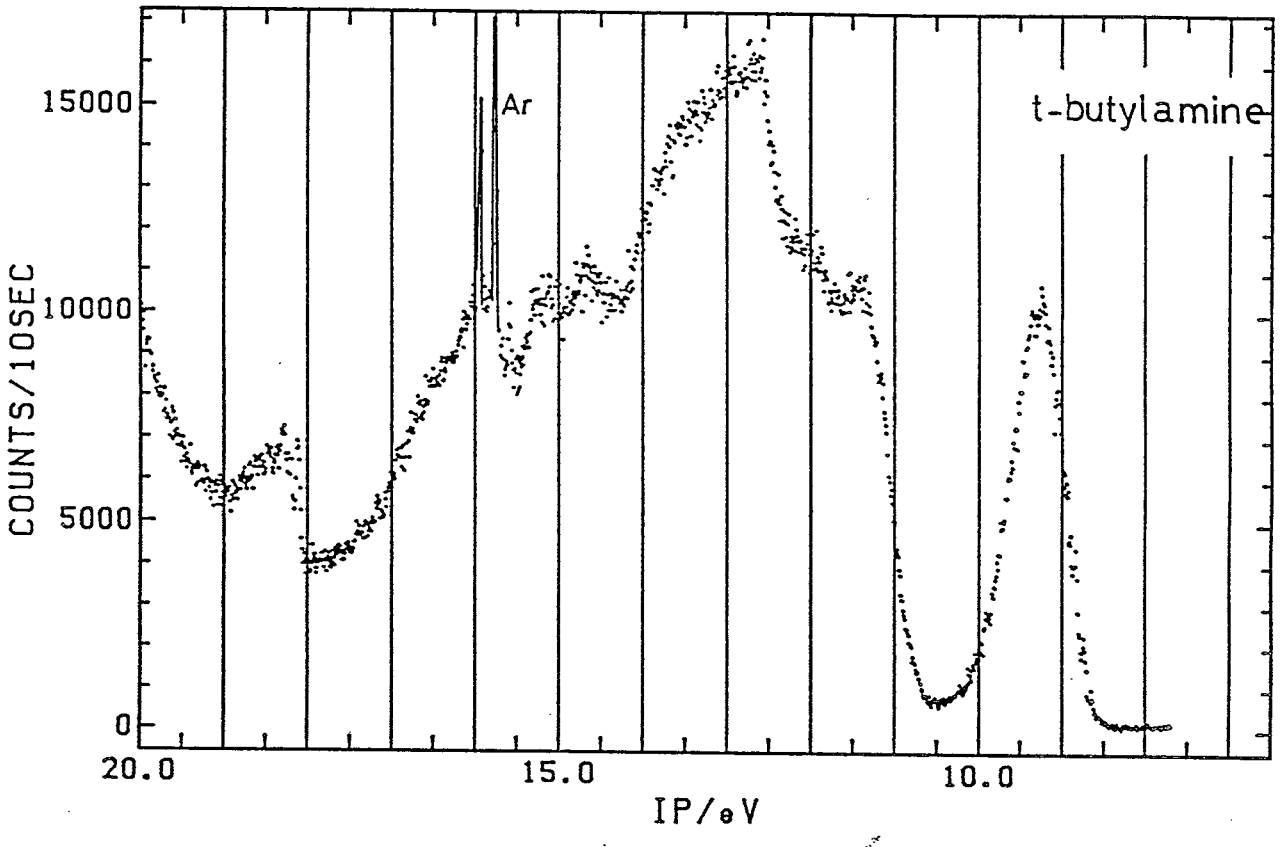
15000
10000
5000
0
COUNTS/10SEC
Ar
t-butylamine
20.0
15.0
10.0
IP/eV

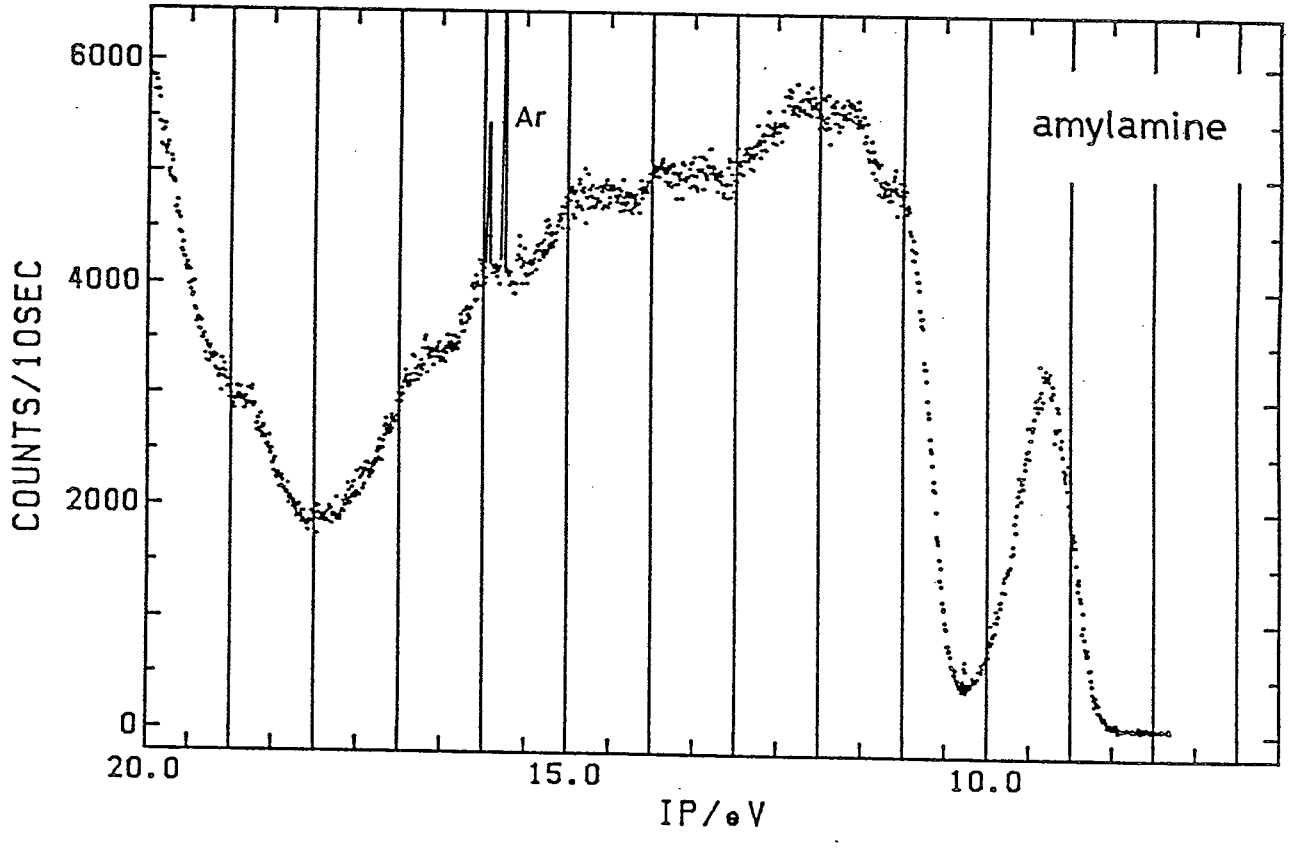
6000
4000
2000
0
COUNTS/10SEC
Ar
amylamine
20.0
15.0
10.0
IP/eV

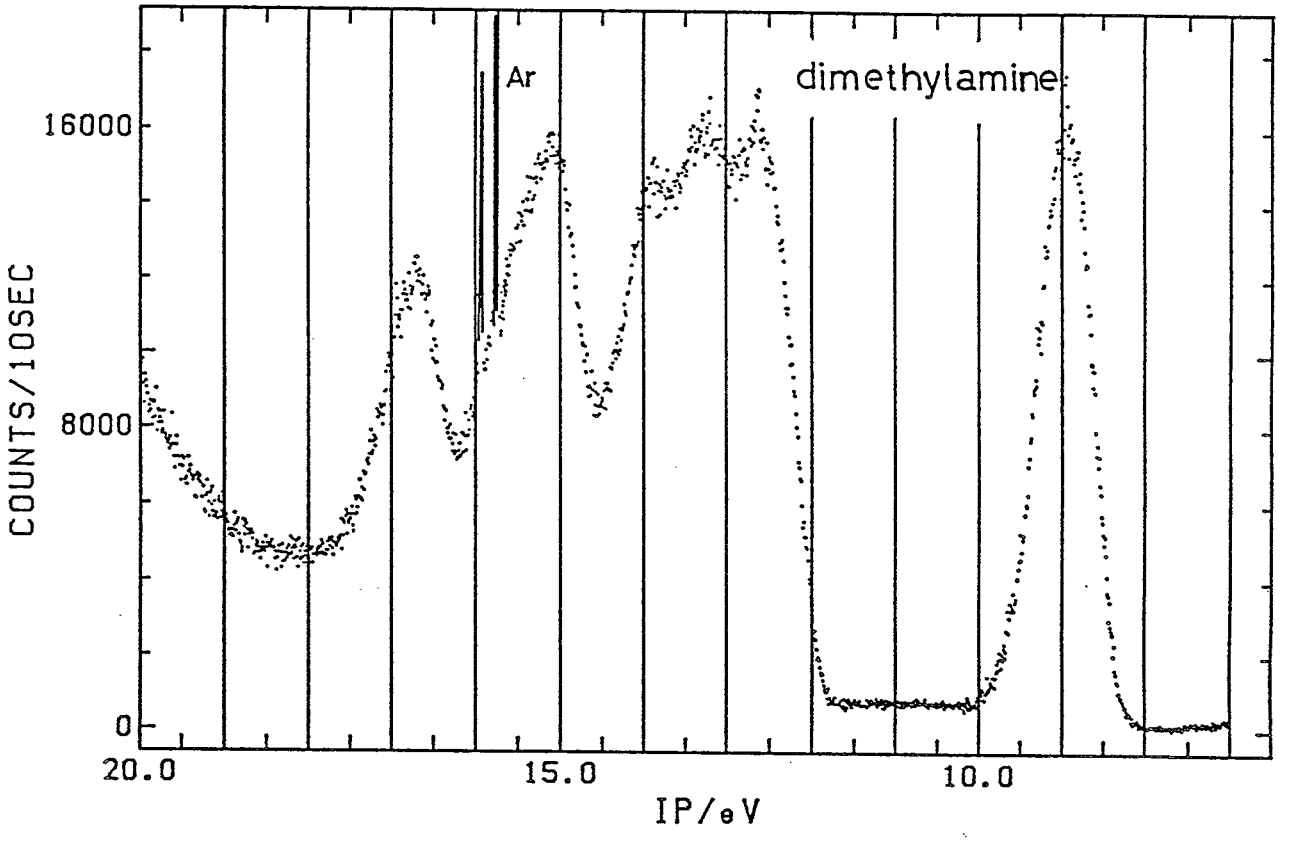
Ar
dimethylamine
16000
8000
0
COUNTS/10SEC
20.0
15.0
10.0
IP/eV

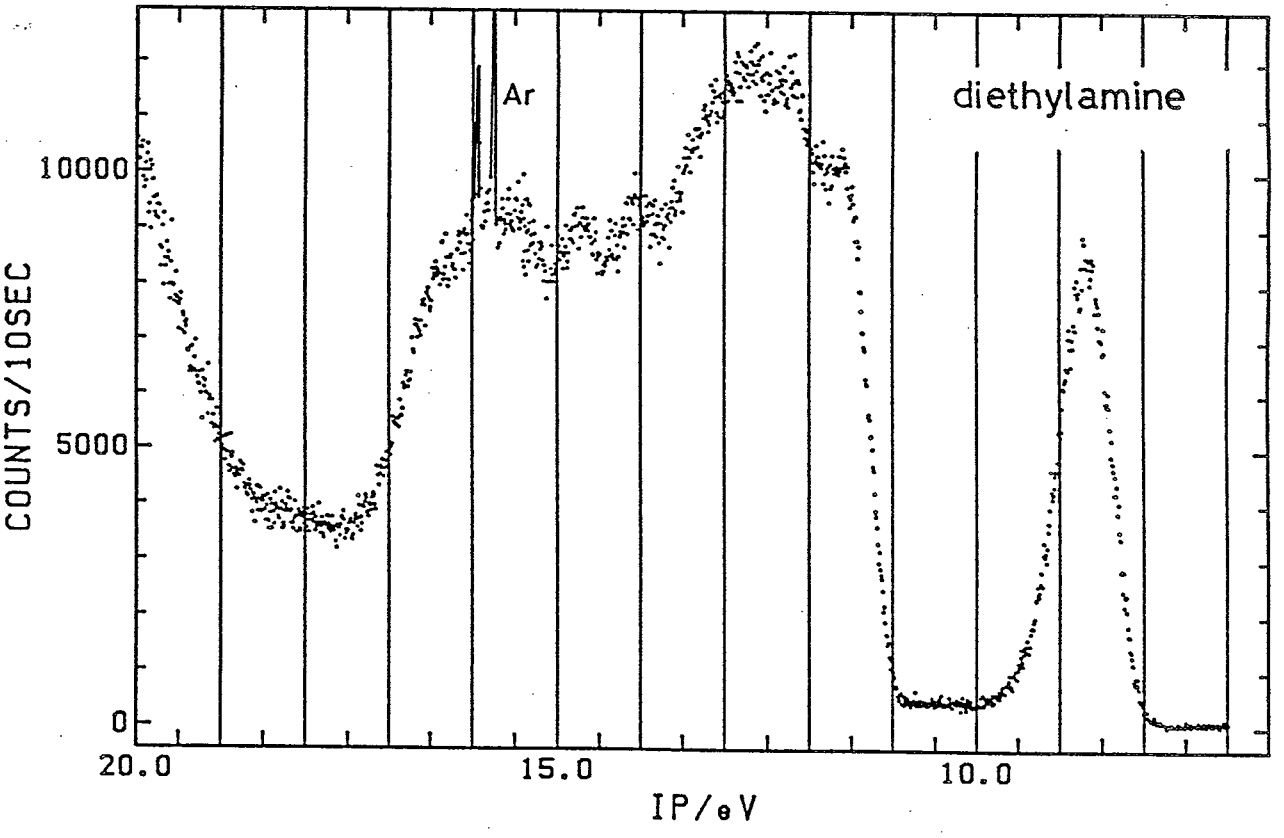
Ar
diethylamine
10000
5000
0
COUNTS/10SEC
20.0
15.0
10.0
IP/eV

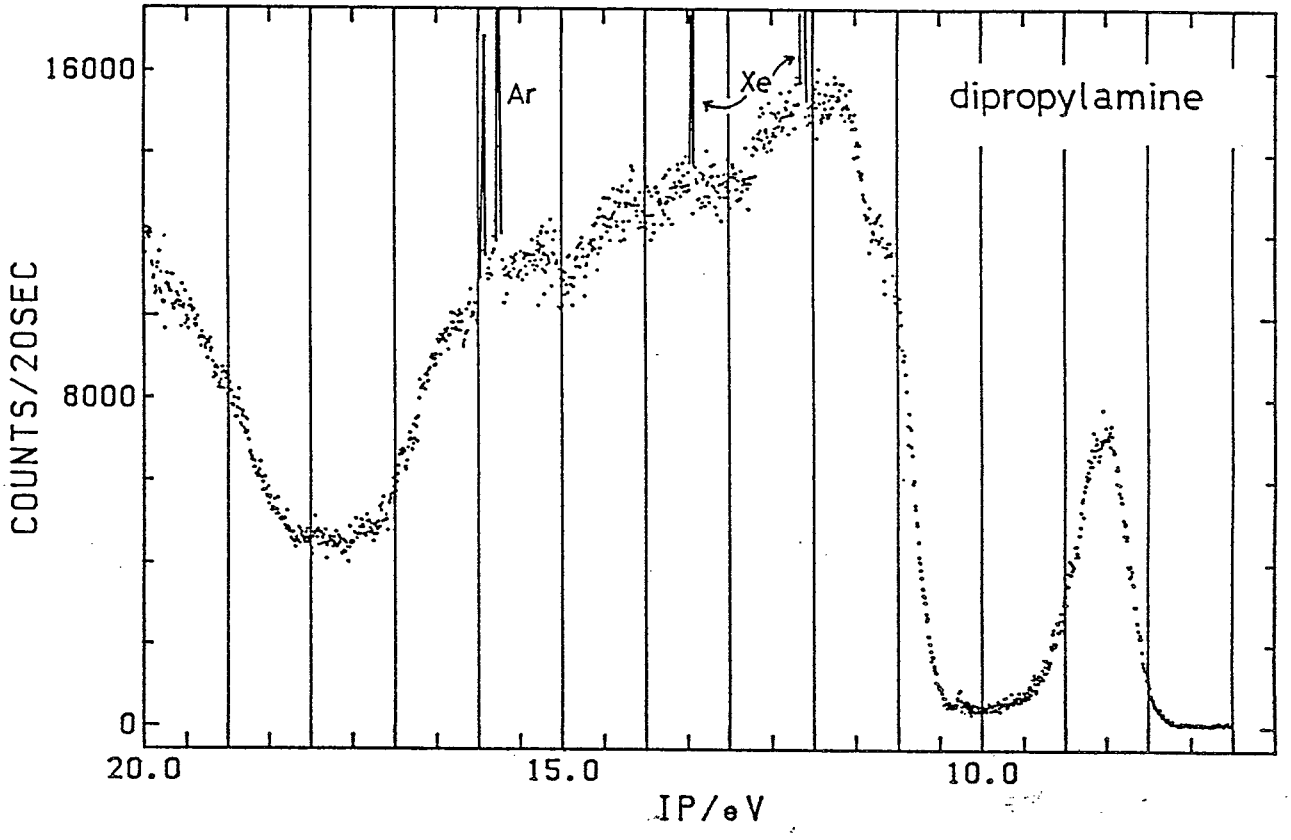
16000
8000
0
COUNTS/20SEC
Ar
Xe
dipropylamine
20.0
15.0
10.0
IP/eV

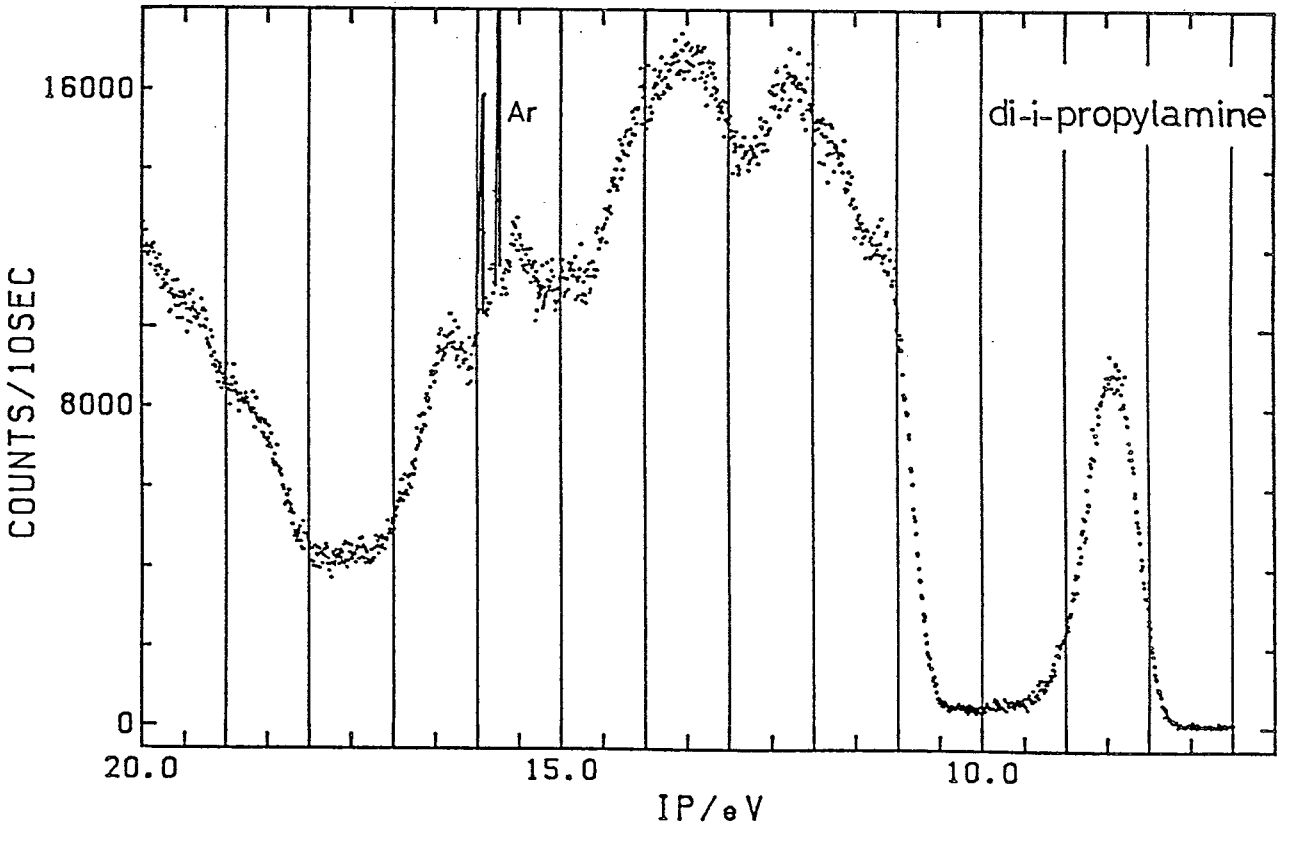
16000
8000
0
COUNTS/10SEC
Ar
di-i-propylamine
20.0
15.0
10.0
IP/eV

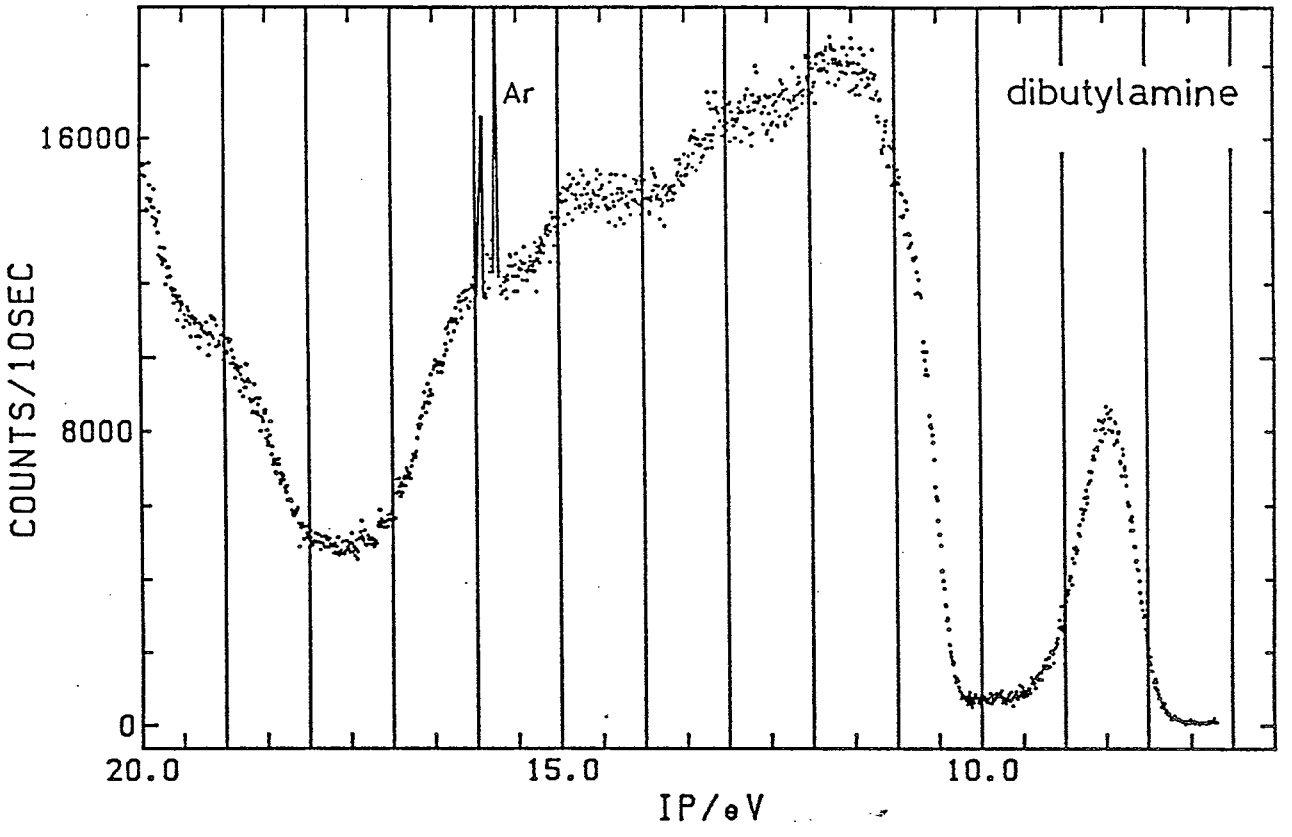
Ar
dibutylamine
16000
8000
0
COUNTS/10SEC
20.0
15.0
10.0
IP/eV

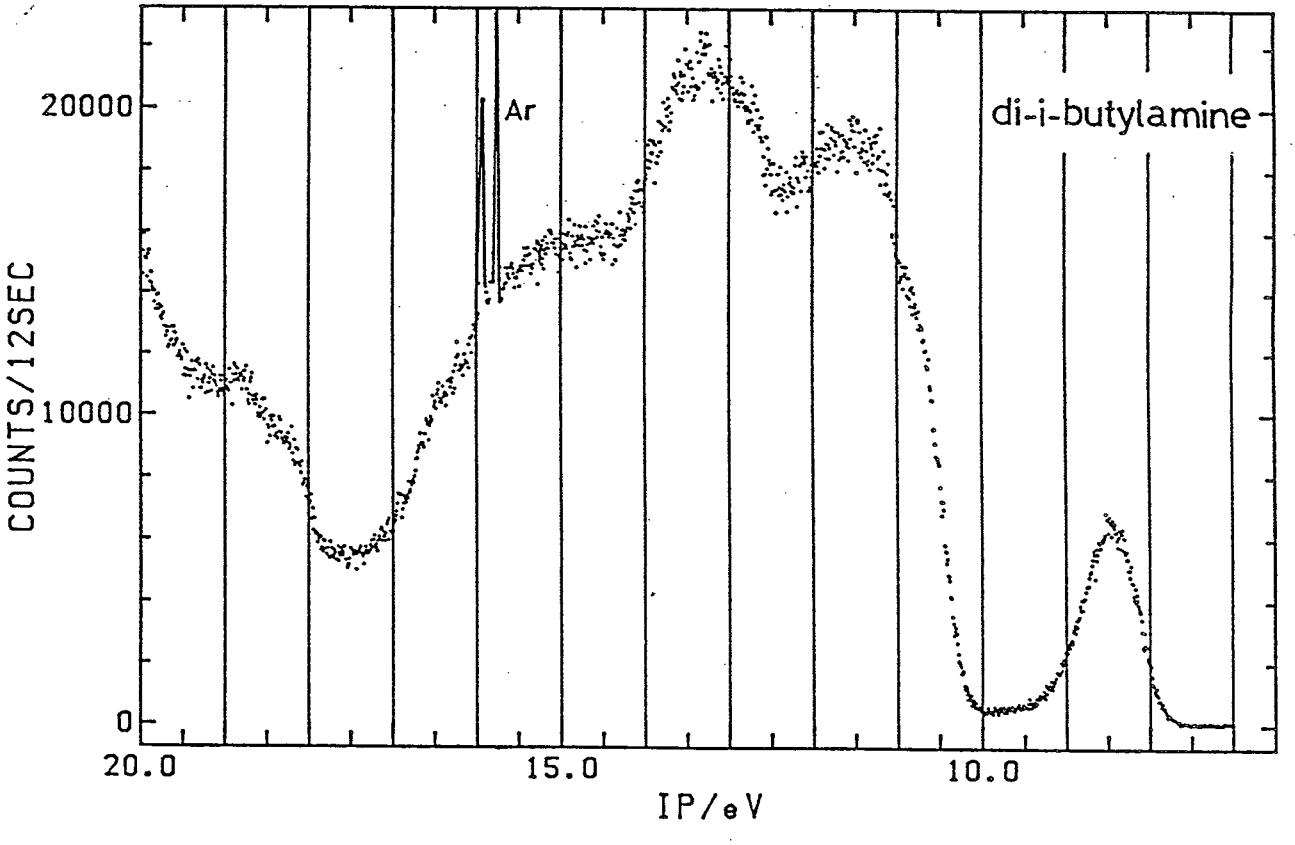
Ar
di-i-butylamine
20000
10000
0
COUNTS/12SEC
20.0
15.0
10.0
IP/eV

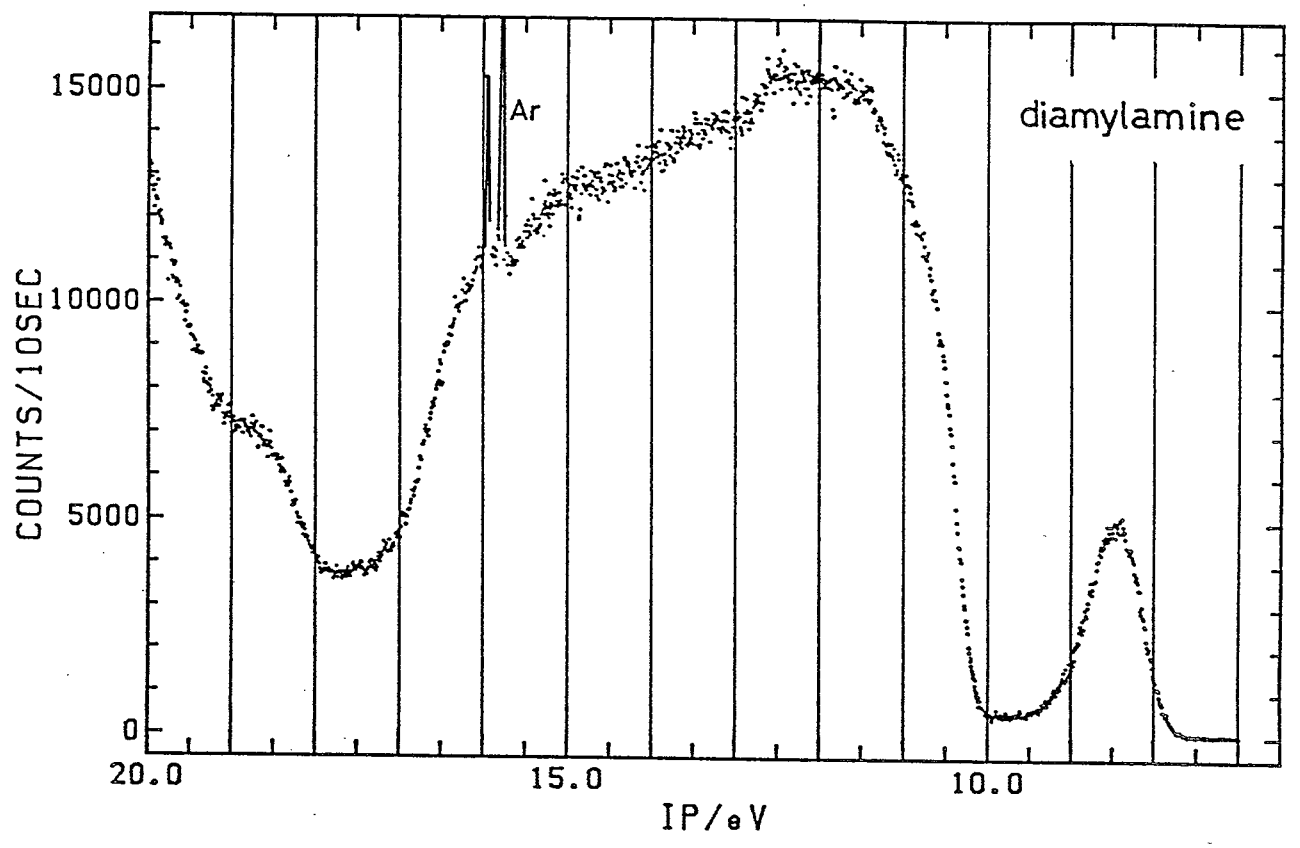
15000
10000
5000
0
COUNTS/10SEC
Ar
diamylamine
20.0
15.0
10.0
IP/eV

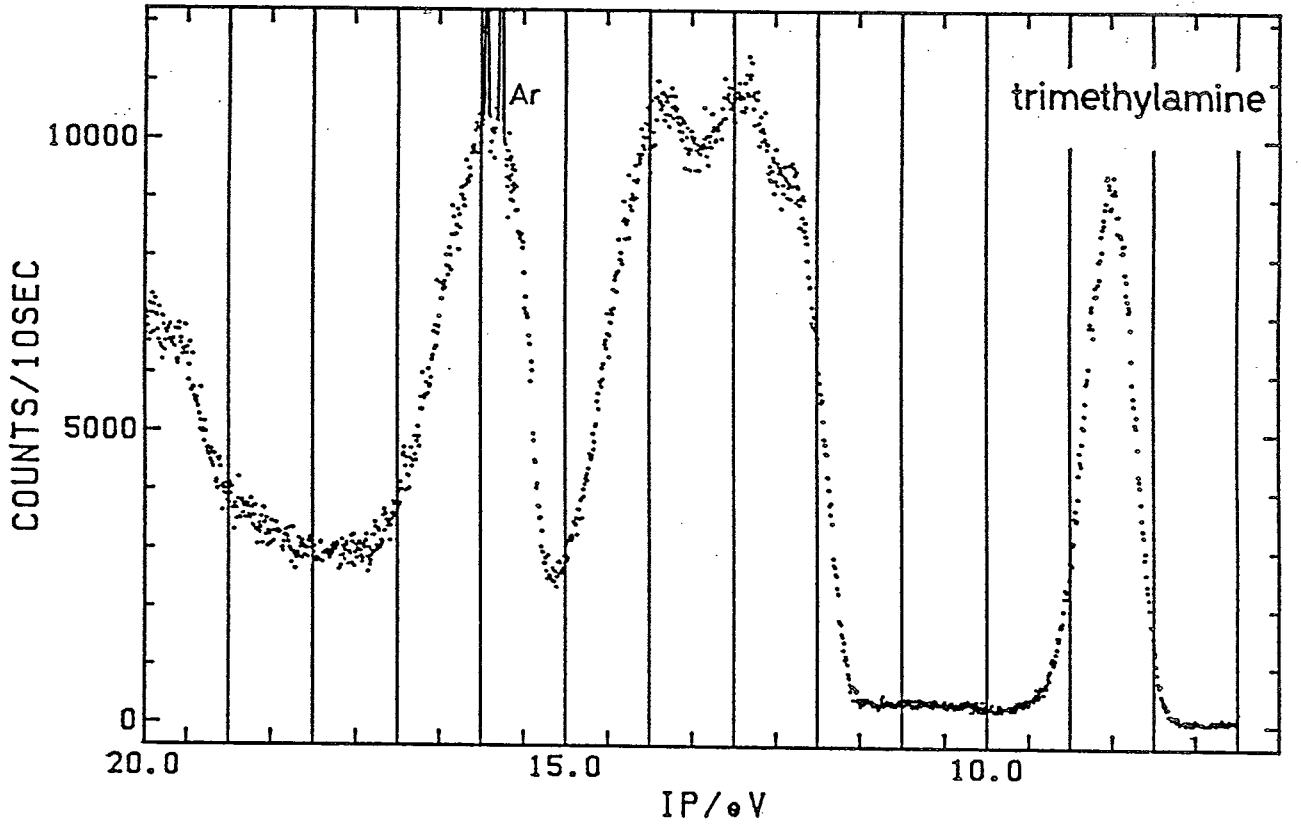
10000
5000
0
COUNTS/10SEC
Ar
trimethylamine
20.0
15.0
10.0
IP/eV

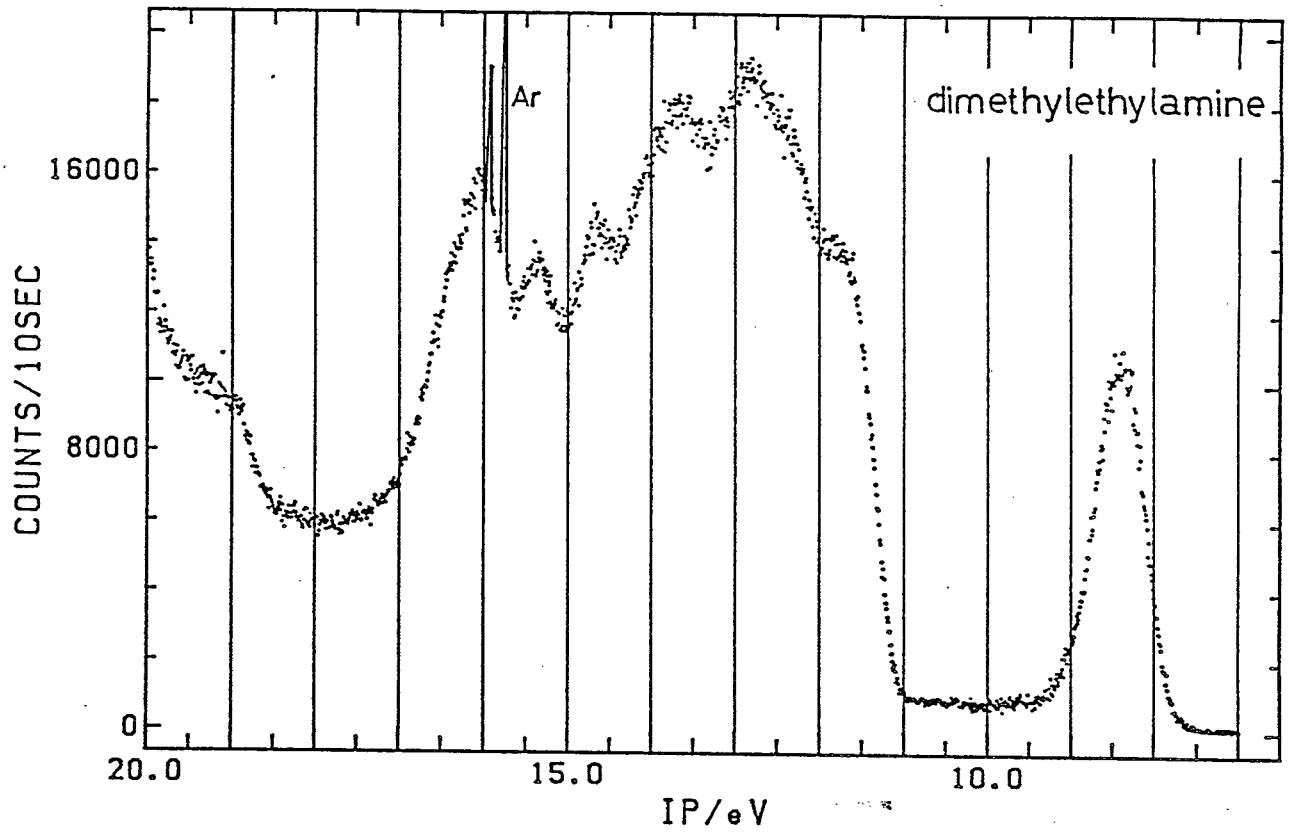
Ar
dimethylethylamine
16000
8000
0
COUNTS/10SEC
20.0
15.0
10.0
IP/eV

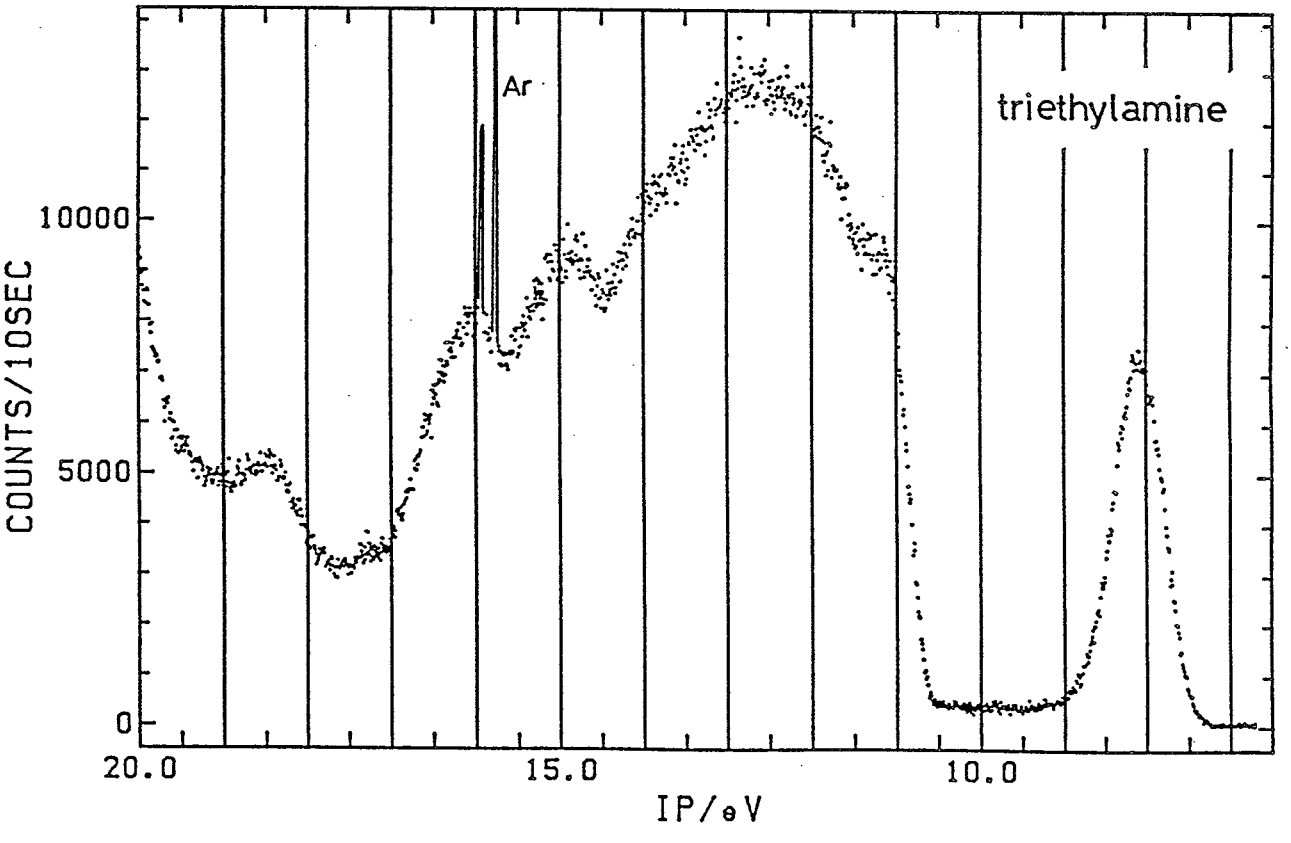
Ar
triethylamine
10000
5000
0
COUNTS/10SEC
20.0
15.0
10.0
IP/eV

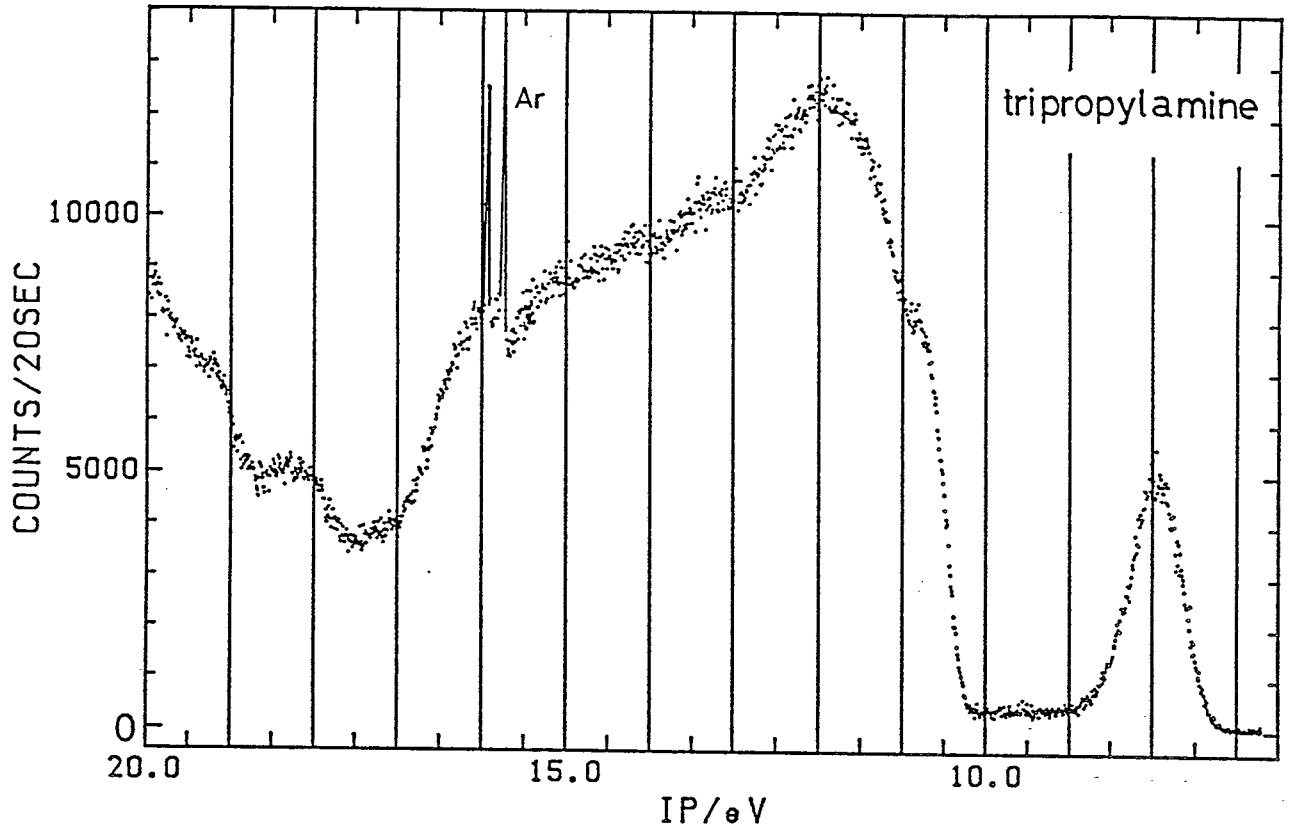
tripropylamine
Ar
10000
5000
0
COUNTS/20SEC
20.0
15.0
10.0
IP/eV

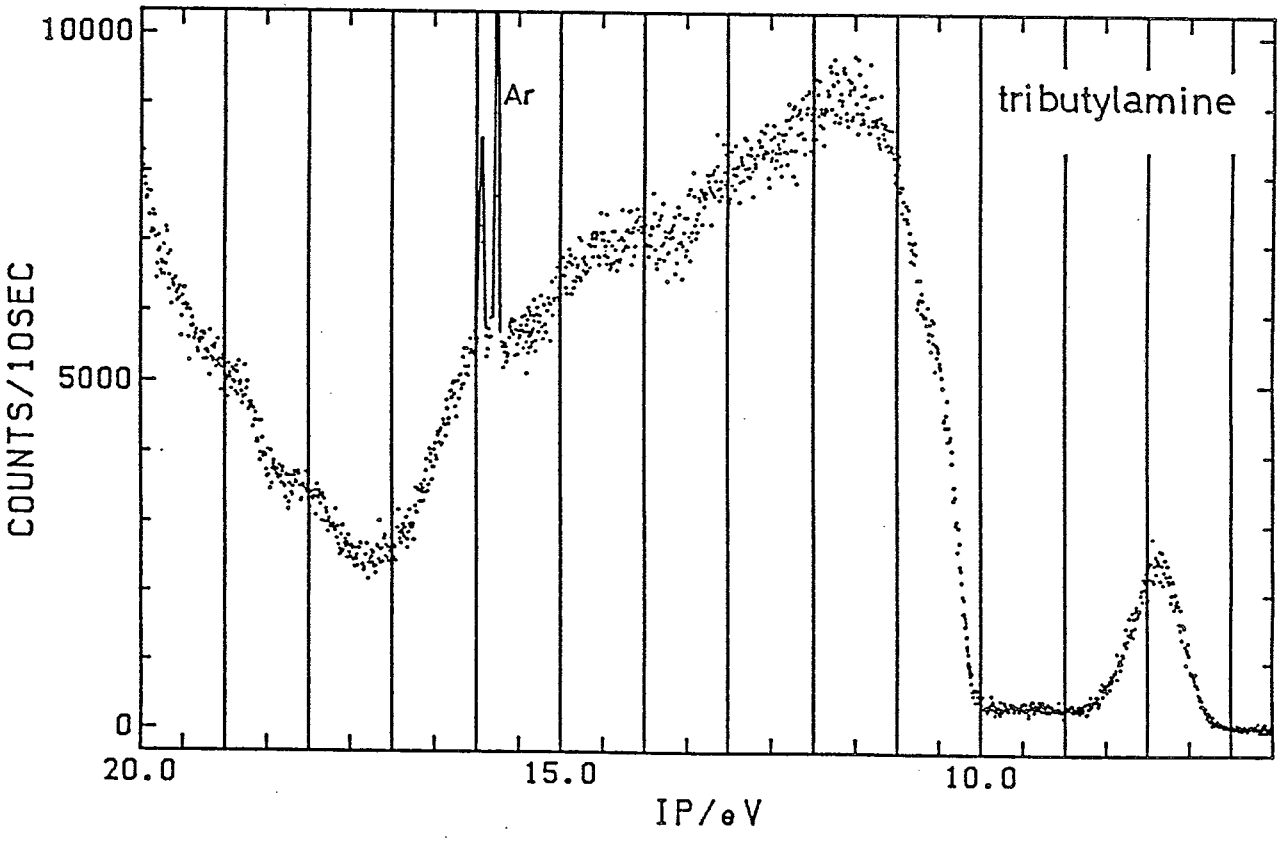
tributylamine
Ar
10000
5000
0
COUNTS/10SEC
20.0
15.0
10.0
IP/eV

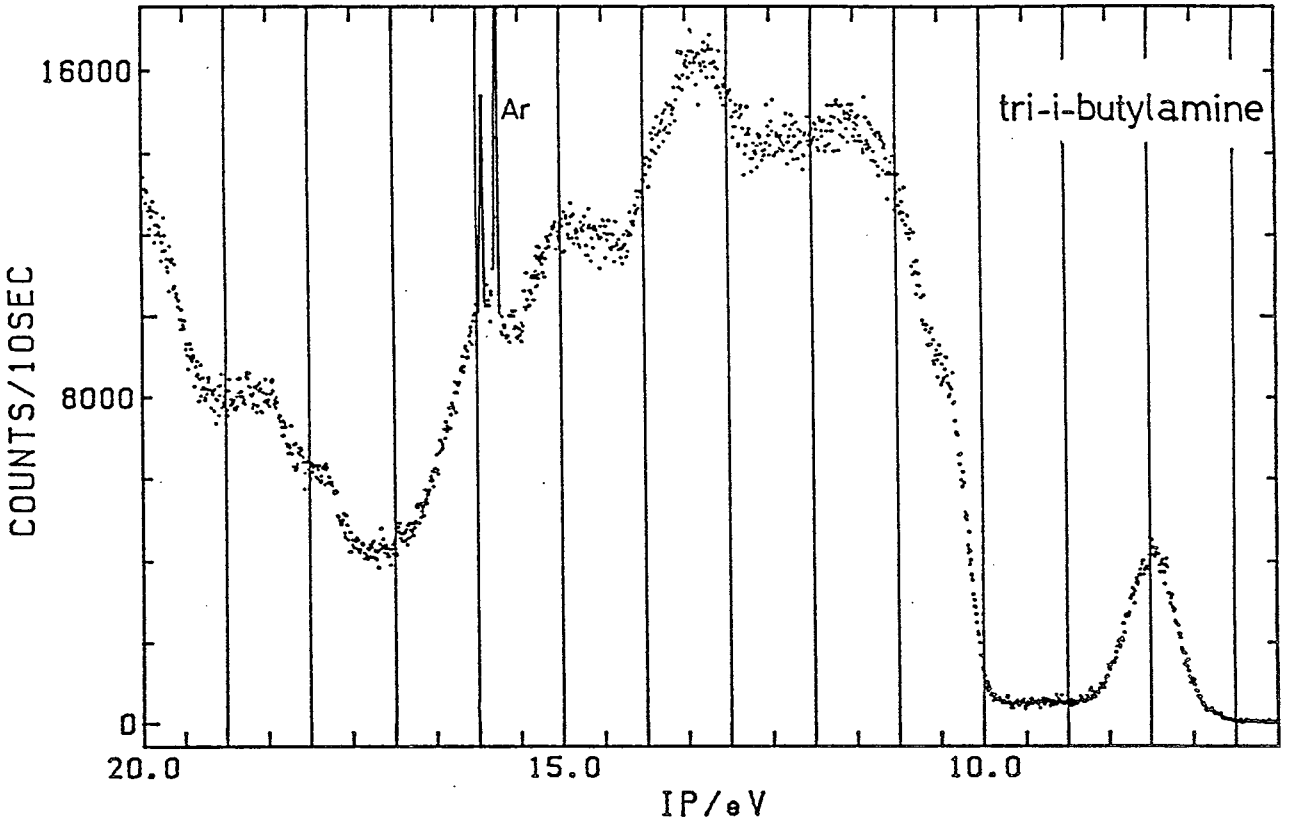
16000
8000
0
COUNTS/10SEC
Ar
tri-i-butylamine
20.0
15.0
10.0
IP/eV

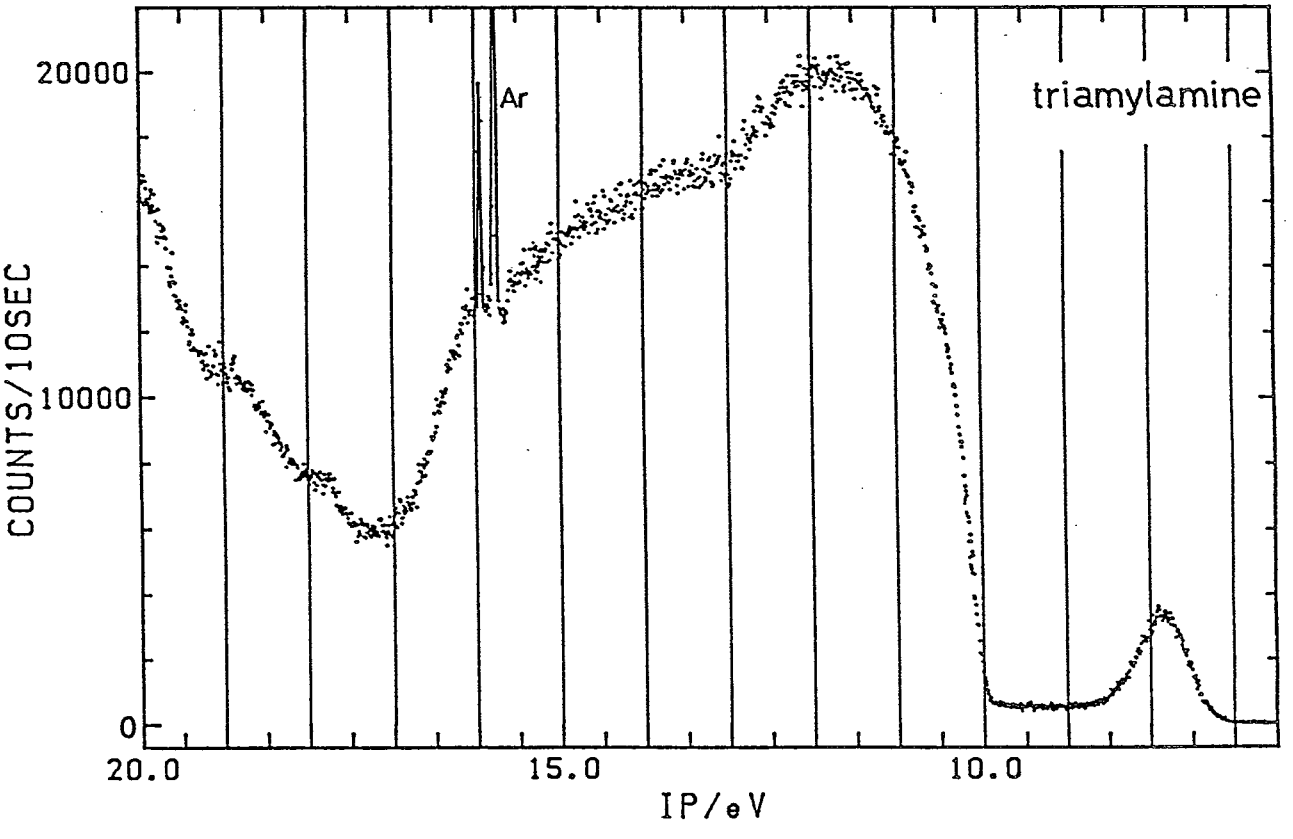
20000
10000
0
COUNTS/10SEC
Ar
triamylamine
20.0
15.0
10.0
IP/eV

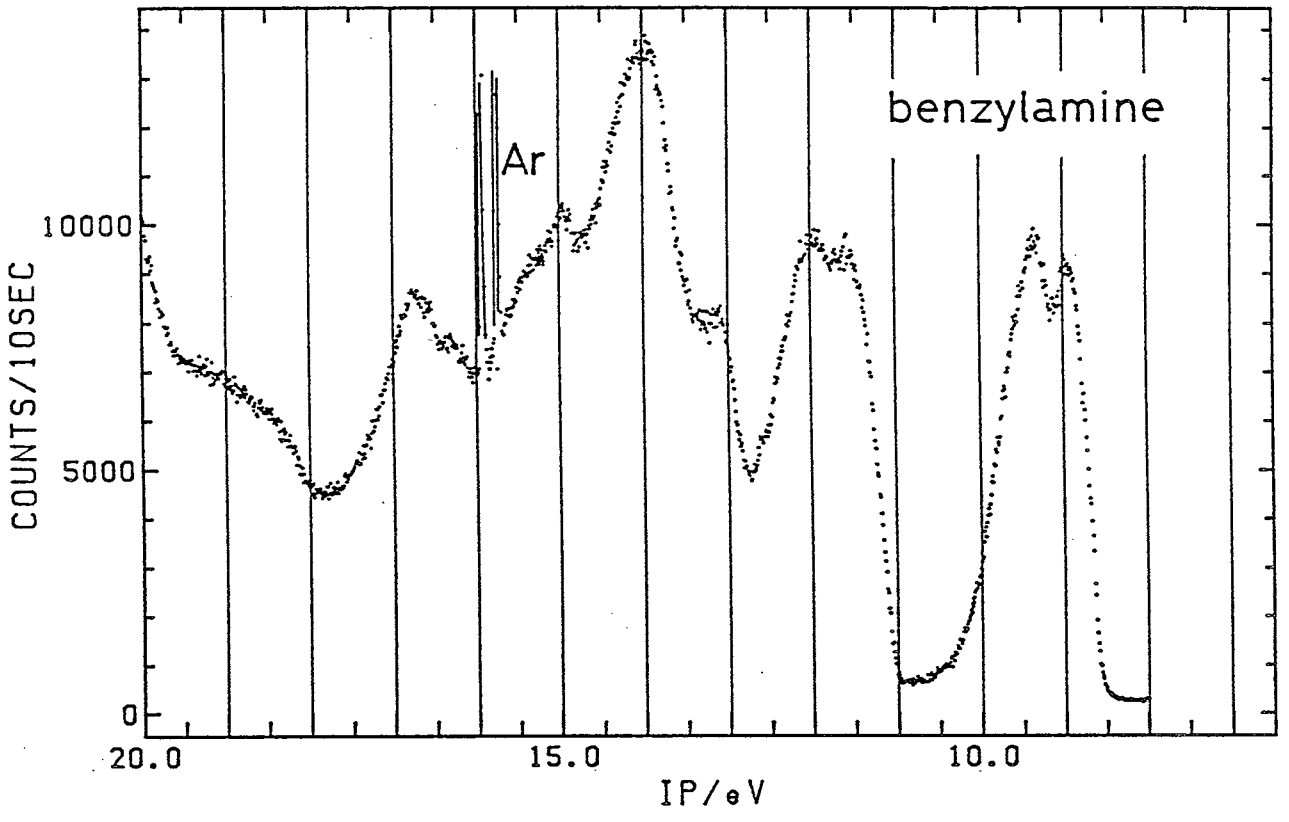
benzylamine
Ar
10000
5000
0
COUNTS/10SEC
20.0
15.0
10.0
IP/eV

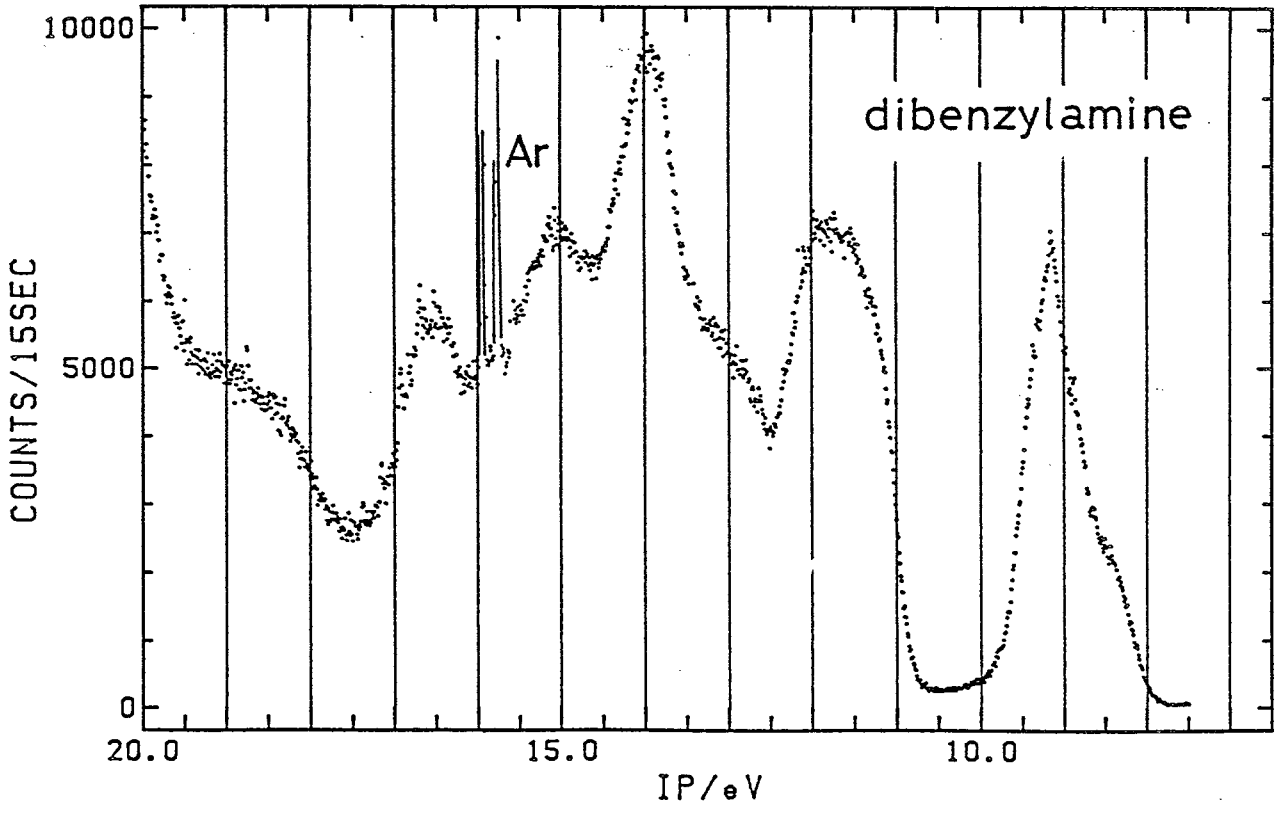
dibenzylamine
Ar
10000
5000
0
COUNTS/15SEC
20.0
15.0
10.0
IP/eV

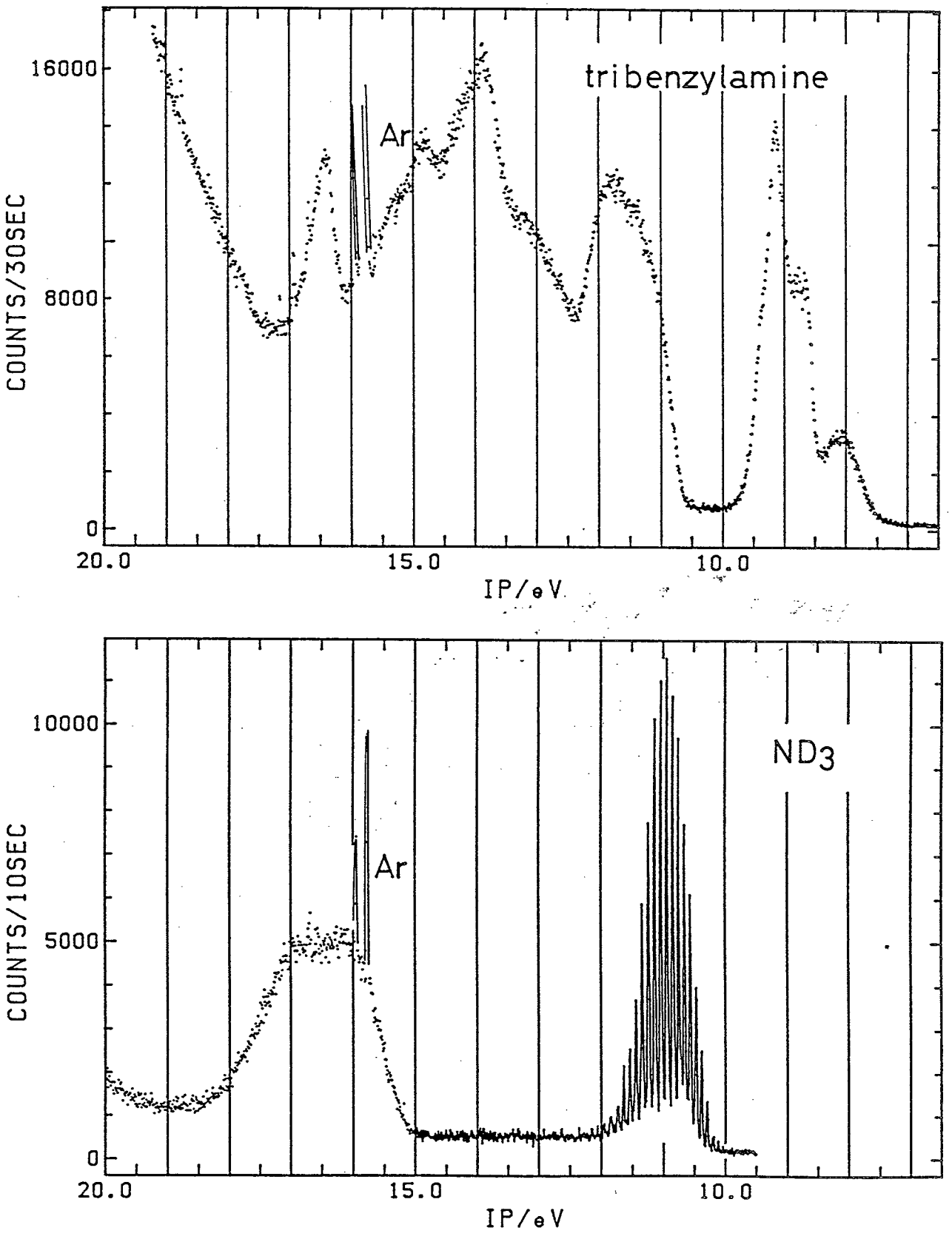
16000
8000
0
COUNTS/30SEC
tribenzylamine
Ar
20.0
15.0
10.0
IP/eV
10000
5000
0
COUNTS/10SEC
Ar
ND3
20.0
15.0
10.0
IP/eV

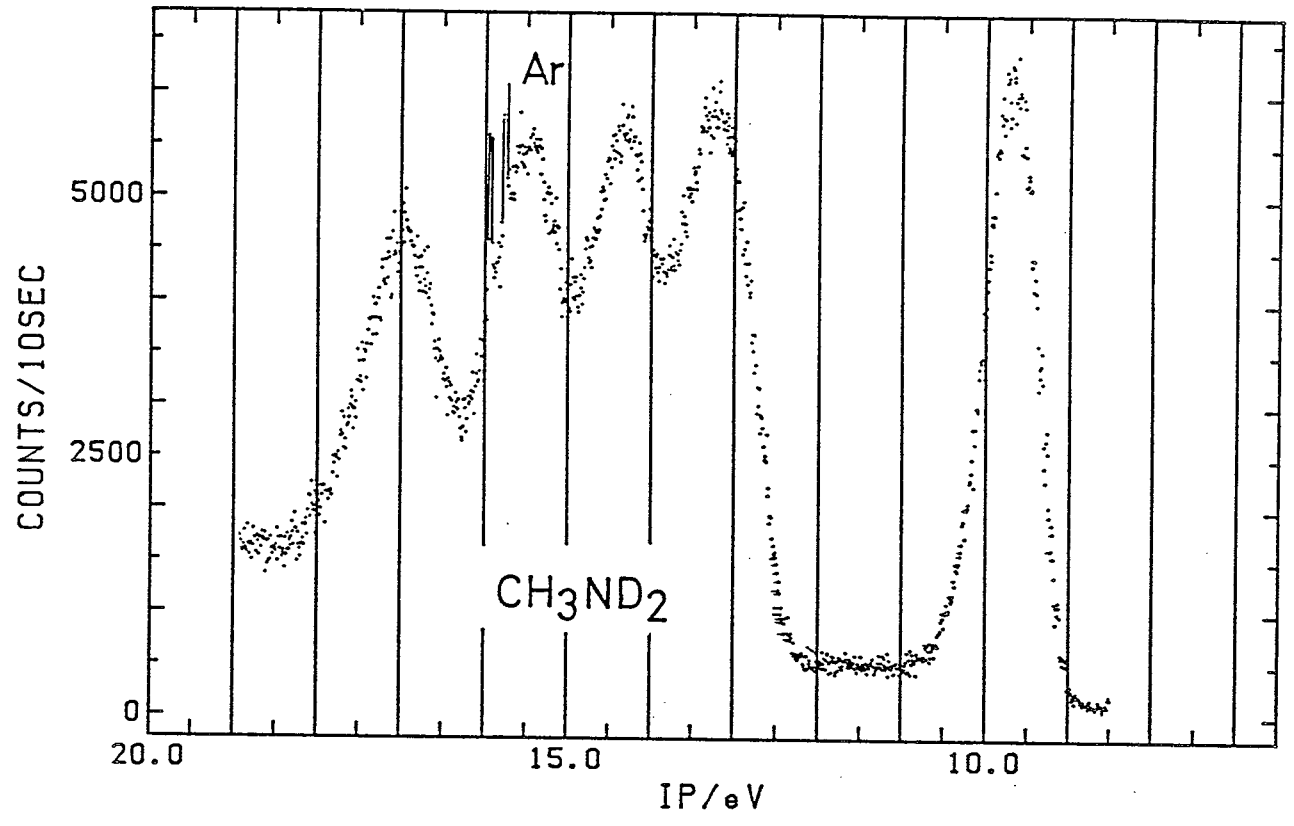
Ar
CH3ND2
5000
2500
0
COUNTS/10SEC
20.0
15.0
10.0
IP/eV

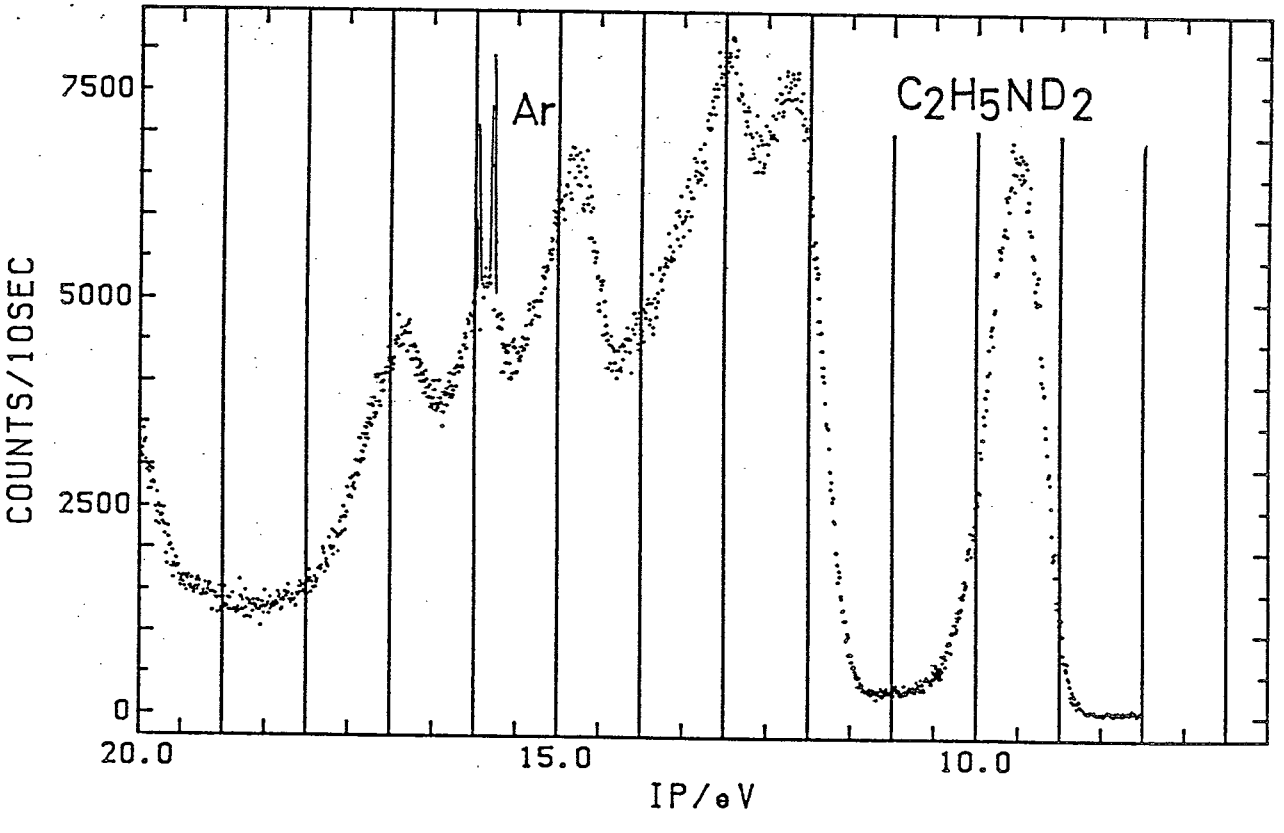
Ar
C2H5ND2
7500
5000
2500
0
COUNTS/10SEC
20.0
15.0
10.0
IP/eV

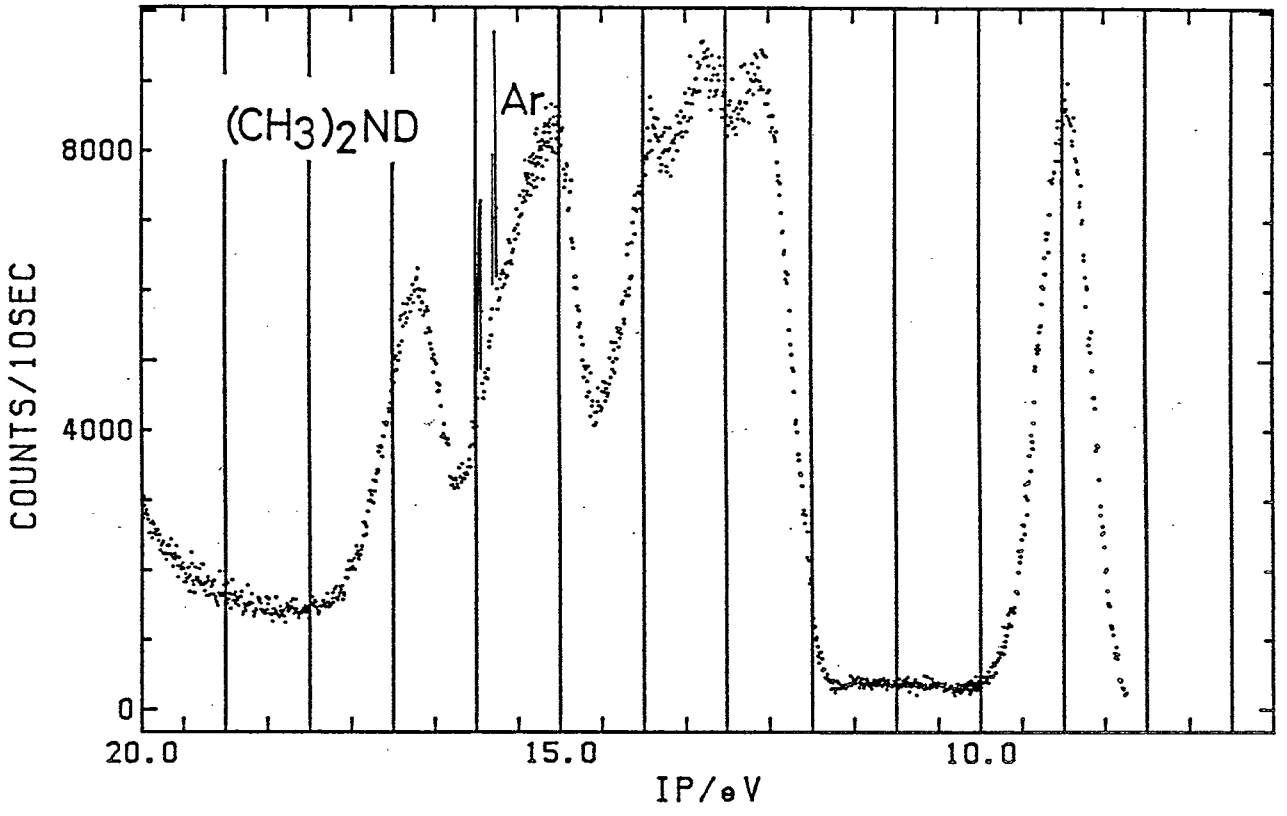
(CH3)2ND
Ar
8000
4000
0
COUNTS/10SEC
20.0
15.0
10.0
IP/eV

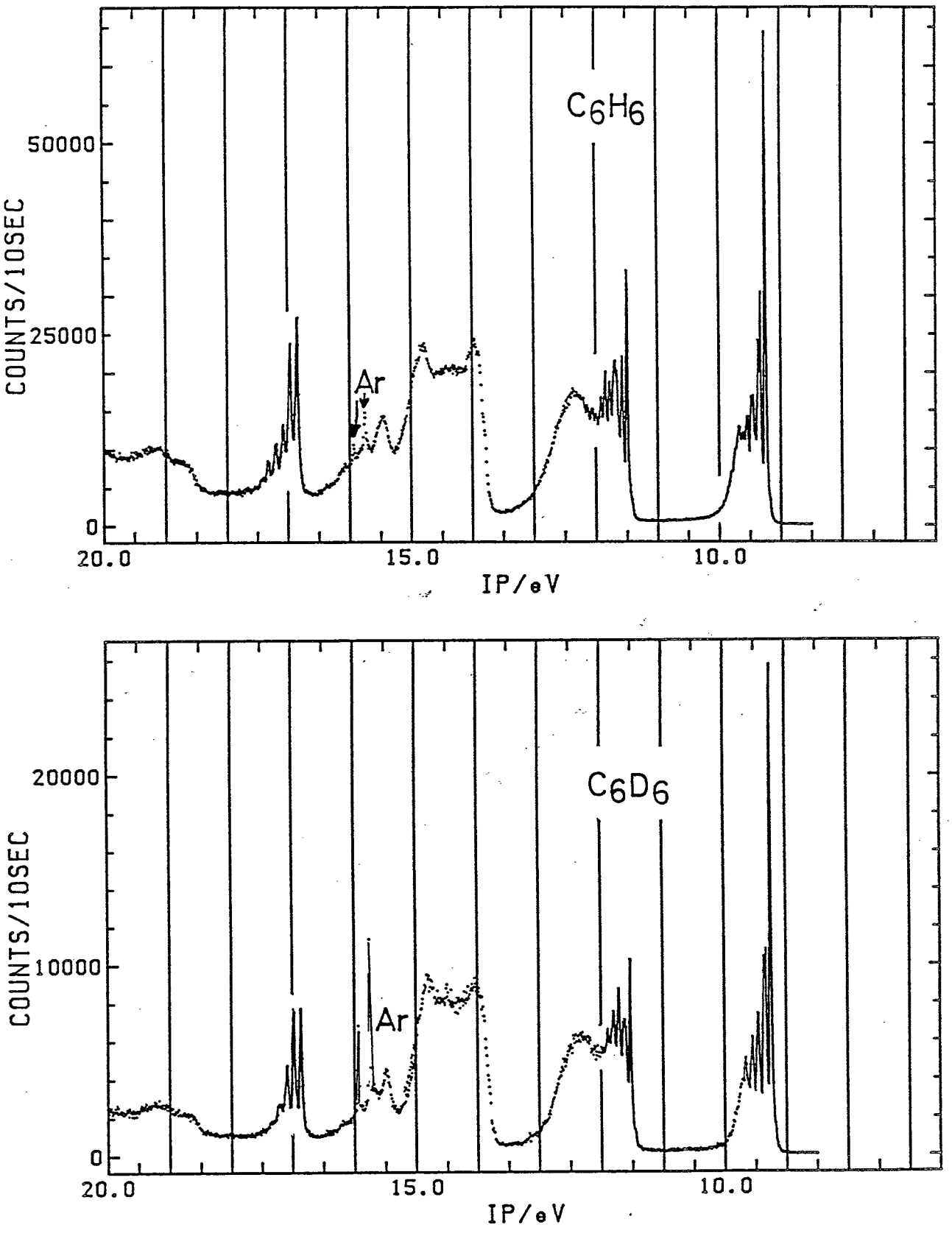
C6H6
50000
25000
0
COUNTS/10SEC
Ar
20.0
15.0
10.0
IP/eV
C6D6
20000
10000
0
COUNTS/10SEC
Ar
20.0
15.0
10.0
IP/eV